Thickness Resonances Dispersion Characteristics of a Lossy Piezoceramic Plate with Electrodes of Arbitrary Conductivity

Alex A. Mezheritsky, Alex V. Mezheritsky,

adapted from the article published in the journal IEEE UFFC, October 2007.

ABSTRACT - A theoretical description of the dissipative phenomena in the wave dispersion related to the "energy-trap" effect in a thickness-vibrating infinite thickness-polarized piezoceramic plate with resistive electrodes is presented. The 3-D equations of linear piezoelectricity with quasi-electrostatic approximation were extended to include losses attributed to the bulk electro-mechanical damping in solid (complex material constants) and the resistance in electrodes. These equations were used to obtain symmetric and antisymmetric solutions of plane harmonic waves of arbitrary direction and to investigate the eigen-modes of thickness longitudinal (*TL*) up to 3rd harmonic and shear (*TSh*) up to 9th harmonic vibrations of odd- and even-orders. The effects of internal and electrode energy dissipation parameters on the wave propagation under regimes ranging from a short-circuit (s.c.) condition through the resonance of the *RC*-type relaxation dispersion to an open-circuit (o.c.) condition are examined in detail for PZT piezoceramics with three characteristic *TL*-mode energy-trap figure-of-merit $\dot{c}_{33}^{D}/\dot{c}_{44}^{E}$ values – less, near equal and higher 4 – when the second harmonic spurious *TSh* resonance lies below the fundamental *TL* resonance, inside its resonance-antiresonance frequency interval, and above the *TL* antiresonance, respectively. Calculated lateral wave-number dispersion dependences on frequency and electrode resistance are found to follow the universal scaling formula similar to those for dielectrics characterization. Formally represented as a Cole-Cole diagram of the complex lateral wave-number, the dispersion branches basically exhibit Debye-like and modified Devidson-Cole dependences. Varying the dissipation parameters of internal loss and electrode conductivity, the interaction of different branches was demonstrated by analytical and numerical analysis.

For the purposes of dispersion characterization of at least any thickness resonance near the wave-number origin, the following Theorem was stated: the ratio of two characteristic determinants, specifically constructed from the boundary conditions to describe the eigenmodes of the o.c. and s.c. piezoelectric plate, in the limit of zero lateral wave-number, is equal to the basic elementary-mode normalized admittance. As was found based on the Theorem, the complex lateral wave-numbers near the basic and non-basic *TL* and *TSh* resonances reveal some simple representations related to the respective elementary admittance and showing the connection between the propagation and excitation problems in a continuous piezoactive medium.

e- mail: aam80@optonline.net , mav5@optonline.net (CC: amezheritsky@ieee.org)

I. INTRODUCTION

Piezoplates made of piezoelectric ceramics [1],[2] with 6-mm symmetry are widely used as high-frequency resonators, transducers, and monolithic filters employing thickness vibrational modes [3],[4]. In an elementary theory neglecting transverse effects and other spurious modes influence, in a relatively thin piezoceramic plate $\Psi \times \Upsilon \times 2b$ (Fig. 1a,b) with thickness polarization ($\vec{\mathrm{P}}$) and electrodes respectively on $\Psi \times \Upsilon$ and $\Psi \times 2b$ plate surfaces, two basic thickness elementary *TL*- and *TSh*-modes can be excited [1],[5] by the uniform in the major plane electric field $\vec{E}^*$, with respective piezoresonator's (PR) impedances *Z*:

$$Z \cdot \mathrm{i}\omega C_{33}^S = 1 - \mathrm{k}_t^2 \tan \mathrm{K}_{\langle TL \rangle} \big/ \mathrm{K}_{\langle TL \rangle} , \tag{1}$$

$$\left(Z \cdot \mathrm{i}\omega C_{11}^T \right)^{-1} = 1 - \tilde{\mathrm{k}}_{15}^2 + \tilde{\mathrm{k}}_{15}^2 \tan \mathrm{K}_{\langle TSh \rangle} \big/ \mathrm{K}_{\langle TSh \rangle} \quad , \tag{2}$$

where $C_{33}^S = \varepsilon_{33}^S \, \Psi \, \Upsilon / 2b$ and $C_{11}^T = \varepsilon_{11}^T \, 2b\Psi / \Upsilon$ are the PR capacitance, $\mathrm{k}_t^2 = e_{33}^2 \big/ c_{33}^D \, \varepsilon_{33}^S$ and $\tilde{\mathrm{k}}_{15}^2 = e_{15}^2 \big/ c_{44}^D \, \varepsilon_{11}^S$ are the *TL*- and *TSh*-mode coefficients of electro-mechanical coupling (CEMC) squared, $\mathrm{K}_{\langle TL \rangle}^2 = \omega^2 \rho b^2 \big/ c_{33}^D$ and $\mathrm{K}_{\langle TSh \rangle}^2 = \omega^2 \rho b^2 \big/ c_{44}^E$ are the *TL* and *TSh* elementary mode wave-numbers squared, $2b$ is the PR thickness, ρ is the piezomaterial density, $\omega = 2\pi f$ is the frequency, $\mathrm{i} = \sqrt{-1}$. The standard [6] notations and the SI system of units are used for the material constants: piezocoefficients e_{ij} (h_{ij}, d_{ij}), dielectric permittivity $\varepsilon_{ij}^{T,S}$ at constant stress ***T*** and strain ***S***, elastic stiffness $c_{ij}^{E,D}$ (compliance $s_{ij}^{E,D}$) at constant strength ***E*** and induction ***D*** of an electric field. To take into account internal losses, the material coefficients are phenomenologically expressed as complex [7] with respective imaginary parts responsible for mechanical, dielectric, and piezoelectric energy dissipation.

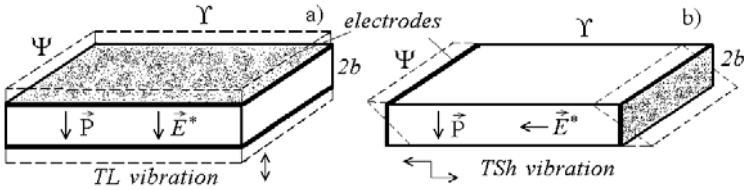

Fig. 1 a,b . *Thickness-polarized PR plates with TL (a) and TSh (b) elementary vibrations.*

The PR admittance is actually related to the extended concept of dielectric permittivity as a charge (induction)-to-voltage ratio. Then, the relationships (1),(2) can be expressed in a generalized form as an effective dielectric permittivity of a PR

$$\varepsilon^S \cdot \hat{\mathrm{Y}} = \Re / \omega Z \qquad \text{with} \qquad \hat{\mathrm{Y}} \equiv \hat{\mathrm{Y}}_{\langle TL|TSh \rangle} = \mathrm{i}\left(1 \mp \mathrm{k}^2 \tan \mathrm{K}/\mathrm{K}\right)^{\mp 1} \quad , \tag{3}$$

where $\hat{\mathrm{Y}}_{\langle TL,TSh \rangle}$ is the dimensionless normalized admittance of the respective elementary mode, $\Re$ is the PR dimension factor, then for the elementary *TL*-mode (Fig. 1a): $\mathrm{K} = \mathrm{K}_{\langle TL \rangle}$, $\mathrm{k}^2 = \mathrm{k}_t^2$, $\Re = 2b/\Psi \, \Upsilon$, $\varepsilon^S = \varepsilon_{33}^S$; for the elementary *TSh*-mode (Fig. 1b): $\mathrm{K} = \mathrm{K}_{\langle TSh \rangle}$, $\mathrm{k}^2 = \mathrm{k}_{15}^2 \equiv \tilde{\mathrm{k}}_{15}^2 \big/ \left(1 - \tilde{\mathrm{k}}_{15}^2\right)$, $\Re = \Upsilon / 2b\Psi$, $\varepsilon^S = \varepsilon_{11}^S$. The typical frequency responses of a PR have both the resonance f_r and antiresonance f_a frequencies [6],[8]

determined by the real elastic stiffness $\dot{c}_{ij}^{E,D}$; only odd-order harmonics ($n=1,3,5...$) of the basic resonances can be excited in the elementary PRs. The resonance and antiresonance peaks sharpness is determined basically by the complex elastic stiffness $c_{ij}^{E,D}=\dot{c}_{ij}^{E,D}(1+\mathrm{i}/Q_{ij}^{E,D})$ with respective quality factors $Q_{ij}^{E,D}$ [9] whose difference can reach as much as 3 times due to high piezoeffect in piezoceramics.

In general, thickness vibrations of a real PR are very complicated due to the influence of competing modes and the effects that are caused by planar boundary conditions. Coupling of different modes typically occurs in the vicinity of the lowest fundamental thickness resonances [4],[7],[10]-[16], so that the basic *TL*-mode with a coupled *TSh* vibration, or the basic *TSh*-mode with coupled flexure-twist vibrations, can provide under certain conditions the "energy-trapping" effect widely used in frequency selection devices. The PZT-piezoceramics is characterized by the wide range of the figure-of-merit $\dot{c}_{33}^{D}/\dot{c}_{44}^{E}$ from approximately 2.3 for far-tetragonal compositions up to 9 for soft piezoceramics near morphotropic phase boundary [1,2].

The 3-D equations of linear piezoelectricity, including mechanical damping and electric conductivity, were used in [13] to obtain solutions of plane bulk harmonic Lamb waves [1],[14] in an infinite piezoelectric plate with general symmetry. Four lowest dispersion curves were computed and plotted for real frequencies and complex lateral wave numbers $\xi(\omega)$ in a wide frequency range near the fundamental resonances. All branches are complex due to dissipation, and there are no longer any cut-off frequencies as those existing for the non-dissipative waves where a significant characteristic change of dispersion curves occurs. The relatively newly discovered edge mode, which is a combined motion of the even-order *TSh* and odd-order *TL* vibrations, was explained theoretically [10] from a branch with complex wave-number. The fields distribution in a vibrating body can be calculated based on finite element method – boundary element method, however the connection of such a calculation with the dispersion relations is not obvious.

Useful dispersion properties can be extracted from a simple fact – by supposing the only condition that determinants of the characteristic matrices are even functions of both ξ^2 and ω^2 [4]. When the determinant equals zero, there is a root for dispersion relationship in the primary form $\zeta_m^2(\omega^2)$, then as a first-order approximation $\zeta_m^2 \propto \omega^2-\bar{\omega}_0^2$ in a vicinity of the complex resonance with $\bar{\omega}_0^2=\omega_0^2\left(1+\mathrm{i}/Q\right)$, where $\bar{\omega}_0^2$ is proportional to the lossy elastic stiffness $\dot{c}_{ij}\left(1+\mathrm{i}/Q\right)$ with the quality factor *Q*. It follows that at the resonance there is an absolute minimum $\zeta_m^2\left(\omega=\omega_0\right)\propto \pm\mathrm{i}\,\omega_0^2/Q$ with the complex wave-number $min\ \zeta_m\left(\omega=\omega_0\right)\approx\left(\pm1-\mathrm{i}\right)n/\sqrt{Q}$ inversely proportional to $\sqrt{Q}$ [15]. In piezoelectrics the difference (shift) between s.c. and o.c. branches near the resonance appears to be proportional to CEMC squared.

Ingebrigtsen's approach [17],[18], primarily developed for the 1-D electrical behavior description of the surface acoustic waves in an interdigital piezo-transducer array, is based on the effective dielectric permittivity $\varepsilon^*(\xi)$ concept. As $\varepsilon^*(\xi)$ as a parameter of the surface potential distribution is an even function of the wave-number ξ, its frequency dependence between the s.c. resonance pole ($\xi=\zeta_r$) and o.c. zero

antiresonance ($\xi = \zeta_a$) provides a convenient approximate form

$$\frac{\varepsilon^*(\xi)}{\varepsilon_0} \approx \Gamma \cdot \frac{\xi^2 - \zeta_a^2}{\xi^2 - \zeta_r^2} \quad , \tag{4}$$

where Γ is a constant. Such approach, applied particularly to the 1-D elementary admittance (3) with the thickness wave-number K, is the basis for a simplified traditional equivalent circuit of a PR [1].

Further development of the concept was conducted in [19] for the harmonic admittance. As was formulated as a general theorem, if the appropriately defined dispersion equation for open electrodes is $\left\|\mathbf{G}(\xi,\omega)\right\| = 0$ to describe the eigenmodes $\xi = \zeta^{oc}(\omega)$, and for short-circuited electrodes is $\left\|\mathbf{\Phi}(\xi,\omega)\right\| = 0$ with $\xi = \zeta^{sc}(\omega)$ of an infinite 1-D periodic surface electrode array, then the harmonic admittance of the piezoelectric structure may be always expressed as the ratio of two determinants

$$Z^{-1}(\xi,\omega) = \left\|\mathbf{G}(\xi,\omega)\right\| \Big/ \left\|\mathbf{\Phi}(\xi,\omega)\right\| \ . \tag{5}$$

The calculation of the harmonic admittance and finding the dispersion equations for the eigenmodes of the infinite periodic electrode array are usually considered as two independent concepts - the excitation problem and the propagation problem. It was shown that these two problems [19] are in reality very closely connected.

The thinner piezoplate thickness used in practice, the thinner electrode thickness is required and limited methods can be applied for electrode deposition. The electrode resistivity effect can not be properly described by discrete equivalent circuit elements with an additional resistance (R_{el}), as such the PR is a system with distributed parameters involving local acoustic and electric interactions. The effect of resistive electrodes and/or bulk conductivity on elastic waves in piezoelectrics relates to a common phenomenon of dielectric dispersion [18],[21]-[23]. Most of relaxation processes in dielectrics – frequency behavior of the effective complex dielectric constant $\varepsilon^*(\omega) = \mathrm{Re}\,\varepsilon^* - \mathrm{i}\,\mathrm{Im}\varepsilon^*$ – are generally described by the Havriliak-Negami empirical expression [22]-[24] with two exponential parameters

$$\varepsilon^*(\omega) = \varepsilon_\infty + \frac{\varepsilon_0 - \varepsilon_\infty}{\left[1 + (\mathrm{i}\omega\tau)^\alpha\right]^\beta} \quad , \tag{6}$$

where ε_∞ is the high frequency permittivity, ε_0 is the static, low frequency permittivity, and $\tau = RC$ is the characteristic relaxation time of the medium with effective resistive R and capacitive C components. The exponents α and β describe the asymmetry and broadness of the corresponding dielectric dispersion curve, and depend mainly on the structure configuration (anisotropy degree). For $\beta = 1,\ 0 < \alpha \le 1$ it is known as the Cole-Cole; for $0 < \beta \le 1,\ \alpha = 1$ as the Davidson-Cole equation. The Debye expression with $\beta = \alpha = 1$ corresponds to a single isotropic relaxation mechanism describing the “loss tangent” in a dielectric medium, with a maximum in $\mathrm{Im}\,\varepsilon^*$ at the dielectric resonance $\omega\tau = 1$. Traditionally plotted real and imaginary parts of the dielectric constant as a function of frequency is called a Cole-Cole diagram – an ideal semicircle arc for Debye dispersion, and linear at high frequencies and with arc-like shape at low frequencies

for Davidson-Cole dispersion.

As was shown from the dispersion equations for acoustic waves in conductive solid medium, such as piezoelectric semiconductors [25], the character of interaction of the elastic waves with free bulk charges (unit conductivity σ) is largely determined by the effective complex dielectric permittivity

$$\varepsilon^*(\tau) = \varepsilon^T + \frac{\sigma}{\mathrm{i}\,\omega} = \varepsilon^T \left(\frac{\mathrm{i}\,\omega\tau}{1+\mathrm{i}\,\omega\tau} \right)^{-1} . \qquad (7)$$

Free chargers are fully screening the electric fields in the wave at relatively low frequencies where wave velocity is determined by the elastic constant s^E under constant electric field *E*, the influence of free charges at relatively high frequencies are negligible and wave velocity is determined by the elastic constant $s^D = s^E\left(1-\mathrm{k}^2\right)$ under constant electric induction *D*. Clearly, the effective elastic compliance $s^*(\tau)$ behaves itself in the same way forming the lateral phase velocity dispersion under bulk conductivity:

$$s^*(\tau) = s^E\left(1-\mathrm{k}^2\frac{\mathrm{i}\,\omega\tau}{1+\mathrm{i}\,\omega\tau}\right) = s^D\left(1+\frac{\mathrm{k}^2}{1-\mathrm{k}^2}\cdot\frac{1}{1+\mathrm{i}\,\omega\tau}\right) , \qquad (8)$$

where $\tau = \varepsilon^T/\sigma$ is the *Maxwell* charge relaxation time, k^2 is the respective material CEMC squared.

The dispersion dependences can be interpreted in the term of conductivity at a constant given frequency as τ is mainly dependable on conductivity. In the literature, the interaction of acoustic waves in piezoelectrics with conductivity of free charges was described for various structures: bulk waves and conductivity in piezoelectric semiconductors; surface waves in a piezoelectric substrate with electrodes – fully covered or interdigital, metal or semi-conductive, located directly on the surface, or with a gap [20], as conductive fluid [21]. Because of high electromechanical coupling, the interaction of the bulk acoustic waves with the electrode system is relatively strong, and a velocity change as large as 50% can be achieved by altering the surface conductivity. The results obtained reveal great prospects of using such properties to create acousto-electronic devices with controllable characteristics. A simple fixture principle, related to the problem, with two contact points on the resistive electrode was proposed [15] providing deep sharpening and exact determination of the PR resonances. The present original theoretical research is studying the influence of electrode resistivity on the dispersion of bulk plane acoustic waves near the thickness resonances of a lossy piezoplate.

II. GOVERNING EQUATIONS for PLANE WAVES in a PIEZOCERAMIC PLATE

The plane waves in the $x-z$ plane of an infinite in both *x*-*y* directions and thickness-polarized plate (Fig. 2 a,b) are considered for certainty, so that no gradients exist in the y - direction. The relevant linear equations of piezoelectricity are as follows:

$$T_x = c_{11}^E\cdot u_{x,\,x} + c_{13}^E\cdot u_{z,\,z} + e_{31}\cdot\varphi_{,\,z} \quad , \qquad T_z = c_{13}^E\cdot u_{x,\,x} + c_{33}^E\cdot u_{z,\,z} + e_{33}\cdot\varphi_{,\,z} \quad ,$$

$$T_{xz} = c_{44}^E\cdot\left(u_{x,\,z} + u_{z,\,x}\right) + e_{15}\cdot\varphi_{,\,x} \quad ,$$

$$D_z = e_{31}\cdot u_{x,x} + e_{33}\cdot u_{z,z} - \varepsilon_{33}^S\cdot\varphi_{,z}\ , \qquad D_x = e_{15}\cdot\left(u_{x,z}+u_{z,x}\right) - \varepsilon_{11}^S\cdot\varphi_{,x}\ , \tag{9}$$

where $\boldsymbol{T}$ is the stress, $\boldsymbol{E}$ and $\boldsymbol{D}$ are the electric field strength and induction, φ is the electric potential with $E_{x(z)} = -\varphi_{,x(z)}$, $\vec{u}$ is the mechanical displacement [13]. The equations of motion and charge are:

$$\rho u_{z,\mathrm{tt}} = T_{z,z} + T_{xz,x}\ , \qquad \rho u_{x,\mathrm{tt}} = T_{x,x} + T_{xz,z}\ , \qquad D_{x,x} + D_{z,z} = 0\ . \tag{10}$$

All material constants are supposed to be complex, responsible for respective internal losses [7], time dependence is taken as $e^{+\mathrm{i}\omega\mathrm{t}}$. The common solution for plane waves can be expressed as exponential functions of z and x coordinates with respective thickness K_z and lateral ξ_x wave-numbers:

$$\left\{u_z, u_x, \varphi\right\}(x,z) = A_{\{z,x,\varphi\}}\cdot\exp\left(\mathrm{i}\omega\mathrm{t} - \mathrm{i}K_z\cdot z - \mathrm{i}\xi_x\cdot x\right), \tag{11}$$

or in a normalized (to half-thickness *b*) form:

$$\left\{\overline{u}_z, \overline{u}_x, \overline{\varphi}\right\} = \overline{A}_{\{z,x,\varphi\}}\cdot\exp(\mathrm{i}\omega\mathrm{t} - \mathrm{i}K\cdot\overline{z} - \mathrm{i}\xi\cdot\overline{x}), \tag{12}$$

where $\left\{\overline{u}_z, \overline{u}_x, \overline{\varphi}\right\} = \left\{u_z, u_x, \varphi\right\}/b$, $\overline{A}_{\{z,x,\varphi\}} = A_{\{z,x,\varphi\}}/b$, $\left\{K,\xi\right\} = \left\{K_z,\xi_x\right\}\cdot b$, $\left\{\overline{x},\overline{z}\right\} = \left\{x,z\right\}/b$.

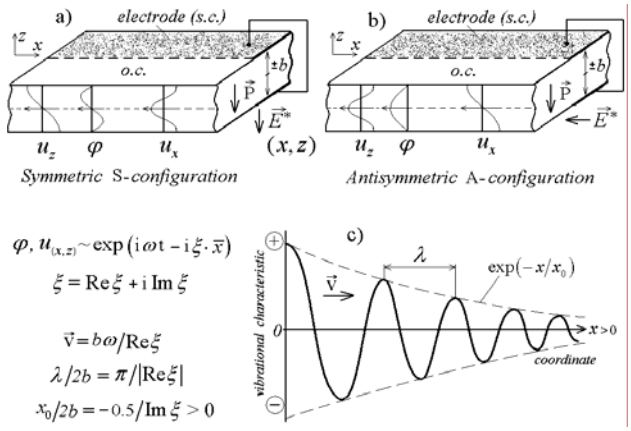

Fig. 2 a,b,c . *An infinite thickness-polarized piezoceramic plate with schematic mechanical and electrical (o.c., s.c.) fields thickness distribution shown for* **S-** *(a) and* **A-** *(b) configurations, and basics for the lateral dispersion parameter ξ with the space decaying wave amplitudes in the major plane (c).*

As schematically shown in Fig. 2c for a simple single vibrational mode, the complex lateral wave-number ξ describes the plane wave with phase velocity $\vec{\mathrm{v}}$ and wave-length λ, exponentially decaying with a characteristic distance x_0. The phase propagation direction depends on the $\mathrm{Re}\,\xi$ sign and, in general, is not indicative of the wave direction of energy transfer defined by the group velocity $\partial\omega/\partial\xi$ [14]. Clearly, energy conservation requires that the real part of $-\mathrm{i}\xi\overline{x}$ be negative, so that negative $\mathrm{Im}\,\xi < 0$ provides physically correct attenuation with zero wave amplitude in the infinity for $x \to +\infty$. Two types of independent orthogonal solutions exist, traditionally called "symmetric" (**S-**configuration) and "antisymmetric" (**A-**configuration) ones, following to the symmetry of the mechanical displacements (u_x) in respect to the middle plane of a plate. Generally both these cases correspond to the elementary *TL*- and *TSh*-vibrations (Fig. 1) excited by the respective longitudinal (thickness-excited) [1] and transverse [5] electric fields $\vec{E}^*$. It is assumed further that the electrode mass does not cause any mechanical perturbations [13].

A. ***Equations of Motion and Charge***

Substituting the equations of piezoelectricity (9) into the motion and charge equations (10), in a matrix form

$$\left|\mathbf{B}\right|\cdot\begin{vmatrix}-\overline{A}_x\\ \overline{A}_z\\ \overline{A}_\varphi\end{vmatrix}=0\ ,\qquad \left|\mathbf{B}\right|=\begin{vmatrix} K\xi\left(c_{44}^E+c_{13}^E\right) & -\left(\omega^2\rho b^2-\xi^2c_{44}^E\right)+K^2c_{33}^E & K^2e_{33}+\xi^2e_{15}\\ \left(\omega^2\rho b^2-\xi^2c_{11}^E\right)-K^2c_{44}^E & -K\xi\left(c_{44}^E+c_{13}^E\right) & -K\xi\left(e_{31}+e_{15}\right)\\ -K\xi\left(e_{31}+e_{15}\right) & -\left(K^2e_{33}+\xi^2e_{15}\right) & K^2\varepsilon_{33}^S+\xi^2\varepsilon_{11}^S\end{vmatrix}\ . \quad (13)$$

The determinant $\left\|\mathbf{B}\right\|=0$ must vanish for non-trivial solutions, which provides a bi-cubic characteristic equation

$$\left(\frac{K^2}{\xi^2}\right)^3-\left(\frac{K^2}{\xi^2}\right)^2\cdot\left\{\frac{c_{11}^E}{c_{44}^E}\left(\frac{\omega^2\rho b^2}{c_{11}^E\ \xi^2}-1\right)+\frac{c^*}{c_{33}^D}\left(\frac{\omega^2\rho b^2}{c^*\ \xi^2}-1\right)+\frac{2e_{33}\left(e_{15}+e_{31}\right)}{\varepsilon_{33}^S c_{33}^D}\left(1+\frac{c_{13}^E}{c_{44}^E}\right)-\left(1-\mathrm{k}_t^2\right)\frac{\left(e_{15}+e_{31}\right)^2}{\varepsilon_{33}^S c_{44}^E}+\frac{c_{44}^E}{c_{33}^D}\left(1+\frac{c_{13}^E}{c_{44}^E}\right)^2\right\}+$$

$$+\left(\frac{K^2}{\xi^2}\right)\cdot\left\{\frac{c_{11}^E}{c_{44}^E}\frac{c^*}{c_{33}^D}\left(\frac{\omega^2\rho b^2}{c_{11}^E\ \xi^2}-1\right)\left(\frac{\omega^2\rho b^2}{c^*\ \xi^2}-1\right)-\frac{c_{44}^E}{c_{33}^D}\frac{\varepsilon_{11}^S}{\varepsilon_{33}^S}\left[1+\frac{\left(e_{15}+e_{31}\right)^2}{\varepsilon_{11}^S c_{44}^E}\right]\left(\frac{\omega^2\rho b^2}{c_{44}^E\ \xi^2}-1\right)-\frac{c_{44}^E}{c_{33}^D}\frac{\varepsilon_{11}^S}{\varepsilon_{33}^S}\left[\mathrm{k}_{15}^2\left(1+2\frac{c_{13}^E}{c_{44}^E}\right)+\frac{2e_{15}e_{31}}{\varepsilon_{11}^S c_{44}^E}\left(1+\frac{c_{13}^E}{c_{44}^E}\right)+\left(1+\frac{c_{13}^E}{c_{44}^E}\right)^2\right]\right\}+$$

$$+\frac{\varepsilon_{11}^S}{\varepsilon_{33}^S}\frac{c_{44}^D}{c_{33}^D}\frac{c_{11}^E}{c_{44}^E}\left(\frac{\omega^2\rho b^2}{c_{11}^E\ \xi^2}-1\right)\left(\frac{\omega^2\rho b^2}{c_{44}^D\ \xi^2}-1\right)\ =\ 0 \qquad (14)$$

where $c_{33}^E=c_{33}^D\left(1-\mathrm{k}_t^2\right)$, $c_{44}^E=c_{44}^D\left(1-\tilde{\mathrm{k}}_{15}^2\right)=c_{44}^D\big/\left(1+\mathrm{k}_{15}^2\right)$ and $c^*=c_{44}^E+c_{33}^E\,\varepsilon_{11}^S\big/\varepsilon_{33}^S+2e_{33}e_{15}\big/\varepsilon_{33}^S$.

This 3-D problem is reduced to a 2-D one with coupled thickness and lateral wave-numbers common for both **S-** and **A-** configurations - there are three roots $K_{(j)}^2(\xi^2,\omega^2)$ with respective sets $\overline{A}_{\{x,z,\varphi\}(j)}$, where $j=1,2,3$ is the order of the roots (Appendix II-2). Solving (13) we particularly have for the amplitudes

$$\overline{A}_{\{z,\,\varphi\}}=\left(K/\xi\right)\cdot\tilde{A}_{\{z,\,\varphi\}}\cdot\overline{A}_x\ ,\qquad \text{where}$$

$$\tilde{A}_z=\xi^2\cdot H^{-1}\left\{\left(e_{31}+e_{15}\right)\left(e_{33}K^2+e_{15}\xi^2\right)+\left(c_{44}^E+c_{13}^E\right)\left(\varepsilon_{33}^S K^2+\varepsilon_{11}^S\xi^2\right)\right\}\ , \qquad (15)$$

$$\tilde{A}_\varphi=\xi^2\cdot H^{-1}\left\{\left(e_{31}+e_{15}\right)\left(\omega^2\rho b^2-c_{33}^E\cdot K^2-c_{44}^E\cdot\xi^2\right)+\left(c_{44}^E+c_{13}^E\right)\left(e_{33}K^2+e_{15}\xi^2\right)\right\}, \qquad (16)$$

$$H=\left(c_{33}^E K^2+c_{44}^E\xi^2-\omega^2\rho b^2\right)\left(\varepsilon_{33}^S K^2+\varepsilon_{11}^S\xi^2\right)+\left(e_{33}K^2+e_{15}\xi^2\right)^2 \qquad (17)$$

For further eigen-values consideration it is supposed $\overline{A}_x=1$ in (15)-(17), so that $\overline{A}_{\{z,\,\varphi\}}=\left(K/\xi\right)\cdot\tilde{A}_{\{z,\,\varphi\}}$.

B. ***Boundary Conditions for Short-Circuit and Open-Circuit Regimes***

The boundary conditions on major surfaces for mechanical stress are

$$\overline{T}_z\big|_{\overline{z}=\pm1}=0\ ,\qquad \overline{T}_{xz}\big|_{\overline{z}=\pm1}=0\ , \qquad (18)$$

and classical limit s.c. (ideal short-circuited electrodes) and o.c. (electrodeless plate with the electric potential floating freely and the current vanishing) electrical boundary conditions are

$$\overline{\varphi}\big|_{\overline{z}=\pm1}=0\quad \text{(s.c.)}\ ,\qquad \overline{D}_z\big|_{\overline{z}=\pm1}=0\quad \text{(o.c.)}\ . \qquad (19)$$

The solutions for the **S-**configuration (basic *TL*-mode) are expressed in the form

$$\overline{u}_x=-\sin(\xi\,\overline{x})\cdot\sum\nolimits_j^3 L_j\,\overline{A}_{x(j)}\cdot\cos(K_{(j)}\cdot\overline{z})\ ,\qquad \overline{u}_z=\cos(\xi\,\overline{x})\cdot\sum\nolimits_j^3 L_j\,\overline{A}_{z(j)}\cdot\sin(K_{(j)}\cdot\overline{z}),$$

$$\bar{\varphi} = \cos(\xi\,\bar{x})\cdot\sum\nolimits_j^3 L_j\,\bar{A}_{\varphi(j)}\cdot\sin(K_{(j)}\cdot\bar{z})\ , \tag{20}$$

and the solutions for the **A-**configuration (basic *TSh*-mode) are

$$\bar{u}_x = \cos(\xi\,\bar{x})\cdot\sum\nolimits_j^3 L_j\,\bar{A}_{x(j)}\cdot\sin(K_{(j)}\cdot\bar{z})\ ,\qquad \bar{u}_z = -\sin(\xi\,\bar{x})\cdot\sum\nolimits_j^3 L_j\,\bar{A}_{z(j)}\cdot\cos(K_{(j)}\cdot\bar{z})\,,$$

$$\bar{\varphi} = -\sin(\xi\,\bar{x})\cdot\sum\nolimits_j^3 L_j\,\bar{A}_{\varphi(j)}\cdot\cos(K_{(j)}\cdot\bar{z})\ , \tag{21}$$

The dimensionless L_j weighting coefficients mean equal relative shares of partial solutions with $A_{\{z,\,\varphi\}(j)}$ amplitudes in each characteristic (20),(21). For the **S-** or **A-** ($\mathrm{S|A}$) cases, with respectively the s.c. and o.c. conditions on the electrodes

$$\left\|\begin{matrix}\varphi\\ T_z\\ T_{xz}\end{matrix}\right\|_{\bar{z}=\pm 1} = 0\ ,\ \text{then}\ \left|\mathbf{\Phi}\left\langle \mathrm{S|A}\right\rangle\right|\cdot\left|\begin{matrix}L_1\\ L_2\\ L_3\end{matrix}\right| = 0\,,\qquad \text{and}\qquad \left\|\begin{matrix}D_z\\ T_z\\ T_{xz}\end{matrix}\right\|_{\bar{z}=\pm 1} = 0\ ,\ \text{then}\ \left|\mathbf{G}\left\langle \mathrm{S|A}\right\rangle\right|\cdot\left|\begin{matrix}L_1\\ L_2\\ L_3\end{matrix}\right| = 0\ . \tag{22}$$

To satisfy the above conditions and extract the primary non-trivial solutions $\xi^2 = (\zeta_m^{sc,\,oc})^2(\omega^2)$, the respective determinants of the boundary-conditions characteristic matrices must vanish

$$\left\|\mathbf{\Phi}\left\langle \mathrm{S|A}\right\rangle\right\| = 0\quad \text{(s.c.)}\qquad \text{and}\qquad \left\|\mathbf{G}\left\langle \mathrm{S|A}\right\rangle\right\| = 0\quad \text{(o.c.)}. \tag{23}$$

Conducting elementary transformations for the determinants, we have:

$$\left\|\mathbf{\Phi}\left\langle \mathrm{S|A}\right\rangle\right\| = \left\|\mathbf{M}\left\langle \mathrm{S|A}\right\rangle\right\|\cdot\frac{b}{\varepsilon_{33}^S}\cdot\frac{1}{\xi^2}\cdot\left\{\frac{c_{44}^E c_{33}^E\, e_{33}}{b^3}\right\}\ \text{ and }\ \left\|\mathbf{G}\left\langle \mathrm{S|A}\right\rangle\right\| = \left\|\mathbf{N}\left\langle \mathrm{S|A}\right\rangle\right\|\cdot\frac{1}{\xi^2}\cdot\left\{\frac{c_{44}^E c_{33}^E\, e_{33}}{b^3}\right\}\ , \tag{24-25}$$

where for the $\mathrm{S|A}$ - configurations:

$$\mathbf{M}\left\langle \mathrm{S}\middle|\mathrm{A}\right\rangle_{1j} = \mp\frac{\varepsilon_{33}^S}{e_{33}}\cdot K_{(j)}\,\tilde{A}_{\varphi\,(j)}\cdot\left\langle \sin\middle|\cos\right\rangle(K_{(j)})\ ,$$

$$\mathbf{N}\left\langle \mathrm{S}\middle|\mathrm{A}\right\rangle_{1j} = \left[\frac{e_{31}}{e_{33}}\xi^2 - K_{(j)}^2\cdot\tilde{A}_{z\,(j)} + \frac{\varepsilon_{33}^S}{e_{33}}\cdot K_{(j)}^2\cdot\tilde{A}_{\varphi\,(j)}\right]\cdot\left\langle \cos\middle|\sin\right\rangle(K_{(j)})\ ,$$

$$\mathbf{M}\left\langle \mathrm{S}\middle|\mathrm{A}\right\rangle_{2j} = \mathbf{N}\left\langle \mathrm{S}\middle|\mathrm{A}\right\rangle_{2j} = \left[\frac{c_{13}^E}{c_{33}^E}\xi^2 - K_{(j)}^2\cdot\tilde{A}_{z\,(j)} - \frac{e_{33}}{c_{33}^E}\cdot K_{(j)}^2\cdot\tilde{A}_{\varphi\,(j)}\right]\cdot\left\langle \cos\middle|\sin\right\rangle(K_{(j)})\,,$$

$$\mathbf{M}\left\langle \mathrm{S}\middle|\mathrm{A}\right\rangle_{3j} = \mathbf{N}\left\langle \mathrm{S}\middle|\mathrm{A}\right\rangle_{3j} = \left[1 - \tilde{A}_{z\,(j)} - \frac{e_{15}}{c_{44}^E}\cdot\tilde{A}_{\varphi\,(j)}\right]\cdot K_{(j)}\cdot\left\langle \sin\middle|\cos\right\rangle(K_{(j)})\ . \tag{26}$$

The determinants of the matrices $\left|\mathbf{M}\left\langle \mathrm{S|A}\right\rangle\right|$ and $\left|\mathbf{N}\left\langle \mathrm{S|A}\right\rangle\right|$ have the same dimension, and their corresponding pairs, $\left\|\mathbf{M}\mathrm{S}\right\|$ and $\left\|\mathbf{N}\mathrm{S}\right\|$, $\left\|\mathbf{M}\mathrm{A}\right\|\cdot\xi$ and $\left\|\mathbf{N}\mathrm{A}\right\|\cdot\xi^{-1}$, are finite at $\xi\to 0$. Solving (14),(23) is a problem about eigen-values, or eigen-states, which provides the relationship between frequency ω and lateral wave-number ζ known as a dispersion relation. Final original solutions are symmetric in respect to the lateral wave-number and are expressed in a mathematically correct form $\zeta_m^2(\omega^2)$, while for its application in the wave propagation physical analysis it needs to be transformed into $\zeta_m(\omega)$ with the physical limitations mentioned. Note, as a further stage of analysis, for a real finite PR plate with a lateral boundary, its coupled frequency

spectrum can be found in a similar procedure with equal weighting shares of all partial solutions related to the roots ζ_m in the m-summation for planar directions [26].

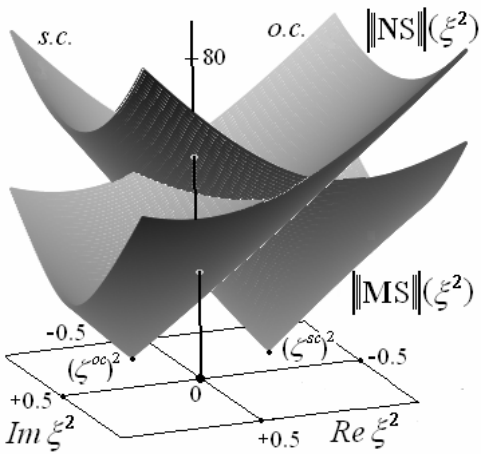

Fig. 3. *Typical surfaces of the* **S-***configuration dispersion matrices (module of the complex determinants (24),(25)) in the* ξ^2*-plane for* $\left|\xi^2\right|<1$ *near the fundamental TL antiresonance with* $\chi_{(TL)}=-0.03$ (70). *PZT-5A,* $Q=100$.

C. *Characteristic Matrices at the Dispersion Origin - The Theorem*

Obviously, the characteristic dispersion matrices at the origin ($\xi=0$) refer to an elementary 1-D case. The existence of such a presentation is formulated as a general **Theorem**, which is stated as follows:

Theorem. The ratio of two matrix determinants constructed from the boundary condition equations for a finite piezoelectric plate with the open-circuited and short-circuited major surfaces, with respectively $\left|\mathbf{G}\left\langle \mathrm{S|A}\right\rangle\right|$ and $\left|\mathbf{\Phi}\left\langle \mathrm{S|A}\right\rangle\right|$ characteristic matrices in the symmetric **S-**configuration (antisymmetric **A-**configuration), in the limit of zero lateral wave-number $\xi\to 0$ is equal to the normalized complex admittance $\widehat{\mathrm{Y}}$ of the basic elementary mode, particularly:
for the **S-**configuration with the basic S-*TL* mode

$$\left(-\frac{b}{\varepsilon_{33}^{S}}\right)\cdot\left(\frac{\left\|\mathbf{G}\mathrm{S}\right\|}{\left\|\mathbf{\Phi}\mathrm{S}\right\|}\right)\Bigg|_{\xi\to 0}=\left\{1-\mathrm{k}_t^2\,\frac{\tan\left(\omega b\sqrt{\rho/c_{33}^{D}}\right)}{\omega b\sqrt{\rho/c_{33}^{D}}}\right\}^{-1}\equiv -\mathrm{i}\cdot\widehat{\mathrm{Y}}_{\langle TL\rangle}\ , \tag{27}$$

for the **A-**configuration with the basic A-*TSh* mode

$$\left(-\frac{b}{\varepsilon_{11}^{S}}\right)\cdot\left(\xi^{-2}\frac{\left\|\mathbf{G}\mathrm{A}\right\|}{\left\|\mathbf{\Phi}\mathrm{A}\right\|}\right)\Bigg|_{\xi\to 0}=1+\mathrm{k}_{15}^2\,\frac{\tan\left(\omega b\sqrt{\rho/c_{44}^{E}}\right)}{\omega b\sqrt{\rho/c_{44}^{E}}}\equiv -\mathrm{i}\cdot\widehat{\mathrm{Y}}_{\langle TSh\rangle}\ . \tag{28}$$

The proof of the Theorem is presented in Appendix I. Typical surfaces of the o.c. and s.c. dispersion matrices in the ξ^2-plane are shown in Fig. 3, and generally they represent right cones (linear) near the origin at $\left|\xi^2\right|<1$. Basics for the Theorem are clear from the initial equations (9)-(11), where for $\xi\to 0$ the only elementary *TL*-mode parameters (c_{33}^{E}, e_{33}, ε_{33}^{S}) are remaining (ξ is a factor with all other material constants). In the contrary, the initial equations, being multiple or divided by ξ (or by ξ^2 totally for the matrix ratio (28)), have the only elementary *TSh*-mode parameters dominant and remaining at $\xi\to 0$.

D. *Piezoceramic Plate with Electrodes of Finite Conductivity*

D1. *Electrical Boundary Condition for a Dielectric Plate with Resistive Electrodes*

The basic equation describing the electrical potential distribution $\varphi(x)$ along the resistive non-inertial electrodes with the unit conductivity σ and thickness h_{el} can be established from the continuity of currents along the electrode (Fig. 4) - for an elementary electrode cell with length dx (unit width) the difference of the currents on its left I_1 and right I_2 sides equals the current I_3 caused by the surface normal electrical inductance $D_z\big|_{\overline{z}=\pm 1}$. On the boundary "dielectric – resistive electrode", there are equal tangent components of the electric field and equal normal components of the electrical induction (density of free charges q) [23]. Note the positive *z*-direction is opposed to the circuitry loop direction in the plate, as shown in Fig. 4. Inside the upper electrode ($\overline{z}=1$) for the established space-coordinates, $I_1 - I_2 = I_3$ with $E_x = -\varphi_{,x}$, then:

$$I_1 - I_2 = \sigma h_{el}\left(E_{x_1} - E_{x_2}\right) = \sigma h_{el}\cdot\varphi_{+,\,xx}\cdot dx\ , \qquad I_3 = q_{+,\,\mathrm{t}} = -D_{z,\,\mathrm{t}}\cdot dx = -\mathrm{i}\omega D_z\cdot dx\ , \tag{29}$$

$$\varphi_{+,\,xx} + \mathrm{i}\omega\breve{R}_{el}\cdot D_z = 0\ , \tag{30}$$

where $\breve{R}_{el} = 1/\sigma h_{el}$ is the unit surface running electrode resistance. As a general equation for both electrodes

$$\pm\overline{\varphi}_{,\,xx}\Big|_{\overline{z}=\pm 1} = -\mathrm{i}\omega\breve{R}_{el}\cdot\overline{D}_z\Big|_{\overline{z}=\pm 1}\ , \tag{31}$$

with $\varphi\big|_{\overline{z}=+1} = -\varphi\big|_{\overline{z}=-1}$ and $D_z\big|_{\overline{z}=+1} = D_z\big|_{\overline{z}=-1}$ for symmetric **S**-configuration ,

and $\varphi\big|_{\overline{z}=+1} = \varphi\big|_{\overline{z}=-1}$ and $D_z\big|_{\overline{z}=+1} = -D_z\big|_{\overline{z}=-1}$ for antisymmetric **A**-configuration.

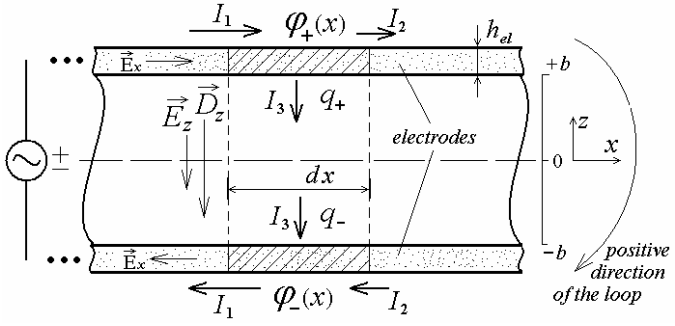

Fig. 4. *Schematic of the electric field configuration in a dielectric plate (bulk field $\vec{E}_z$) with thin layer electrodes (surface field $\vec{E}_x$).*

D2. "*Discrete" R-C (R-Z) Model – Introductory Parameters*

The following introductory consideration covers the discrete *R-C* and *R-Z* simple models (like a classical 3-1 piezocomposite), with respectively capacitive admittance and uncoupled elementary bulk impedance of the *TL* vibrations in the **S**-configuration, to explain further the results of general analysis. It is the case when the admittance of a plate segment at any frequency is strictly proportional to its square, so no lateral electric field components occur inside the plate body [28]. As $I_3 = \mathrm{i}\omega\varphi_+\cdot 2\breve{C}dx$ and $I_3 = 2\varphi_+\cdot\breve{Z}^{-1}dx$, respectively, where $\breve{C}\ \left(\breve{C}_0 = \varepsilon_{33}^S/2b\right)$ and $\breve{Z}^{-1} = \omega\breve{C}_0\widehat{\mathrm{Y}}_{\langle TL\rangle}$ are the unit surface running dielectric capacitance and *TL*-

mode elementary admittance (1), then according to (30) for $\overline{\varphi} = \varphi_{\pm}/b = \overline{\varphi}\big|_{\overline{x}=\pm 1}$:

$$\overline{\varphi}_{,\overline{x}\,\overline{x}} + \mu^2 \cdot \overline{\varphi} = 0 \qquad \text{with} \tag{32}$$

$$\mu^2 = -\mathrm{i}2b^2\omega\breve{C}\breve{R}_{el} \qquad \text{and} \qquad \mu^2 = -b^2\, 2\breve{R}_{el}/\breve{Z} \tag{33}$$

respectively for a capacitive dielectric body and for a generalized "uncoupled" case – all as discrete elements. The common solution for the surface potential is a set of exponential functions $\overline{\varphi}(\overline{x}) = B\exp(-\mathrm{i}\mu\cdot\overline{x})$ with two symmetric roots $\pm\mu$, where *B* is a coefficient.

For a capacitive case $\mu^2 = -2\mathrm{i}\,P^2$, then in the units of $P \equiv b\sqrt{\omega\breve{C}\breve{R}_{el}} > 0$ there are roots $\pm(1-\mathrm{i})P$. For an infinite plate with $x > 0$ and $x < 0$, and for a finite plate with a planar boundary, they are both in force. For an infinite plate with $x > 0$ (for simplicity and certainty), the only physically correct solution provides fully decaying wave in the infinity with $\mathrm{Im}\,\mu < 0$:

$$\mu = +(1-\mathrm{i})b\sqrt{\omega\breve{C}\breve{R}_{el}} \equiv \sqrt{\omega/\omega_0}\cdot P_0 - \mathrm{i}\sqrt{\omega/\omega_0}\cdot P_0 = P - \mathrm{i}\,P \quad , \tag{34}$$

where $P_0^2 = b^2\omega_0\breve{C}\breve{R}_{el} \sim (\omega_0 b)\cdot(\varepsilon_{33}^S/\sigma)$, ω_0 is some reference frequency (resonance). Only dispersion roots under such conditions will be further considered. Such electric field distribution corresponds to a case of phase-shift potential rotation along the electrode surface as a wave with the wave-number $\lambda/2b = \pi/P$, decay distance $x_0/2b = 0.5/P$ and phase velocity $\tilde{\mathrm{v}} = +\omega b/P$ (Fig. 2c).

Analogously for the "uncoupled" *TL* elementary mode case, in a set of two roots $\mu = \mathrm{Re}\,\mu + \mathrm{i}\,\mathrm{Im}\,\mu =$ $= \pm\sqrt{-b^2\, 2\breve{R}_{el}/\breve{Z}}$, the only one is taken into account with negative $\mathrm{Im}\,\mu < 0$. As the elementary PR admittance can be represented as $\breve{Z}^{-1} = \mathrm{Re}\,\breve{Z}^{-1} + \mathrm{i}\,\mathrm{Im}\,\breve{Z}^{-1} = \left|\breve{Z}\right|^{-1} e^{\mathrm{i}\phi}$, where $\phi \in (-\pi/2, +\pi/2)$ is its phase, then

$$\mu = -e^{\mathrm{i}0.5(\pi+\phi)}\cdot b\sqrt{2\breve{R}_{el}\left|\breve{Z}\right|^{-1}} \quad . \tag{35}$$

The PR impedance near the resonance has capacitive, inductive, or active character. At the *TL* resonance (*r*) or antiresonance (*a*) frequencies, when the elementary PR impedance is active $\breve{Z} = \breve{R}_{r(a)}$, the distribution parameter $\mu = -\mathrm{i}\,b\sqrt{2\breve{R}_{el}/\breve{R}_{r(a)}}$ is pure imaginary. The inductive character of $\breve{Z}$ provides the root $\mu \propto (-1-\mathrm{i})$ with $\mathrm{Im}\,\mu < 0$ and hence $\mathrm{Re}\,\mu < 0$ (opposite phase velocity to the capacitive case). From the three characteristic cases, it follows that for $x > 0$ the wave is always decaying, it travels in positive *x*-direction outside the PR resonance-antiresonance frequency interval (capacitive case with $\mathrm{Re}\,\mu > 0$), and in opposite negative *x*-direction inside the resonance-antiresonance frequency interval (inductive case with $\mathrm{Re}\,\mu < 0$). Such a transition is continuous on frequency, so that the case with $\mathrm{Re}\,\mu = 0$ corresponds to the resonance or antiresonance frequency (decaying distribution without space oscillations).

D3. ***Dielectric (Non-Piezoelectric) "Continuous" Plate with Resistive Electrodes***

For a pure electrical case with zero piezoeffect in a dielectric plate, the actual thickness and lateral electric field distribution can be described with a similar eigen-value approach (9)-(11),(20),(21),(31) providing the relationship for the thickness and lateral wave-numbers $K^2 + \nu\,\xi^2 = 0$ from the charge equation, where $\nu = \varepsilon_{11}/\varepsilon_{33}$ is the parameter of dielectric anisotropy. Finally there are two orthogonal equations for the **S**- and **A**-configurations, respectively

$$\xi \cdot \tan\left(\mathrm{i}\xi\sqrt{\nu}\right) = 2P^2\sqrt{\nu} \qquad \text{and} \qquad \xi \cdot \cot\left(\mathrm{i}\xi\sqrt{\nu}\right) = -2P^2\sqrt{\nu} \tag{36}$$

with $P^2 = b^2\omega\breve{C}_{33}\breve{R}_{el} \in (0,\infty)$. There are two infinite sets of solutions $\xi = \zeta_m$ with respectively {odd $m\hat{\Phi}$ } branches in **S**-configuration, and {even $m\hat{\Phi}$ } branches in **A**-configuration, $m = 1,2,3,4...$ (Figs. 5,6). For the lowest $1\hat{\Phi}$ branch at $P << 1$, there is $\zeta_{\{1\hat{\Phi}\}} \cong (1-\mathrm{i})P$ coinciding with those of the discrete model. For the branch at $P \to \infty$, the lateral field distribution is as $\sim \exp(-0.5\pi\bar{x})$ with a characteristic decay distance $\bar{x}_0 \simeq 1$ related to the edge-effect of field distribution from a dot surface charge.

D4. ***Piezoceramic Plate with Resistive Electrodes – Dispersion Equation***

In the case of resistive electrodes, each elementary unit plate volume is acoustically coupled with and electrically loaded by surrounding regions. From (12),(31) it follows a general electrical boundary condition for both **S**- and **A**-configurations corresponding to resistive electrodes and taking an intermediate disposition between classical o.c. and s.c. regimes:

$$\xi^2 \cdot \left(\pm\bar{\varphi}\big|_{\bar{z}=\pm 1}\right) - \mathrm{i}\omega\breve{R}_{el}b^2 \cdot \bar{D}_{\bar{z}}\Big|_{\bar{z}=\pm 1} = 0 \ . \tag{37}$$

Then, together with the mechanical boundary conditions (22), the dispersion equation is:

$$\xi^2 \cdot \left\|\mathbf{\Phi}\left\langle \mathrm{S}|\mathrm{A}\right\rangle\right\| - \mathrm{i}b^2\omega\breve{R}_{el} \cdot \left\|\mathbf{G}\left\langle \mathrm{S}|\mathrm{A}\right\rangle\right\| = 0 \ , \quad \text{or} \tag{38}$$

$$\xi^2 \cdot \left\|\mathbf{M}\left\langle \mathrm{S}|\mathrm{A}\right\rangle\right\| - 2\,\mathrm{i}\,P^2 \cdot \left\|\mathbf{N}\left\langle \mathrm{S}|\mathrm{A}\right\rangle\right\| = 0 \tag{39}$$

for corresponding **S**- (basic *TL*-mode) and **A**- (basic *TSh*-mode) configurations, where $\breve{R}_{el} = 1/h_{el}\sigma$, $\breve{C}_0 = \varepsilon_{33}^S/2b$, $P^2 = b^2\omega\breve{C}_0\breve{R}_{el} = \omega\tau$, $\tau = b^2\breve{R}_{el}\breve{C}_0$ is the dielectric relaxation time. The matrix determinants (39) provide roots $\xi^2 = \zeta_m^2(P)$ with their limit values for each branch $\zeta_m(P \to 0) = \zeta_m^{sc}$ of s.c. and $\zeta_m(P \to \infty) = \zeta_m^{oc}$ of o.c. classical conditions.

According to the Theorem, for sufficiently small $\left|\xi^2\right| << 1$, we have (38) a root for the **S**-configuration:

$$\zeta_{\{1\hat{\Phi}\}}^2 \cong \mathrm{i}b^2\omega\breve{R}_{el} \cdot \frac{\left\|\mathbf{G}\mathrm{S}\right\|}{\left\|\mathbf{\Phi}\mathrm{S}\right\|}\bigg|_{\xi^2 \to 0} = -b^2\omega\breve{R}_{el} \cdot \left(\varepsilon_{33}^S/b\right)\hat{\mathrm{Y}}_{\langle TL\rangle} = -b^2\,2\breve{R}_{el}/\breve{Z} \equiv \mu^2 \ , \tag{40}$$

so that it coincides with (33) for an "uncoupled discrete case", is linear proportional to $\breve{R}_{el}$ and elementary *TL* admittance $\breve{Z}^{-1}$, so that the origin $\xi = 0$ is a dispersion solution at $\breve{R}_{el} \to 0$ (ideal electrode) and forms a dispersion branch $\zeta^{sc}_{\{1\Phi\}} = 0$. For the **A**-configuration $\mathrm{i}b^2\omega\breve{R}_{el}\cdot\left(\xi^{-2}\left\|\mathbf{G}\mathrm{A}\right\|/\left\|\mathbf{\Phi}\mathrm{A}\right\|\right) = 1$, so that there is no solution at the origin $\xi = 0$ at $\breve{R}_{el} \to 0$.

According to (37), the surface free charges density occurs on the electrode accompanying the wave propagation $q = -D_z\big|_{\bar{z}=+1} = \mathrm{i}\left(\varphi\cdot\breve{C}_0\right)\left(\zeta_m/P\right)^2$, where $\left(\varphi\cdot\breve{C}_0\right)$ is the pure capacitive charge. Note that at $P \to 0$ the space-periodic potential amplitude $\varphi \to 0$ on the getting equipotential electrode surface.

III. RESULTS of DISPERSION ANALYSIS and DISCUSSION

The effects of internal dissipation and electrode resistivity in the range from the ideal electrodes (s.c.) condition through the *RC*-type relaxation resonance up to fully electrodeless (o.c.) condition on the wave propagation are examined in detail for PZT ceramics with three characteristic values of the *TL*-mode energy-trap figure-of-merit $\dot{c}^D_{33}/\dot{c}^E_{44}\left(\dot{c}^E_{33}/\dot{c}^E_{44}\right) = 3.0(2.4)$, 4.4(3.5), 7.0(5.4) – less, near equal and higher 4 – when the second harmonic spurious *TSh* resonance in the **S**-configuration lies respectively below the fundamental *TL* resonance, inside its resonance-antiresonance frequency interval, and above the *TL* antiresonance. The results of calculations of the lateral dimensionless wave-number $\zeta_m(\omega, P)$ dispersion branches up to as much as 2π in magnitude in their combined frequency and dissipation dependences for three corresponding piezoceramics are presented in MULTIMEDIA files: M1<S|A> for $PbTiO_3$, M2<S|A> for PZT-35, M3<S|A> for PZT-5A [1],[2], respectively for **S**- and **A**-configurations. A low-frequency cumulative fragment for PZT-5A is presented in Fig. 5 a,b. In the conducted analysis the only c^D_{ij} elastic constants with their quality factors $Q = Q^{E,D}_{ij}$ were used as complex, while the other parameters involved in (9),(14) were taken as real, nevertheless providing the dielectric ε^T_{ij} and piezoelectric d_{ij} constants complex as well as in the traditional approach [7]. The following frequency parameters $\omega^2\rho b^2 = (1+\chi)^2(\pi/2)^2\dot{c}_{ij}$ of the resonance frequency displacement $\chi = \omega/\omega_0 - 1$ were used, where $\omega_0 = (\pi/2b)\sqrt{\dot{c}_{ij}/\rho}$ with $\dot{c}_{ij} = \dot{c}^D_{33}$, $\chi = \chi_{(TL:1)}$ for **S**- (1), and $\dot{c}_{ij} = \dot{c}^E_{44}$, $\chi = \chi_{(TSh:2)}$ for **A**- (2) configurations, corresponding to the major soft (*TSh*) and hard (*TL*) vibrational mode types [6],[8]. The "resonance" and "antiresonance" terms primarily refer here to the elementary normalized admittance $\widehat{\mathrm{Y}}_{\langle TL,\,TSh\rangle}$ for certainty, accompanying with $\zeta^{oc,\,sc}_m \to 0$ of a corresponding branch as shown.

There are planar ($\widehat{R}$), odd-order *TL* ($m\widehat{E}^-$) and even-order *TSh* ($m\widehat{E}^+$) mode branches for **S**-, and flexure ($\widehat{F}$), odd-order *TSh* ($m\widehat{E}^+$) and even-order *TL* ($m\widehat{E}^-$) mode branches for **A**-configurations, and respective potential branches ($m\widehat{\Phi}$). As the planar phase velocity of a wave is $\vec{\mathrm{v}} = b\,\omega/\mathrm{Re}\,\zeta$, then $\mathrm{Re}\,\zeta > 0$ corres-

ponds to forward-wave modes, traveling in positive direction, and $\mathrm{Re}\,\zeta < 0$ refers to backward-wave modes.

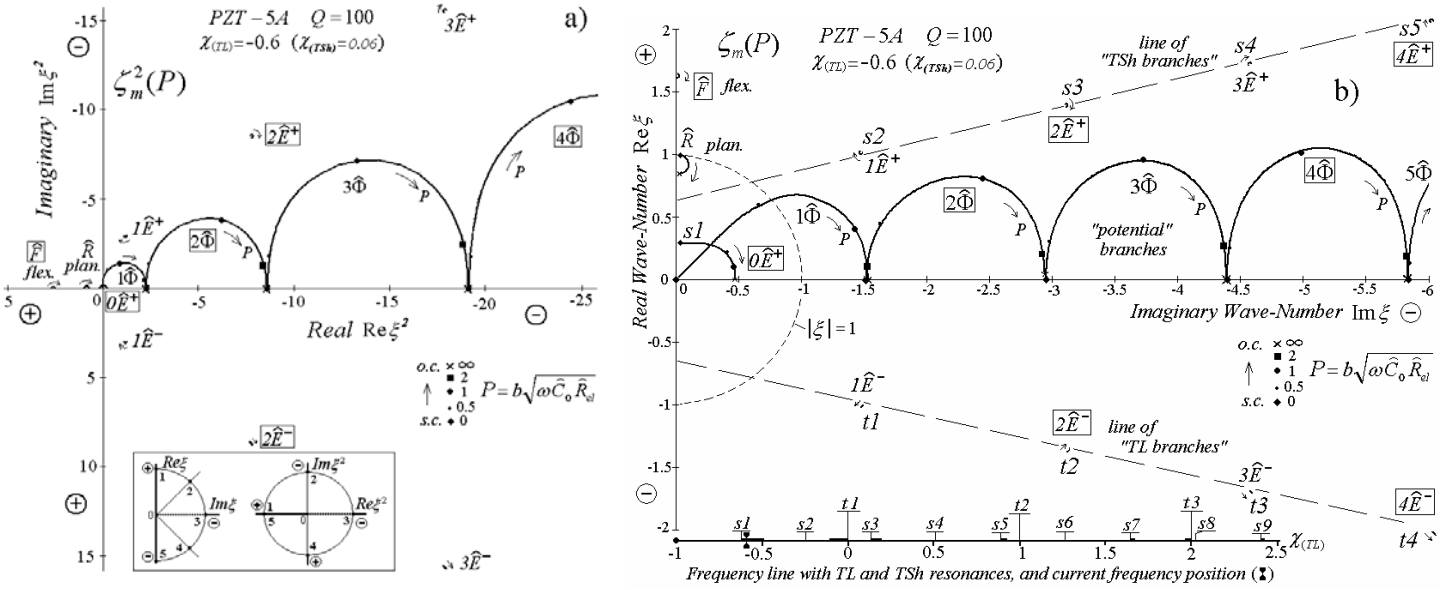

Fig. 5 a,b . *Cumulative dispersion branches* $\zeta_m^2(P)$ *(a) and* $\zeta_m(P)$ *(b) for both* **S-** *and* **A-***configurations of a lossy PR plate with resistive electrodes (39) at a frequency near the fundamental "*A*-TSh:1" resonance (PZT-5A). Inserted (a) shows a transformation from complex* ξ^2*- to* ξ*-plane with major axes. The branches with notation in a frame relate to the* **A-***configuration, without a frame – to the* **S-***configuration. The "*$t\,n_{TL}$*" and "*$s\,n_{TSh}$*" branches are related to and form the respective n-order TL and TSh resonances. The* $|\xi| \le 1$ *circle (b) is the scope of the Statement (Chapter III-B).*

The ξ^2-plane representation of dispersion is more important for the mathematical analysis as a primary parameter of characteristic functions of certain symmetry, while the ξ-plane representation is more informative for practical applications in the wave propagation analysis. For the last one, mathematically, two solutions are close to each other with maximum interaction, when either they are close in the ξ-plane, or when they are both pure real (Fig. 5a, inserted). Particularly as seen from the MULTIMEDIA files, the edge mode [10] is a result of the $1\widehat{E}^-$ *TL* and $1\widehat{E}^+$ *TSh* branches interaction. Note that according to conform reflections, a "half circle-to-circle" transformation takes place for a square function, so it seems there is no restriction on the ξ^2 sign. Major branches exhibit a clock-wise "rotation" with the resistance parameter *P* increasing. Comparing the presented branches classification with those in the classical Lamb wave description [14] for the modes propagating in the plate with predominantly real (lossless) wave-numbers, each branch $m\widehat{E}^{\pm}$ corresponds to a certain Lamb mode for the frequencies higher the corresponding thickness resonance, with the following relationships of notations: $\widehat{R} \to \mathrm{S}_0$ Lamb mode, $1\widehat{E}^{\pm} \to \mathrm{S}_{<1|2>}$, … for **S-** , and $\widehat{F} \to \mathrm{A}_0$ Lamb mode, $0\widehat{E}^{+} \to \mathrm{A}_1$, $2\widehat{E}^{\pm} \to \mathrm{A}_{<2|3,4>}$, … for **A-**configuration, depending on the $\dot{c}_{33}^D / \dot{c}_{44}^E$ parameter mostly for higher-order modes.

A. ***General Properties of Dispersion Surfaces***

The initial position of the dispersion characteristics can be considered as corresponding to $\omega \to 0$ for the limit s.c. and o.c. regimes and is close to presented in Fig. 5. According to the motion and charge equations (14), there are three roots $\left(K^2/\xi^2\right)\Big|_{\omega\to 0}$ independent of ξ^2 at $\omega \to 0$: the first root $\simeq -1+\left(\sim \mathrm{i}/Q\right)$ and two other complex conjugate roots $\simeq -1 \pm \mathrm{i}\cdot 0.5$. The exact solutions differing in the limits $\sim \pm 0.2$ depend on elastic, dielectric, and piezoelectric anisotropy. Then, as can be seen from the boundary conditions, there are several infinite sets of eigen solutions (branches) ζ_m^2. One set related to the first root provides the s.c. and o.c. solutions of "electrical potential" branches $\{m\hat{\Phi}\}$ – particularly for the **S**-configuration $\zeta_m^{sc} \simeq -\mathrm{i}(m-1)\pi/2$ when $\sin K_{(1)} \simeq 0$, and $\zeta_m^{oc} \simeq -\mathrm{i}\, m\pi/2$ when respectively $\cos K_{(1)} \simeq 0$ in the characteristic matrices (24)-(26), where $m = 1,3,5...\infty$ is the branch order. Similar s.c. and o.c. "potential" solutions exist for the **A**-configuration with accordingly zero cosine/sine and even branch orders $m = 2,4,6...\infty$. The other two conjugate roots basically provide two infinite sets of dispersion solutions for the respective *TSh* and *TL* complex branches $\{m\hat{E}^{\pm}\}$ with near equal $\mathrm{Im}\,\zeta_m$ in each pair at least for $\omega << \omega_0$ of any thickness (*TL*, *TSh*) resonance (Fig. 5b), so that:

$$\zeta_{\{m\hat{\Phi}\}}^{oc} \cong \zeta_{\{(m+1)\hat{\Phi}\}}^{sc} \cong \mathrm{i}\cdot \mathrm{Im}\,\zeta_{\{m\hat{E}^{\pm}\}}^{sc,\,oc} \cong -\mathrm{i}\, m\pi/2\ , \tag{41}$$

where $m = 1,2,3...$, with $\zeta_{\{1\hat{\Phi}\}}^{sc} = 0$ and

$$\mathrm{Re}\,\zeta_{\{m\hat{E}^{\pm}\}}^{sc,\,oc} \simeq \pm\left(\pi/4\right)\left(1+0.4\,m\right). \tag{42}$$

As the basic frequency factor in (14) is $(\omega^2\rho b^2/c_{ij} - \xi^2)$, with frequency increasing, the characteristic value $|\xi| \approx 0.5\pi\left(\omega/\omega_0\right)$, where ω_0 is a fundamental thickness resonance, is a measure of consecutive distortion of the dispersion pattern formed by the *TL* and *TSh* branches, when the $m \approx \omega/\omega_0$ order $\{m\hat{E}^{\pm}\}$ branches start moving toward the ξ-origin to form further the corresponding thickness resonances (see M1,2,3<S|A> files). Considering the electrode resistivity as a factor of the characteristic relaxation time $\tau = b^2\breve{R}_{el}\breve{C}_0$ in $P^2 = \omega\tau$ (39), the real and imaginary parts of $\zeta_m(P) = \mathrm{Re}\,\zeta_m(P) + \mathrm{i}\,\mathrm{Im}\,\zeta_m(P)$ are found to follow the universal scaling formula – the Cole-Cole diagram of the lateral complex wave-numbers remains very close to a semicircle for the $\{\hat{R}\}$, $\{\hat{F}\}$, and $\{m\hat{\Phi}\}$ with $m \geq 1$ branches.

The relaxation dependences of the planar $\{\hat{R}\}(P)$ and flexure $\{\hat{F}\}(P)$ branches are found the following:

$$\zeta_{\{\hat{R},\hat{F}\}}(P) \cong \mathrm{Re}\,\zeta_{\{\hat{R},\hat{F}\}}^{oc} + \Lambda\frac{1}{1+\mathrm{i}\,\omega\tau} = \mathrm{Re}\,\zeta_{\{\hat{R},\hat{F}\}}^{sc} - \Lambda\frac{\mathrm{i}\,\omega\tau}{1+\mathrm{i}\,\omega\tau}\ , \tag{43}$$

where $\Lambda = \mathrm{Re}\,\zeta_{\{\hat{R},\hat{F}\}}^{sc} - \mathrm{Re}\,\zeta_{\{\hat{R},\hat{F}\}}^{oc} \cong 0.5\,\mathrm{k}^2\,\mathrm{Re}\,\zeta_{\{\hat{R},\hat{F}\}}^{sc}$ is the semicircle width, k is the corresponding CEMC. Note that for the branches at $P^2 = \omega\tau \approx 1$, the maximum wave energy loss inside the electrodes takes place.

Such an effect becomes obvious from the elementary planar mode classical description (as S_0, A_0 Lamb waves): the dimensionless lateral wave-numbers of a planar mode $(\zeta^{sc})^2 = \omega^2 \rho b^2 s^E$, $(\zeta^{oc})^2 \cong \omega^2 \rho b^2 s^D$, where $s^D = s^E(1-\mathrm{k}^2)$, $s^{E,D} = \dot{s}^{E,D}(1-\mathrm{i}/Q^{E,D})$, k is the planar CEMC (for example, $s_{11}^{E,D}$, k_{31}), then $\zeta^{sc,oc} \cong \omega b\sqrt{\rho \dot{s}^{E,D}}(1-\mathrm{i}/2Q^{E,D})$, $\zeta^{sc} - \zeta^{oc} \simeq \zeta^{sc} \cdot \mathrm{k}^2/2$. For the resistive electrodes according to (8) $\zeta^2(\tau) = \omega^2 \rho b^2 s^*(\tau)$, so that the branch's semicircle diameter is proportional to the planar CEMC squared, and is rising with frequency.

The relaxation dependences of the potential branches $\{m\hat{\Phi}\}(P)$ obey the following:

$$\zeta_{\{m\hat{\Phi}\}}(P) \cong \mathrm{i}\left(\mathrm{Im}\,\zeta^{oc}_{\{m\hat{\Phi}\}} + \Lambda \frac{1}{1+\mathrm{i}\,\omega\tau} \right) = \mathrm{i}\left(\mathrm{Im}\,\zeta^{sc}_{\{m\hat{\Phi}\}} - \Lambda \frac{\mathrm{i}\,\omega\tau}{1+\mathrm{i}\,\omega\tau} \right) \quad , \tag{44}$$

where $\Lambda = \mathrm{Im}\,\zeta^{sc}_{\{m\hat{\Phi}\}} - \mathrm{Im}\,\zeta^{oc}_{\{m\hat{\Phi}\}} \cong \pi/2$, $m = 2,3,4...$, with maxima of $\mathrm{Re}\,\zeta_{\{m\hat{\Phi}\}}(P)$ at $P \approx 1$.
The first-order $\{1\hat{\Phi}\}(P)$ potential branch far enough out of any thickness resonance is described by the modified Davidson-Cole relaxation expression

$$\zeta_{\{1\hat{\Phi}\}}(P) \cong \mathrm{i}\,\frac{\mathrm{Im}\,\zeta^{oc}_{\{1\hat{\Phi}\}}}{\left[1+(\mathrm{i}\,\omega\tau)^{-1}\right]^{1/2}} \tag{45}$$

with $\mathrm{Im}\,\zeta^{oc}_{\{1\hat{\Phi}\}} \cong -\pi/2$ and the exponents $\beta = 1/2$ and $\alpha = -1$ (6), which is linear $\zeta_{\{1\hat{\Phi}\}}(P \ll 1) \simeq (1-\mathrm{i})P$ at relatively low and with arc-like shape at relatively high electrode resistivity. The existence and main features of the "potential" branches (44),(45) can be explained by the "dielectric" approach (Chapter II-D3), which are not largely dependent on piezoeffect.

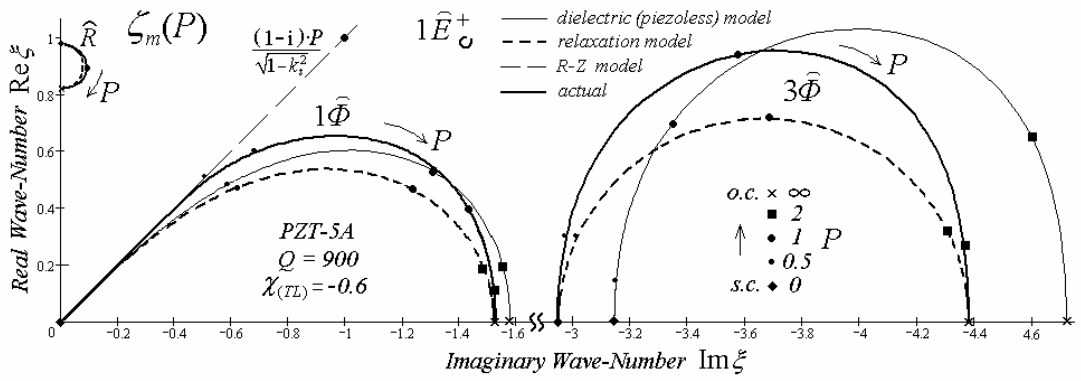

Fig. 6. *Lowest characteristic dispersion curves for a piezoplate and its electrical analogs: ▬ actual exact dispersion (39), ═══ dielectric (piezoless) model (36), - - - relaxation model (43-45) matched on o.c. and s.c. points, ▬ ▬ R-C model (34).* **S**-*configuration for a frequency much less any thickness resonances (PZT-5A).*

The dependence of dispersion relationships on the relaxation time has been analytically and numerically determined, and the results are compared in Fig. 6 with those for the dielectric, relaxation, and *R-C* models. There are two major types of relaxation curves. The electrode resistance dependences of complex $\zeta_m(\omega\tau)$ for the basic branches (out of their interaction), but $1\hat{\Phi}$, largely follow the Debye-like dielectric relaxation

(typical for a spherically isotropic structure) in terms of frequency and relaxation time. The last one ($1\widehat{\Phi}$) exhibits an asymmetric distribution of the modified Davidson-Cole functional form. The Cole-Cole semicircles of a Debye-type relaxation can be satisfactory modeled by an equivalent RC circuit chain with concentrated parameters [22],[23], where maximum dispersion corresponds to the relaxation dielectric resonance with $RC \approx 1$. When the process is restricted to a constant angle with respect to some fixed axis (less "degrees of freedom"), approximate Davidson-Cole relaxation is found [23]. Relaxation effects of the vibration characteristics space distribution described here are part of the general relaxation phenomenon, supposing that time (transient-effects) and space relaxations are related for a distributed system.

As seen from the M1,2,3<S|A> files of the dispersion branches in their performance under frequency variation, when some branch distortion from the ideal form takes place, there is a strong electro-acoustical interaction with some other nearby branches in a higher degree dependent on dissipation parameters.

B. *First-Order Derivative Approximation for the Basic and Non-Basic TL and TSh Resonances*

In a generalized consideration, defining the function $F(\xi)$ as a determinant $\|\mathbf{M}\mathrm{S}\|$ or $\|\mathbf{M}\mathrm{A}\| \cdot \xi$, then the function $U(\xi)$ as $\|\mathbf{N}\mathrm{S}\|$ or $\|\mathbf{N}\mathrm{A}\|(\varepsilon_{33}^{S}/\varepsilon_{11}^{S}) \cdot \xi^{-1}$, respectively for **S-** and **A-**configurations (Appendix I), the functions are supposed to be analytical, symmetric of ξ and finite at $\xi \to 0$. Then at least for $\left|\xi^2\right| << 1$ they can be represented as:

$$F(\xi) = F_0 + F' \cdot \xi^2 + 0.5F'' \cdot (\xi^2)^2 + \ldots, \tag{46}$$

$$U(\xi) = U_0 + U' \cdot \xi^2 + 0.5U'' \cdot (\xi^2)^2 + \ldots, \tag{47}$$

where the independent on ξ coefficients are

$$F_0 = F\big|_{\xi^2=0}\ , \qquad F' = F'_{,\xi^2}\Big|_{\xi^2=0} = 0.5\,F''_{,\xi}\Big|_{\xi=0}\ , \qquad F'' = F''_{,\xi^2}\Big|_{\xi^2=0} = (1/12)\,F^{(4)}_{,\xi}\Big|_{\xi=0}\ ; \tag{48}$$

$$U_0 = U\big|_{\xi^2=0}\ , \qquad U' = U'_{,\xi^2}\Big|_{\xi^2=0} = 0.5\,U''_{,\xi}\Big|_{\xi=0}\ , \qquad U'' = U''_{,\xi^2}\Big|_{\xi^2=0} = (1/12)\,U^{(4)}_{,\xi}\Big|_{\xi=0}\ . \tag{49}$$

Considering (46),(47) as linear functions of ξ^2 (Fig. 3) in a first-order approximation, the dispersion roots at least near any thickness resonance with $\left|(\zeta_m^{sc,\,oc})^2\right| << 1$ can be found as follows:

$$F(\xi) = 0\,, \quad \text{then} \quad \left(\zeta_m^{sc}\right)^{-2} \cong -F'/F_0\ , \tag{50}$$

$$U(\xi) = 0\,, \quad \text{then} \quad \left(\zeta_m^{oc}\right)^{-2} \cong -U'/U_0\ . \tag{51}$$

According to the Theorem $U_0/F_0 = \mathrm{i} \cdot \widehat{\Upsilon}$, then

$$\mathrm{i} \cdot \left(\zeta_m^{oc}\right)^2 \Big/ \left(\zeta_m^{sc}\right)^2 \cong \widehat{\Upsilon} \cdot \left(-F'/U'\right)\ . \tag{52}$$

If in an ideal fully lossless case the o.c. and s.c. branches intersect the ω-axis with $\zeta_m^{oc,\,sc} = 0$ at any *TL* and *TSh* resonance and antiresonance frequencies, then in a lossy case they do not and reach the ξ-plane origin as close as the dissipation factors are low. Generally the graphic surfaces of the absolute functions $F(\xi)$ and

$U(\xi)$ represent a right cone near the origin in the ξ^2 - plane (Fig. 3), and for this reason, as a consequence of a linear dependence, the corresponding roots for the lateral complex wave-numbers are directly related to the respective elementary normalized admittances $\widehat{\mathrm{Y}}=\widehat{\mathrm{Y}}_{\langle TL,TSh\rangle}$. The comparative dispersion curves near the coupled fundamental S-*TL* and second-order S-*TSh* resonances derived with the *first-derivative* method and actual *exact* solutions are shown in Fig.7, which are in a good agreement. The elementary admittance $\widehat{\mathrm{Y}}_{\langle TL,TSh\rangle}$ with its the only basic resonances determines the specific features of the dispersion behavior near thickness resonances of any kind, which consequently are different for the basic *TL* and non-basic *TSh* modes in **S-**, and for the basic *TSh* and non-basic *TL* modes in **A-**configuration.

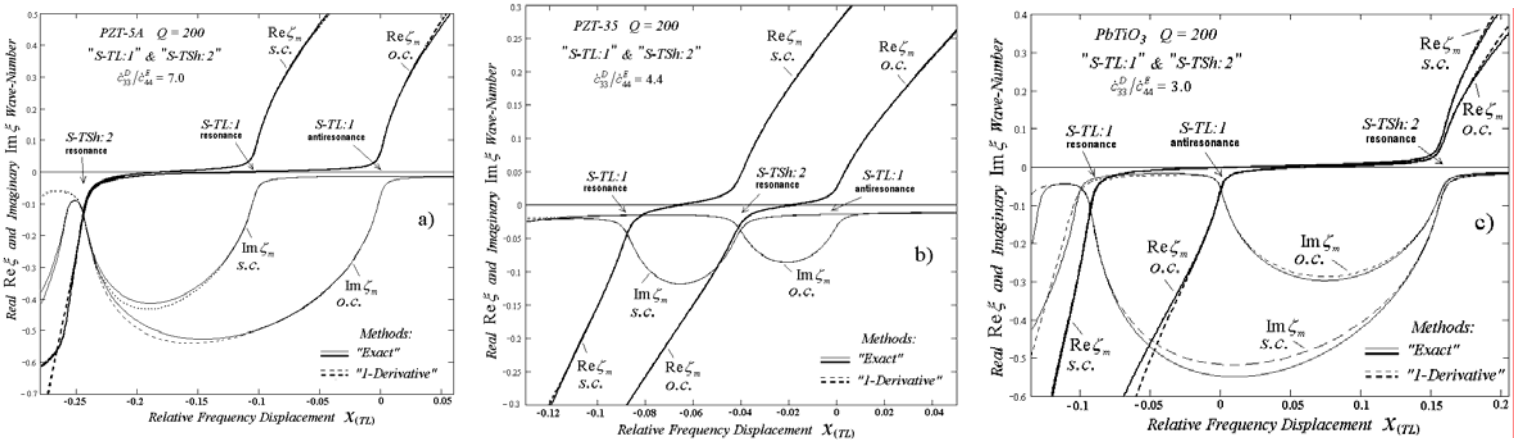

Fig. 7 a,b,c . *Comparative o.c. and s.c. dispersion curves near the coupled fundamental* "S-*TL:* $n=1$" *and second-order* "S-*TSh:* $n=2$" *resonances for exact solutions (23) and those numerically obtained by the "first-derivative" method (50),(51) for the three PZT-5A (a), PZT-35 (b), PbTiO$_3$ (c) piezoceramics.*

The derivative of some 3x3 matrix determinant $\|\mathrm{X}\|$ can be expressed as a sum of derivatives of the partial matrix elements with $\sin|\cos K_{(j)}$ functions as in (22)-(26):

$$\text{if} \quad \|\mathrm{X}\| = \begin{Vmatrix} X_{1j} \\ X_{2j} \\ X_{3j} \end{Vmatrix}, \quad j=1,2,3, \quad \text{then} \quad \mathrm{X}' \equiv \|\mathrm{X}\|'_{,\xi^2} = \begin{Vmatrix} X'_{1j,\xi^2} \\ X_{2j} \\ X_{3j} \end{Vmatrix} + \begin{Vmatrix} X_{1j} \\ X'_{2j,\xi^2} \\ X_{3j} \end{Vmatrix} + \begin{Vmatrix} X_{1j} \\ X_{2j} \\ X'_{3j,\xi^2} \end{Vmatrix}. \qquad (53)$$

In the S-configuration the matrix derivatives (50),(51) are ultimately divided by $U_0 \propto const \cdot \cos \mathrm{K}_{\langle TL\rangle} \cdot \sin \mathrm{K}_{\langle TSh\rangle}$, and in the **A**-configuration they are divided by $F_0 \propto const \cdot \sin \mathrm{K}_{\langle TL\rangle} \cdot \cos \mathrm{K}_{\langle TSh\rangle}$ (Appendix I). Each component of the sum for the matrix derivative contains a *const* from the first matrix column, $\sin|\cos \mathrm{K}_{\langle TL\rangle}$ functions as a factor from the second matrix column, and $\sin|\cos \mathrm{K}_{\langle TSh\rangle}$ functions as a factor from the third matrix column. Grouping the terms, the main body of the matrix derivative can be finally represented in general as follows, particularly for the **S**-configuration

(coefficients with a lower "~" sign):

$$\left(\zeta_m^{sc}\right)^{-2} \cong -\frac{F'}{F_0} = \frac{F'}{U_0}\cdot\left(-\frac{U_0}{F_0}\right) \equiv \underset{\sim}{\Omega}^{sc}\cdot\left(-\mathrm{i}\widehat{\mathrm{Y}}_{\langle TL\rangle}\right) \ , \tag{54}$$

$$\left(\zeta_m^{oc}\right)^{-2} \cong -\frac{U'}{U_0} \equiv \underset{\sim}{\Omega}^{oc} \ , \tag{55}$$

$$\underset{\sim}{\Omega}^{sc|oc} = \frac{F'\left|\left(-U'\right)\right.}{U_0} \equiv \ -\frac{1}{2}\underset{\sim}{\Delta}_0^{sc|oc} - \underset{\sim}{\Delta}_1^{sc|oc}\ \frac{\tan \mathrm{K}_{\langle TL\rangle}}{\mathrm{K}_{\langle TL\rangle}}\frac{\cot \mathrm{K}_{\langle TSh\rangle}}{\mathrm{K}_{\langle TSh\rangle}} - \frac{1}{2}\underset{\sim}{\Delta}_2^{sc|oc}\ \frac{\tan \mathrm{K}_{\langle TL\rangle}}{\mathrm{K}_{\langle TL\rangle}} + \frac{1}{2}\underset{\sim}{\Delta}_3^{sc|oc}\ \frac{\cot \mathrm{K}_{\langle TSh\rangle}}{\mathrm{K}_{\langle TSh\rangle}} =$$

$$= -\frac{1}{2}\underset{\sim}{\theta}_0^{sc|oc} + \frac{1}{4}\underset{\sim}{\theta}_1^{sc|oc}\left(1-2\,\underset{\sim}{\theta}_2^{sc|oc}\ \frac{\tan \mathrm{K}_{\langle TL\rangle}}{\mathrm{K}_{\langle TL\rangle}}\right)\left(1+2\,\underset{\sim}{\theta}_3^{sc|oc}\ \frac{\cot \mathrm{K}_{\langle TSh\rangle}}{\mathrm{K}_{\langle TSh\rangle}}\right) \ , \tag{56}$$

where $\underset{\sim}{\theta}_3 = \underset{\sim}{\Delta}_1/\underset{\sim}{\Delta}_2$, $\underset{\sim}{\theta}_2 = \underset{\sim}{\Delta}_1/\underset{\sim}{\Delta}_3$, $\underset{\sim}{\theta}_1 = \underset{\sim}{\Delta}_2\,\underset{\sim}{\Delta}_3/\underset{\sim}{\Delta}_1$, $\underset{\sim}{\theta}_0 = \underset{\sim}{\Delta}_0 + \underset{\sim}{\theta}_1/2$ for the s.c. and o.c. regimes, respectively.

The material dimensionless coefficients $\underset{\sim}{\Delta}_i^{sc,\,oc}$, $i = 0,1,2,3$, are of the order of 1, their finite algebraic expressions do not contain trigonometric functions, particularly (Appendix II):

$$\underset{\sim}{\Delta}_3^{sc} = \vartheta_{1(3)} \ , \qquad \underset{\sim}{\Delta}_3^{oc} = \vartheta_{1(3)}\left(1+2\,\kappa_{TSh}^2\right) , \tag{57}$$

$$\underset{\sim}{\Delta}_2^{sc} = \vartheta_{1(2)} - \nu\,\mathrm{k}_t^2 + \frac{c_{33}^D}{\omega^2\rho b^2}\cdot\left\{\approx\left(\mathrm{k}_t^2 - \frac{e_{33}e_{15}}{c_{33}^D\varepsilon_{33}^S}\right)\right\} \cong \vartheta_{1(2)}\left(1-\kappa_{TL}^2\right) \quad , \qquad \underset{\sim}{\Delta}_2^{oc} = \vartheta_{1(2)} \ , \tag{58}$$

$$\underset{\sim}{\Delta}_1^{sc} = \frac{c_{33}^D}{c_{44}^E}\aleph^2 + \frac{1}{2}\mathrm{k}_t^2\cdot\vartheta_{1(3)} \ \cong \ 1 + \frac{1}{2}\mathrm{k}_t^2\cdot\vartheta_{1(3)} + \sqrt{\nu}\,\frac{\mathrm{k}_{15}\,\mathrm{k}_t}{\sqrt{c_{33}^D/c_{44}^E}} \ ,$$

$$\underset{\sim}{\Delta}_1^{oc} = \frac{c_{33}^D}{c_{44}^E}\left[\aleph + \frac{e_{33}e_{15}}{c_{33}^D\varepsilon_{33}^S}\right]^2 \ \cong \ 1 + \sqrt{c_{33}^D/c_{44}^E}\cdot\sqrt{\nu}\,\mathrm{k}_{15}\mathrm{k}_t \ , \tag{59}$$

where $\aleph = \left\{1 + \frac{c_{13}^E}{c_{33}^D} + \frac{e_{33}\left(e_{31}+e_{15}\right)}{c_{33}^D\varepsilon_{33}^S}\right\}\Big/\left(\frac{c_{33}^D}{c_{44}^E} - 1\right)$, $\kappa_{TL}^2 = \mathrm{k}_t^2\,\nu/\vartheta_{1(2)}$, $\kappa_{TSh}^2 = \mathrm{k}_{15}^2\,\nu/\vartheta_{1(3)}$.

Substituting (46),(47) into (39), we have the equation for $\zeta_m\left(\omega, P\right)$ in its electrode resistivity dependence as a first-order derivative approximation near the origin $\left|\xi^2\right| << 1$:

$$\underset{\sim}{\Omega}^{sc}\cdot\xi^4 + \left[2\,\mathrm{i}\,P^2\cdot\underset{\sim}{\Omega}^{oc} - \left(-\mathrm{i}\widehat{\mathrm{Y}}_{\langle TL\rangle}\right)^{-1}\right]\cdot\xi^2 - 2\,\mathrm{i}\,P^2 =$$

$$= \left(\zeta_m^{sc}\right)^{-2}\cdot\xi^4 + \left[2\,\mathrm{i}\,P^2\left(-\mathrm{i}\widehat{\mathrm{Y}}_{\langle TL\rangle}\right)\cdot\left(\zeta_m^{oc}\right)^{-2} - 1\right]\cdot\xi^2 - 2\,\mathrm{i}\,P^2\left(-\mathrm{i}\widehat{\mathrm{Y}}_{\langle TL\rangle}\right) \ = \ 0 \tag{60}$$

There are two roots for $\zeta_m^2\left(\omega, P\right)$, so two different branches exist near the origin forming the resonance.

Analogously for the **A**-configuration (coefficients with a lower "–" sign):

$$\left(\zeta_m^{sc}\right)^{-2} \cong -\frac{F'}{F_0} \equiv \underline{\Omega}^{sc} \quad , \tag{61}$$

$$\left(\zeta_m^{oc}\right)^{-2} \cong -\frac{U'}{U_0} = \frac{U'}{F_0}\left(-\frac{F_0}{U_0}\right) \equiv \underline{\Omega}^{oc}\cdot\left(-\mathrm{i}\widehat{\mathrm{Y}}_{\langle TSh\rangle}\right)^{-1}, \tag{62}$$

$$\underline{\Omega}^{sc|oc} = \frac{\left(-F'\right)\left|U'\right.}{F_0} \equiv -\frac{1}{2}\underline{\Delta}_0^{sc|oc} - \underline{\Delta}_1^{sc|oc}\,\frac{\tan \mathrm{K}_{\langle TSh\rangle}}{\mathrm{K}_{\langle TSh\rangle}}\frac{\cot \mathrm{K}_{\langle TL\rangle}}{\mathrm{K}_{\langle TL\rangle}} - \frac{1}{2}\underline{\Delta}_2^{sc|oc}\,\frac{\tan \mathrm{K}_{\langle TSh\rangle}}{\mathrm{K}_{\langle TSh\rangle}} + \frac{1}{2}\underline{\Delta}_3^{sc|oc}\,\frac{\cot \mathrm{K}_{\langle TL\rangle}}{\mathrm{K}_{\langle TL\rangle}} =$$

$$= -\frac{1}{2}\underline{\theta}_0^{sc|oc} + \frac{1}{4}\underline{\theta}_1^{sc|oc}\left(1-2\underline{\theta}_2^{sc|oc}\,\frac{\tan \mathrm{K}_{\langle TSh\rangle}}{\mathrm{K}_{\langle TSh\rangle}}\right)\left(1+2\underline{\theta}_3^{sc|oc}\,\frac{\cot \mathrm{K}_{\langle TL\rangle}}{\mathrm{K}_{\langle TL\rangle}}\right), \tag{63}$$

where $\underline{\theta}_3 = \underline{\Delta}_1/\underline{\Delta}_2$, $\underline{\theta}_2 = \underline{\Delta}_1/\underline{\Delta}_3$, $\underline{\theta}_1 = \underline{\Delta}_2\underline{\Delta}_3/\underline{\Delta}_1$, $\underline{\theta}_0 = \underline{\Delta}_0 + \underline{\theta}_1/2$ for the s.c. and o.c. regimes, respectively.

The material dimensionless coefficients $\underline{\Delta}_i^{sc,\,oc}$, $i = 0,1,2,3$, are of the order of 1, particularly:

$$\underline{\Delta}_3^{sc} = \vartheta_{1(2)}\left(1-2\kappa_{TL}^2\right), \qquad \underline{\Delta}_3^{oc} = \vartheta_{1(2)}, \tag{64}$$

$$\underline{\Delta}_2^{sc} = \vartheta_{1(3)}, \qquad \underline{\Delta}_2^{oc} = \vartheta_{1(3)} + \nu\,\mathrm{k}_{15}^2 - \frac{c_{44}^E}{\omega^2\rho b^2}\cdot\left\{\approx\left(\frac{e_{33}e_{15}}{c_{44}^E\varepsilon_{11}^S} - \mathrm{k}_{15}^2\right)\right\} \cong \vartheta_{1(3)}\left(1+\kappa_{TSh}^2\right), \tag{65}$$

$$\underline{\Delta}_1^{sc} = \frac{c_{33}^D}{c_{44}^E}\aleph^2 \;\cong\; 1+\sqrt{\nu}\,\frac{\mathrm{k}_{15}\mathrm{k}_t}{\sqrt{c_{33}^D/c_{44}^E}},$$

$$\underline{\Delta}_1^{oc} = \frac{c_{33}^D}{c_{44}^E}\left[\aleph + \frac{e_{33}e_{15}}{c_{33}^D\varepsilon_{33}^S}\right]^2 - \frac{1}{2}\mathrm{k}_{15}^2\cdot\vartheta_{1(2)} \;\cong\; 1+\sqrt{c_{33}^D/c_{44}^E}\cdot\sqrt{\nu}\,\mathrm{k}_{15}\mathrm{k}_t - \frac{1}{2}\mathrm{k}_{15}^2\cdot\vartheta_{1(2)}. \tag{66}$$

Substituting (46),(47) into (39), we have the expression for $\zeta_m\left(\omega,P\right)$ in its electrode resistivity dependence as a first-order derivative approximation near the origin $\left|\xi^2\right| << 1$:

$$\zeta_m^{-2}\left(\omega,P\right) = \frac{\underline{\Omega}^{sc} + 2\,\mathrm{i}\,\nu P^2\cdot\underline{\Omega}^{oc}}{1+2\,\mathrm{i}\,\nu P^2\cdot\left(-\mathrm{i}\widehat{\mathrm{Y}}_{\langle TSh\rangle}\right)} = \frac{\left(-\mathrm{i}\widehat{\mathrm{Y}}_{\langle TSh\rangle}\right)^{-1}\left(\zeta_m^{sc}\right)^{-2} + 2\,\mathrm{i}\,\nu P^2\left(\zeta_m^{oc}\right)^{-2}}{\left(-\mathrm{i}\widehat{\mathrm{Y}}_{\langle TSh\rangle}\right)^{-1} + 2\,\mathrm{i}\,\nu P^2} \tag{67}$$

where $\nu = \varepsilon_{11}^S/\varepsilon_{33}^S$, with a single branch near the origin forming the resonance..

The thickness wave-number derivative parameters $\vartheta_{1(j)}$ (Appendix II) involved can be easily found from (14) by differentiation. They are material dimensionless constants with typical values $\vartheta_{1(j)} \simeq 1\pm 0.3 > 0$ including isotropic non-polarized state of a piezoceramic, do not depend on frequency (harmonic number) – only on elastic anisotropy and CEMC. As (54)-(67) describe the dispersion near a certain *n*-order thickness resonance, the n^2-factor appears in Δ_2 as an approximation from $2/\mathrm{K}^2 \simeq 8/\pi^2 n^2 \simeq 1/n^2$ (70) vanishing at $n \geq 3$ with typical $e_{33} - e_{15} < e_{33}, e_{15}$. The coefficients $\Delta_0 \simeq \frac{\varepsilon_{11}^S}{\varepsilon_{33}^S}\left[\sim 1\right] - \frac{\left[c_{ij}^{E,D}\right]}{\omega^2\rho b^2}$ are determined by the respective terms related to the lowest potential ($\widehat{\Phi}$) and planar ($\widehat{R},\widehat{F}$) branches roots, so that $\left|\Delta_0(\theta_0)\right| <\approx 1$

are supposed to be not essential near a thickness resonance with $\left\langle \tan\middle|\cot \right\rangle(\mathrm{K}) \to \infty$.

As follows from (56) and (63) of the first-order derivative approach, the two coupled *TL* and *TSh* vibrational modes are separated as factors in their influence on the resulted lateral wave-number. Then, three major characteristic cases can be extracted: pure thickness modes, suppressing and gain a mode by another competing mode, depending on the $\left|\mathrm{K}^2_{\langle TSh\rangle}\middle/\mathrm{K}^2_{\langle TL\rangle}\right| \cong \dot{c}^D_{33}/\dot{c}^E_{44} \in 2.3...9.0$ elastic anisotropy parameter and the $\Delta_i^{sc,\,oc}$ factors. Such a formal description is connected to the physical behavior of the $\{m\widehat{E}^{\pm}\}$ branches and their competitive interaction to form a *TSh* resonance. General variants of the basic and non-basic resonances relative disposition, and hence dispersion types for the $\mathrm{S}\middle|\mathrm{A}$ -configurations, respectively, are:

– (B1) "pure" basic mode odd-order resonance $\left|\tan \mathrm{K}_{\langle TL|TSh\rangle}\right| >> 1$ with non-basic mode $\cot \mathrm{K}_{\langle TSh|TL\rangle} \approx 0$;

– (B2) "pure" non-basic mode even-order resonance $\left|\cot \mathrm{K}_{\langle TSh|TL\rangle}\right| >> 1$ with basic mode $\tan \mathrm{K}_{\langle TL|TSh\rangle} \approx 0$;

– (B3) suppressed non-basic mode resonance $\left|\cot \mathrm{K}_{\langle TSh|TL\rangle}\right| >> 1$ by the coupled basic mode with

$$1/2\theta_2 - \tan \mathrm{K}_{\langle TL|TSh\rangle}\big/\mathrm{K}_{\langle TL|TSh\rangle} \simeq 0\ , \tag{68}$$

and suppressed basic mode resonance $\left|\tan \mathrm{K}_{\langle TL|TSh\rangle}\right| >> 1$ by the coupled non-basic mode with

$$1/2\theta_3 + \cot \mathrm{K}_{\langle TSh|TL\rangle}\big/\mathrm{K}_{\langle TSh|TL\rangle} \simeq 0\,, \tag{69}$$

which are satisfied with respective predominantly real coefficients according to (56) and (63);

– (B4) minimal possible resonance dispersion (gain) due to exactly coincident resonances of the coupled basic $\left|\tan \mathrm{K}_{\langle TL|TSh\rangle}\right| >> 1$ and non-basic $\left|\cot \mathrm{K}_{\langle TSh|TL\rangle}\right| >> 1$ thickness modes.

In the first two cases of "pure" modes, the dispersion of the *TL* and *TSh* resonances is formed by the $\{m\widehat{E}^{-}\}$ and $\{m\widehat{E}^{+}\}$ branches, respectively. The "suppressed" conditions (68),(69) relate to the competing $\{m\widehat{E}^{+}\}$ and $\{m\widehat{E}^{-}\}$ branches to form a *TSh* resonance, generally with different *m*-orders, which are simultaneously trying to reach the ξ-origin. Between these two conditions the joint *TL* and *TSh* resonance provides the pure imaginary dispersion with extremely large decay distance. Anyway, any *TL* resonance is always formed by a $\{m\widehat{E}^{-}\}$ branch.

For further presentation, the elementary mode thickness wave-number is expressed as:

$$\mathrm{K}_{\langle TL,TSh\rangle} = \omega b\sqrt{\rho/c} \cong \frac{\pi}{2}n(1+\chi)\left(1-\mathrm{i}\frac{1}{2Q}\right) = \frac{\pi}{2}n + \frac{\pi}{2}n\left(\chi - \mathrm{i}\frac{1+\chi}{2Q}\right), \tag{70}$$

$$\chi = f/f_{0(n)} - 1, \qquad f_{0(n)} = n\sqrt{\dot{c}/\rho}\,/4b\ ,$$

where for *TL*-mode: $Q = Q^D_{33}$, $c = c^D_{33}$ with $\dot{c} = \mathrm{Re}\left(c^D_{33}\right)$, $f_{0(n)} = f_{(TL:\,n)}$, $\chi = \chi_{(TL:\,n)}$, $n = n_{TL}$;

and for *TSh*-mode: $Q = Q^E_{44}$, $c = c^E_{44}$ with $\dot{c} = \mathrm{Re}\left(c^E_{44}\right)$, $f_{0(n)} = f_{(TSh:\,n)}$, $\chi = \chi_{(TSh:\,n)}$, $n = n_{TSh}$.

Decomposing it on small parameters of frequency displacement χ and losses Q^{-1} near their poles

$$\left.\frac{\tan \mathrm{K}}{\mathrm{K}}\right|_{odd\ n} = -\Xi \quad , \qquad \left.\frac{\cot \mathrm{K}}{\mathrm{K}}\right|_{even\ n} = \Xi \quad , \quad \text{where} \quad \Xi \simeq \mathrm{i}\frac{8}{\pi^2 n^2} Q \frac{1}{1+\mathrm{i}\, y} \quad , \tag{71}$$

with $y = 2Q\chi$ generalized frequency displacement. Particularly, the relative frequency displacements $\chi_{a\,(TL:\,n)}$ and $\chi_{r\,(TSh:\,n)}$ are taken in respect to the $f_{a(TL:\,n)} = n_{TL}\sqrt{\dot{c}^D_{33}/\rho}\,/4b$ antiresonance and $f_{r(TSh:\,n)} = n_{TSh}\sqrt{\dot{c}^E_{44}/\rho}\,/4b$ resonance frequencies of the $\widehat{\mathrm{Y}}_{\langle TL,TSh\rangle}$ corresponding elementary mode with odd $n_{(TL,TSh)}$ harmonic numbers. Then, for the $\widehat{\mathrm{Y}}_{\langle TL\rangle}$ (1) resonance $f_{r(n)}/f_{a(n)} - 1 \simeq -4k_t^2/\pi^2 n_{TL}^2$, and for the $\widehat{\mathrm{Y}}_{\langle TSh\rangle}$ (2) antiresonance $f_{a(n)}/f_{r(n)} - 1 \simeq 4k_{15}^2/\pi^2 n_{TSh}^2$.

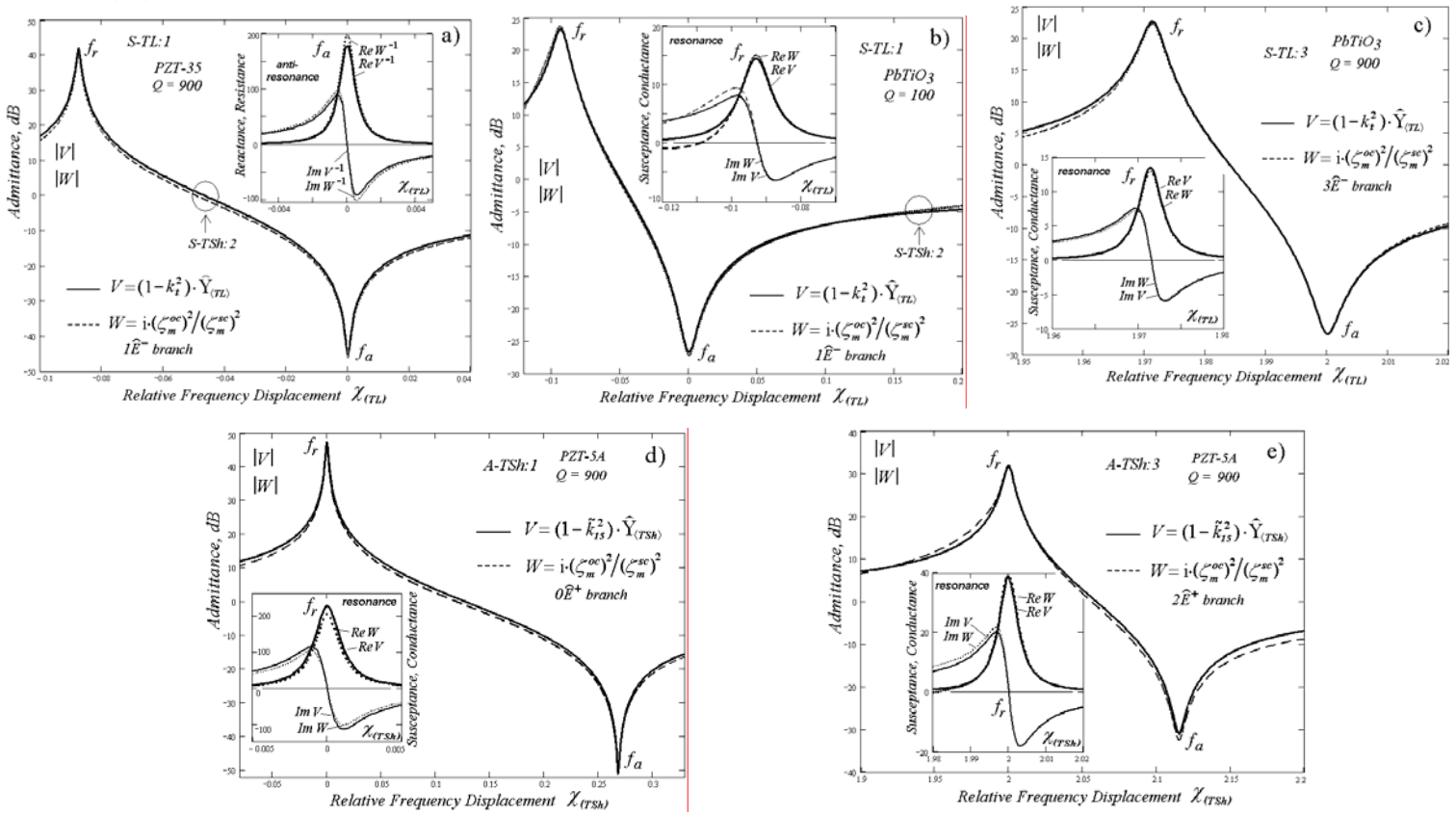

Fig. 8 a,b,c,d,e . *Complex generalized admittance* $V = \left(1 \mp k^2\right)^{\pm 1} \cdot \widehat{\mathrm{Y}}_{\langle TL|TSh\rangle}$ *(3) and actual dispersion ratio* $W = \mathrm{i}(\zeta_m^{oc})^2/(\zeta_m^{sc})^2$ *(23) vs. frequency near the basic fundamental n = 1 and third n = 3* S-*TL and* A-*TSh harmonics for the three piezoceramics. Inserted – the real and imaginary parts (conductance, sucseptance) of the V and W characteristics.*

As $\left(-F'/U'\right)$ in (52) is of the order of 1, the following Statement can be formulated and then is considered in details for the dispersion characterization at thickness resonances of any kind:

Statement. The ratio of the open-circuit $(\zeta_m^{oc})^2$ to short-circuit $(\zeta_m^{sc})^2$ lateral complex wave-numbers squared (as roots of $\left\|\mathbf{G}\langle \mathrm{S|A}\rangle\right\| = 0$ and $\left\|\mathbf{\Phi}\langle \mathrm{S|A}\rangle\right\| = 0$ characteristic matrices, respectively) for a branch with $\left|(\zeta_m^{oc,\,sc})^2\right| << 1$ at least near any pure or coupled thickness resonance is largely determined by the respective normalized elementary complex admittance $\widehat{\mathrm{Y}}_{\langle TL,TSh\rangle}$ in its complex value and frequency dependence.

It follows from the Statement that: a) the dispersion ratio near any basic odd-order thickness resonance-antiresonance coincides with the respective admittance $\widehat{\mathrm{Y}}_{\langle TL,TSh\rangle}$ regardless of the presence of any non-basic thickness resonance; b) near any non-basic even-order thickness resonance far enough out of any basic resonance the dispersion ratio is constant on frequency depending on the respective effective CEMC. Fig. 8 illustrates the phase and amplitude satisfactory coincidence of the lateral dispersion ratio with the elementary complex generalized admittance characteristics near the basic *TL* and *TSh* resonances regardless of the presence of any non-basic thickness resonance, all under a simplified for representation condition for the effective CEMC $\kappa_{TL} \simeq k_t$ and $\kappa_{TSh} \simeq k_{15}$ (56),(63) . The Statement is a useful practical estimate based on the Theorem and is a powerful tool for analyzing the interrelated PR excitation and propagation problems.

B1. *Pure Basic* "S-*TL:odd n*" *and* "A-*TSh:odd n*" *resonances.*

Such a condition for the best performance is provided, for example, for the set of practical values $\dot{c}_{33}^{D}/\dot{c}_{44}^{E} = (3/1)^2,\ (\{5,7,9\}/3)^2,\ (\{9,11,13,15\}/5)^2,\ ... = (n_{odd\ TSh}/n_{odd\ TL})^2$, when the odd-order *TSh*- and *TL*-mode resonances coincide, respectively, and the dispersion branches near the ξ-origin are determined then by the predominant terms with $\Delta_2^{sc,oc}$ coefficients in (56),(58) and (63),(65).

B1-S. For the pure basic "S-*TL: odd n*" resonances with $\left|\tan \mathrm{K}_{\langle TL\rangle}\right| >> 1$ when $\mathrm{K}_{\langle TL\rangle} \simeq \pi n_{TL}/2$ for odd $n_{TL} = 1,3,5...$, near the frequency of some "*TSh: odd n*" resonance with $\cot \mathrm{K}_{\langle TSh\rangle} \approx 0$ (far enough from any non-basic even-order *TSh* resonance, as in an example M1<S> $PbTiO_3$ for S-*TL:3*):

$$\mathrm{i}\left(\zeta_m^{oc}\right)^2 \Big/ \left(\zeta_m^{sc}\right)^2 \ \Big|_{basic}^{\text{S–}TL:\,odd\ n} \cong \left(1-\kappa_{TL}^2\right)\cdot \widehat{\mathrm{Y}}_{\langle TL\rangle}, \tag{72}$$

$$\left(\zeta_m^{sc}\right)^2 \ \Big|_{basic}^{\text{S–}TL:\,odd\ n} \cong -\frac{2}{\vartheta_{1(2)}\left(1-\kappa_{TL}^2\right)}\cdot\frac{\mathrm{K}_{\langle TL\rangle}}{\tan \mathrm{K}_{\langle TL\rangle}}\cdot\frac{1}{\left(-\mathrm{i}\,\widehat{\mathrm{Y}}_{\langle TL\rangle}\right)}\ , \tag{73}$$

$$\left(\zeta_m^{oc}\right)^2 \ \Big|_{basic}^{\text{S–}TL:\,odd\ n} \cong -\frac{2}{\vartheta_{1(2)}}\cdot\frac{\mathrm{K}_{\langle TL\rangle}}{\tan \mathrm{K}_{\langle TL\rangle}}\ , \tag{74}$$

then at the resonance (*r*) and antiresonance (*a*) frequencies respectively

$$\left(\zeta_m^{sc}\right)_a^2 \cong \frac{2}{\vartheta_{1(2)}}\cdot\frac{\mathrm{k}_t^2}{\left(1-\kappa_{TL}^2\right)}\ , \qquad \left(\zeta_m^{oc}\right)_r^2 \cong -\frac{2}{\vartheta_{1(2)}}\cdot \mathrm{k}_t^2\ . \tag{75}$$

Near the *"*S-*TL: odd n"* resonance, decomposing the expressions (73),(74) on relatively small parameters of loss factors and frequency displacements (71), we have

$$\left(\zeta_m^{\langle sc|oc\rangle}\right)^{-2} \ \Big|_{basic}^{\text{S–}TL:\,odd\ n} \simeq \mathrm{i}\,\vartheta_{1(2)}\cdot\frac{4}{\pi^2 n_{TL}^2}\,Q_{\langle r|a\rangle}\frac{1}{1+\mathrm{i}\,y_{\langle r|a\rangle}}\ , \tag{76}$$

with their absolute minimums

$$min\left(\zeta_m^{\langle sc|oc\rangle}\right)_{\langle r|a\rangle} \simeq (1-\mathrm{i})\frac{\pi}{2\sqrt{2\vartheta_{1(2)}}}\cdot\frac{n_{TL}}{\sqrt{Q_{\langle r|a\rangle}}}, \tag{77}$$

where $y_{\langle r|a\rangle}=2Q_{\langle r|a\rangle}\chi_{\langle r|a\rangle}$ is the generalized frequency displacement, the s.c. regime corresponds to the resonance (*r*), and the o.c. regime corresponds to the antiresonance (*a*) of the elementary admittance $\widehat{\mathrm{Y}}_{\langle TL\rangle}$ with its resonance Q_r and antiresonance Q_a quality factors, and resonance $\chi_r=\omega/\omega_{r(n)}-1$ and antiresonance $\chi_a=\omega/\omega_{a(n)}-1$ relative frequency displacements. For the *TL*-mode [27], $Q_r\cong Q_{33}^E$ at the fundamental harmonic $n_{TL}=1$, and $Q_r\cong Q_{33}^D$ at higher harmonics with $n_{TL}\geq 3$, then $Q_a=Q_{33}^D$ for all n_{TL}.

In the **S**-configuration, a *TL* resonance is formed by two $1\widehat{\Phi}$ and $m\widehat{E}^-$ dispersion branches in the region of $\left|\zeta_m(\omega,P)\right|<1$. As found in [15], there are two frequency points of dispersion singularity near the resonance (see M1,2,3<S>), where both the branches have equal wave-numbers (intersection) at a certain electrode resistivity. In a practical view, the dispersion point of singularity determines the range of dispersion linearity so important for some applications [15]. The singularity characteristics of the pure basic *TL* mode can be analytically derived from the quadratic equation (60) under the condition of a singular solution when its determinant equals zero with its real and imaginary parts vanish. As a result for $k_t^2Q/n_{TL}^2>>1$, the lowest "resonance" singularity (*) takes place at the resonance frequency displacement $f^*/f_{r(n)}-1\simeq -1/2Q_r$ at $P^*\simeq k_tQ_r\cdot n_{TL}^2/\sqrt{2\dot{\Delta}_2^{sc}}$ with the joint for both branches lateral wave-number value $\zeta_m^*\simeq(0.5-\mathrm{i})\cdot n_{TL}/Q_r\sqrt{\dot{\Delta}_2^{sc}}$, and hence is mostly dissipative. The second "antiresonance" singularity takes place at the antiresonance frequency displacement $f^*/f_{a(n)}-1\simeq 4k_t^2/\pi^2n_{TL}^2\left(1-2\dot{\kappa}_{TL}^2\right)$ at $P^*\simeq k_t\cdot\sqrt{2/\dot{\Delta}_2^{sc}}$ with the joint lateral wave-number value $\zeta_m^*\simeq(1-0.5\mathrm{i})\cdot k_t\sqrt{2\dot{\Delta}_2^{oc}}/\dot{\Delta}_2^{sc}$, and hence is mostly piezoelectric.

B1-A. For the pure basic "A-*TSh: odd n*" resonances with $\left|\tan \mathrm{K}_{\langle TSh\rangle}\right|>>1$ when $\mathrm{K}_{\langle TSh\rangle}\simeq\pi n_{TSh}/2$, $n_{TSh}=1,3,5...$, near the frequency of some "*TL: odd n*" resonance with $\cot \mathrm{K}_{\langle TL\rangle}\approx 0$ (far enough from any non-basic even-order *TL* resonance, as in examples M1,2,3<A> always for A-*TSh:1*; *PZT-5A* for A-*TSh:3*; $PbTiO_3$ and *PZT-35* for A-*TSh:5*):

$$\mathrm{i}\left(\zeta_m^{oc}\right)^2/\left(\zeta_m^{sc}\right)^2\Big|_{basic}^{\text{A}-TSh:\ odd\ n}\cong\left(1+\kappa_{TSh}^2\right)^{-1}\cdot\widehat{\mathrm{Y}}_{\langle TSh\rangle}\ , \tag{78}$$

$$\left(\zeta_m^{sc}\right)^2\Big|_{basic}^{\text{A}-TSh:\ odd\ n}\cong-\frac{2}{\vartheta_{1(3)}}\cdot\frac{\mathrm{K}_{\langle TSh\rangle}}{\tan \mathrm{K}_{\langle TSh\rangle}}\ , \tag{79}$$

$$\left(\zeta_m^{oc}\right)^2\Big|_{basic}^{\text{A}-TSh:\ odd\ n}\cong-\frac{2}{\vartheta_{1(3)}\left(1+\kappa_{TSh}^2\right)}\cdot\frac{\mathrm{K}_{\langle TSh\rangle}}{\tan \mathrm{K}_{\langle TSh\rangle}}\cdot\left(-\mathrm{i}\,\widehat{\mathrm{Y}}_{\langle TSh\rangle}\right), \tag{80}$$

then at the resonance (*r*) and antiresonance (*a*) frequencies respectively

$$\left(\zeta_m^{sc}\right)_a^2\cong\frac{2}{\vartheta_{1(3)}}\cdot\mathrm{k}_{15}^2\ ,\qquad\left(\zeta_m^{oc}\right)_r^2\cong-\frac{2}{\vartheta_{1(3)}}\cdot\frac{\mathrm{k}_{15}^2}{\left(1+\kappa_{TSh}^2\right)}\ . \tag{81}$$

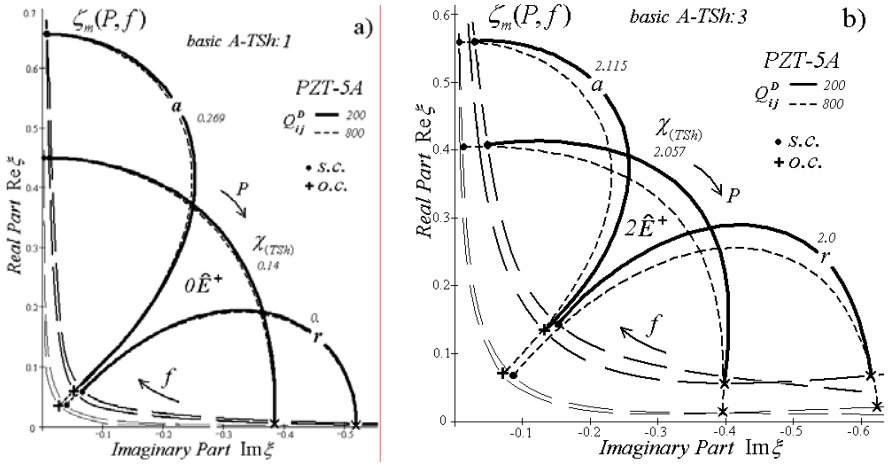

Fig. 9 a,b . *Complex dispersion characteristics* $\zeta_m(P,f)$ *(39) near the basic* A-*TSh:1(a), :3(b) resonances for two quality factor's* Q^D_{ij} *values, material constants for PZT-5A.*

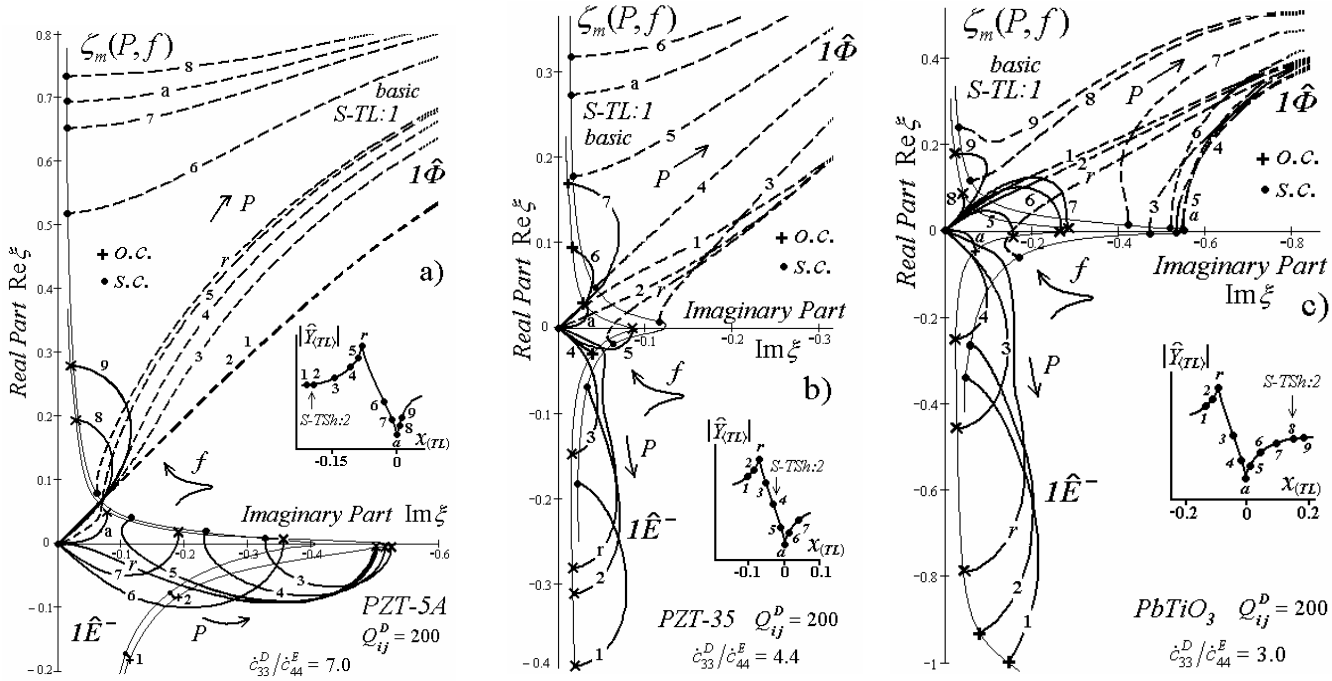

Fig. 10 a,b,c . *Complex dispersion characteristics* $\zeta_m(P,f)$ *(39) near the basic "*S-*TL:1" resonance with quality factor* Q^D_{ij}*=200 , material constants for PZT-5A (a), PZT-35 (b),* $PbTiO_3$ *(c). Inserted – the* $\left|\hat{\mathrm{Y}}_{\langle TL\rangle}\right|$ *characteristic with reference frequencies.*

Near the *"*A-*TSh: odd n"* resonance, decomposing the expressions (79),(80) on relatively small parameters of loss factors and frequency displacement (71), we have

$$\left(\zeta_m^{\langle sc|oc\rangle}\right)^{-2}\Big|_{basic}^{\text{A-}TSh:\,odd\,n} \simeq \mathrm{i}\,\vartheta_{1(3)}\cdot\frac{4}{\pi^2 n_{TSh}^2}\,Q_{\langle r|a\rangle}\frac{1}{1+\mathrm{i}\,y_{\langle r|a\rangle}}\quad , \tag{82}$$

with their absolute minimums

$$min\left(\zeta_m^{\langle sc|oc\rangle}\right)_{\langle r|a\rangle} \simeq (1-\mathrm{i})\frac{\pi}{2\sqrt{2\vartheta_{1(3)}}}\cdot\frac{n_{TSh}}{\sqrt{Q_{\langle r|a\rangle}}}, \tag{83}$$

where $y_{\langle r|a\rangle} = 2Q_{\langle r|a\rangle}\chi_{\langle r|a\rangle}$ is the generalized frequency displacement, the s.c. regime corresponds to the resonance (*r*), and the o.c. regime corresponds to the antiresonance (*a*) of the elementary admittance $\widehat{\mathrm{Y}}_{\langle TSh\rangle}$ with its resonance Q_r and antiresonance Q_a quality factors, and the resonance χ_r and antiresonance χ_a frequency displacements. For the *TSh*-mode [27], $Q_a \cong Q_{44}^D$ at the fundamental harmonic $n_{TSh}=1$, and $Q_a \cong Q_{44}^E$ at higher harmonics with $n_{TSh}\geq 3$, then $Q_r = Q_{44}^E$ for all n_{TSh}.

In the both cases, each ζ_m^{sc} and ζ_m^{oc} wave-number has a minimum (77),(83) at the resonance and antiresonance, respectively. The minima are directly proportional to the harmonic number *n*, inversely proportional to the square root of the resonance or antiresonance quality factors [9],[27] of the respective elementary *TL* (*TSh*) mode, and do not directly depend on CEMC. The numerically calculated dispersion curves (39) and corresponding elementary normalized admittance amplitude-frequency characteristics are shown in Figs. 8-10 , which support the analytical results.

B2. *Pure Non-Basic (Spurious) "S-TSh:even n" and "A-TL:even n" resonances.*

Such a condition for the best performance is provided, for example, for the set of practical values $\dot{c}_{33}^D/\dot{c}_{44}^E = (\{4,6\}/2)^2, (\{8,10,12\}/4)^2, ... = (n_{even\ TSh}/n_{even\ TL})^2$, when the even-order *TSh*- and *TL*-mode resonances coincide, respectively, and the dispersion branches near the ξ-origin are determined then by the predominant terms with $\Delta_3^{sc,oc}$ coefficients in (56),(57) and (63),(64).

B2-S. For the pure non-basic "S-*TSh: even n*" resonances with $\left|\cot \mathrm{K}_{\langle TSh\rangle}\right| >> 1$ when $\mathrm{K}_{\langle TSh\rangle} \simeq \pi n_{TSh}/2$, $n_{TSh} = 2,4,6...$, near the frequency of some "*TL: even n*" resonance with $\tan \mathrm{K}_{\langle TL\rangle} \approx 0$ (far enough from any basic odd-order *TL* resonance, as in ex.: M1,2,3<S> *PZT-5A* and $PbTiO_3$ for S-*TSh:4,6*; *PZT-35* for S-*TSh:4*):

$$\left(\zeta_m^{sc}\right)^2 \Big|_{non-basic}^{S-TSh:\ even\ n} \cong \frac{2}{\vartheta_{1(3)}}\mathrm{K}_{\langle TSh\rangle}\tan \mathrm{K}_{\langle TSh\rangle}\ , \quad \left(\zeta_m^{oc}\right)^2 \Big|_{non-basic}^{S-TSh:\ even\ n} \cong \frac{2}{\vartheta_{1(3)}}\mathrm{K}_{\langle TSh\rangle}\tan \mathrm{K}_{\langle TSh\rangle}\cdot\frac{1}{\left(1+2\kappa_{TSh}^2\right)}\ , \quad (84)$$

then $$\left(\zeta_m^{oc}\right)^2 \Big/ \left(\zeta_m^{sc}\right)^2 \cong \left(1+2\kappa_{TSh}^2\right)^{-1}\ .$$

Supposing $-\mathrm{i}\,\widehat{\mathrm{Y}}_{\langle TL\rangle} \simeq 1$ for an even *TSh* resonance located between some odd basic *TL* resonances, it follows that the wave-numbers ratio is a constant of frequency determined largely by the effective CEMC κ_{TSh}^2 corresponding to a *TSh* (even) resonance. Near the "S-*TSh: even n"* resonance for relatively small frequency displacements (71)

$$\left(\zeta_m^{sc}\right)^{-2} \Big|_{non-basic}^{S-TSh:\ even\ n} \simeq \mathrm{i}\,\vartheta_{1(3)}\cdot\frac{4}{\pi^2 n_{TSh}^2}\,Q_{44}^E\frac{1}{1+\mathrm{i}\,y}\ , \quad (85)$$

with the absolute resonance minimum

$$min\ \zeta_m^{sc}\Big|_{non-basic}^{S-TSh:\ even\ n} \simeq (1-\mathrm{i})\frac{\pi}{2\sqrt{2\vartheta_{1(3)}}}\frac{n_{TSh}}{\sqrt{Q_{44}^E}}\ , \quad (86)$$

where $y = 2Q_{44}^{E}\,\chi_{(TSh:\,n)}$. It is directly proportional to the harmonic number n_{TSh}, and inversely proportional to $\sqrt{Q_{44}^{E}}$ of the shear resonance quality factor only (Fig. 11 a,b).

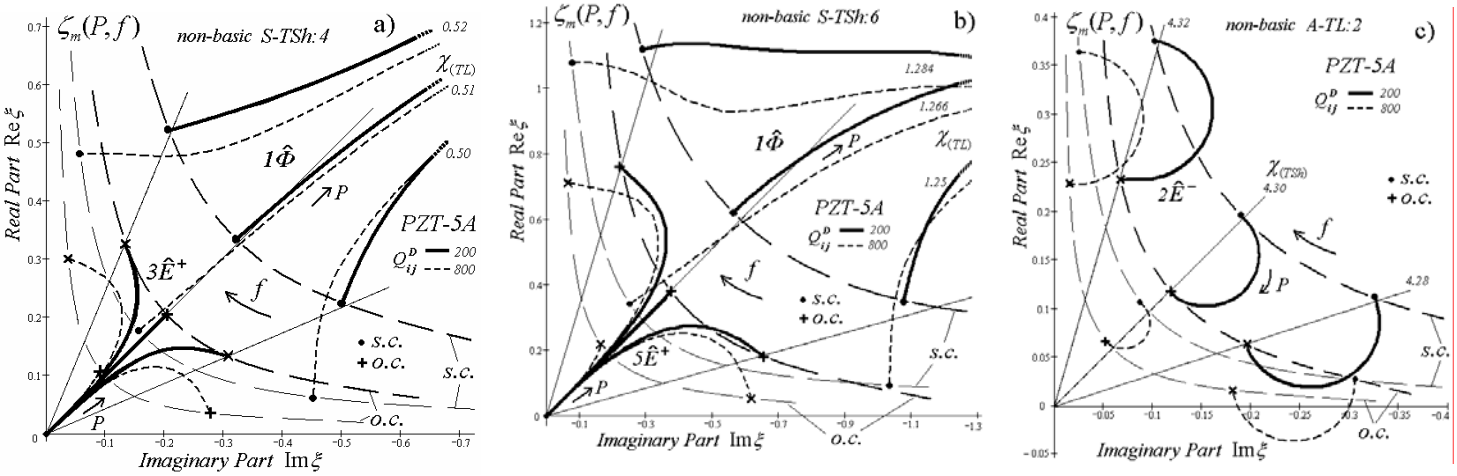

Fig. 11 a,b,c . *Complex dispersion characteristics* $\zeta_m(P,f)$ *(39) near the pure non-basic* S-*TSh: 4(a), :6(b) and* A-*TL: 2(c) resonances for two quality factor's* Q_{ij}^{D} *values, material constants for PZT-5A. The s.c. and o.c. points lie largely on the same ray shown for three frequency displacements.*

B2-A. For the pure non-basic "A-*TL: even n*" resonances with $\left|\cot \mathrm{K}_{\langle TL\rangle}\right| >> 1$ when $\mathrm{K}_{\langle TL\rangle} \simeq \pi n_{TL}/2$, $n_{TL} = 2,4,6...$, near the frequency of some "*TSh: even n*" resonance with $\tan \mathrm{K}_{\langle TSh\rangle} \approx 0$ (far enough from any basic odd *TSh* resonance, as in an example м2<A> *PZT-35* for A-*TL:2*):

$$\left(\zeta_m^{oc}\right)^2 \Big|_{non-basic}^{\text{A}-TL:\,even\ n} \cong \frac{2}{\vartheta_{1(2)}}\mathrm{K}_{\langle TL\rangle}\tan \mathrm{K}_{\langle TL\rangle}\ , \qquad \left(\zeta_m^{sc}\right)^2 \Big|_{non-basic}^{\text{A}-TL:\,even\ n} \cong \frac{2}{\vartheta_{1(2)}}\mathrm{K}_{\langle TL\rangle}\tan \mathrm{K}_{\langle TL\rangle}\cdot\frac{1}{\left(1-2\kappa_{TL}^2\right)}\ , \qquad (87)$$

then $$\left(\zeta_m^{oc}\right)^2 \Big/ \left(\zeta_m^{sc}\right)^2 \cong \left(1-2\kappa_{TL}^2\right).$$

so that the wave-number ratio is a constant determined by the effective CEMC κ_{TL}^2. Near the *"*A-*TL: even n"* resonance for relatively small frequency displacements (71)

$$\left(\zeta_m^{oc}\right)^{-2} \Big|_{non-basic}^{\text{A}-TL:\,even\ n} \simeq \mathrm{i}\,\vartheta_{1(2)}\cdot\frac{4}{\pi^2 n_{TL}^2}\,Q_{33}^{D}\frac{1}{1+\mathrm{i}\,y}\ , \qquad (88)$$

with the absolute resonance minimum

$$min\ \ \zeta_m^{oc}\Big|_{non-basic}^{\text{A}-TL:\,even\ n} \simeq (1-\mathrm{i})\frac{\pi}{2\sqrt{2\vartheta_{1(2)}}}\frac{n_{TL}}{\sqrt{Q_{33}^{D}}}\ , \qquad (89)$$

where $y = 2Q_{33}^{D}\,\chi_{(TL:\,n)}$. It is directly proportional to the harmonic number n_{TL}, and inversely proportional to $\sqrt{Q_{33}^{D}}$ of the *TL* antiresonance quality factor only (Fig. 11 c). For the electrode resistivity dependence of the lateral wave-number with a screen effect related to piezoelectricity, we have according to (67):

$$\zeta_m^{-2}(\omega,P) = \left(\zeta_m^{oc}\right)^{-2}\left(1-\frac{2\kappa_{TL}^2}{1+2\,\mathrm{i}\,\nu P^2}\right)\ . \qquad (90)$$

Summarizing, it particularly follows from the Statement that the resonance $\zeta_m^{sc}(\omega)$ and antiresonance $\zeta_m^{oc}(\omega)$ branches of the basic modes go consequently near the origin of dispersion plane, so that their ratio squared shows classical resonance-antiresonance character. Meantime, as there is no even-order resonances in the elementary mode admittance frequency characteristic (3), the branches of the non-basic modes go and both their absolute minima of $\zeta_m^{sc,\,oc}$ are reached simultaneously (at the same frequency). They both are located on the same ray (Fig. 11) near the resonance and their difference $\left|\zeta_m^{sc}\right| > \left|\zeta_m^{oc}\right|$ is pure piezoelectric, not dissipative. Note, there is equality $\zeta_m^{oc} \equiv \zeta_m^{sc}$ for a non-piezoelectric case with $-\mathrm{i}\widehat{\mathrm{Y}}_{\langle TL,\,TSh\rangle} = 1$.

B3. ***Suppressed Branch for Coupled Basic "S-TL: odd n" with non-Basic "S-TSh: even n", and for Basic "A-TSh: odd n" with non-Basic "A-TL: even n" resonances.***

Any *TL* resonance (basic for **S**- and non-basic for **A**-configuration) is always formed by the respective $m\widehat{E}^-$ branch (Fig. 5). For a certain n_{TSh}-order *TSh* resonance (even-order for **S**- and odd-order for **A**-configuration), it can be formed in two ways depending on the $\dot{c}_{33}^D/\dot{c}_{44}^E$ ratio: by one of the upper $m\widehat{E}^+$ *TSh* branches (Fig. 5) – pure *TSh* resonances under the (B1),(B2) conditions; or by one of the lower $m\widehat{E}^-$ *TL* branches (Fig. 5) when both coupled nearby *TSh* and *TL* resonances are formed consequently by the same $m\widehat{E}^-$ branch under the (B3),(B4) conditions between (68),(69) zeros. In the last case for the **S**-configuration, the "pushed out" $m\widehat{E}^+$ branch is forming the edge mode [10] of the corresponding order.

As typically $\left|\mathrm{K}^2_{\langle TSh\rangle}/\mathrm{K}^2_{\langle TL\rangle}\right| \cong \dot{c}_{33}^D/\dot{c}_{44}^E \in 2.3\ldots9$, for coincident *TL* and *TSh* resonances $n_{TSh}^2 \cong \left(\dot{c}_{33}^D/\dot{c}_{44}^E\right)n_{TL}^2 > > n_{TL}^2$. In the case of **S**-configuration, for the non-basic n_{TSh}-order *"S-TSh: even n"* resonance $\mathrm{K}_{\langle TSh\rangle} \simeq \omega b\sqrt{\rho/\dot{c}_{44}^E} \simeq 0.5\pi\, n_{TSh}$, then the thickness *TL* wave-number is $\mathrm{K}_{\langle TL\rangle} \cong 0.5\pi\, n_{TSh}\Big/\sqrt{\dot{c}_{33}^D/\dot{c}_{44}^E}$. As seen from the expression (56), the effect of the *TL*-mode influence on the *TSh*-resonance dispersion is largely determined by the sign and magnitude of the factor $\left(1-2\underset{\sim}{\theta}_2^{sc|\,oc}\tan\mathrm{K}_{\langle TL\rangle}/\mathrm{K}_{\langle TL\rangle}\right)$. The inverse effect of the non-basic *TSh*-mode influence on the basic n_{TL}-order *TL*-resonance dispersion is largely determined by the sign and magnitude of the factor $\left(1+2\underset{\sim}{\theta}_3^{sc|\,oc}\cot\mathrm{K}_{\langle TSh\rangle}/\mathrm{K}_{\langle TSh\rangle}\right)$ with $\mathrm{K}_{\langle TSh\rangle} \cong 0.5\pi\, n_{TL}\cdot\sqrt{\dot{c}_{33}^D/\dot{c}_{44}^E}$. Analogues procedure can be performed for the **A**-configuration based on (63).

Typically the derivative coefficients $\vartheta_{1(2,3)} \simeq 1\pm0.3$ of the characteristic equation (14), so that the parameters $\theta_{(2,3)} \simeq 1$. After decomposing (68),(69) near the respective *n*-order resonance (71), the corresponding frequency displacements satisfying the aforementioned conditions are

$$\tilde{\chi} \simeq -8\dot{\theta}_{\langle 2|\,3\rangle}\Big/\pi^2 n^2_{\langle odd|even\rangle} \approx -1\Big/n^2_{\langle odd|even\rangle}. \qquad (91)$$

Note that the relative resonance frequency interval of an elementary mode $f_{a(n)}/f_{r(n)}-1\simeq k^2/n^2$ (71) is nearly k^2 less in magnitude. In common for both **S**- and **A**-configurations, it follows as an estimation that any n_{TSh}-order *TSh* resonance is formed by the $m\widehat{E}^-$ *TL*-branch if that resonance frequency is located near some n_{TL}-order *TL*- resonance inside the interval of its relative frequency displacements $\sim\left(-1/n_{TL}^2\ \ldots+1/n_{TSh}^2\right)$.

From the first-derivative approach analysis for the typical for PZT-ceramic interval of the $\dot{c}_{33}^D/\dot{c}_{44}^E$ ratio it follows in particular that:

– the basic "A-*TSh*: $n_{TSh}=1$" resonance is always formed by the $0\widehat{E}^+$ *TSh*-branch, and the non-basic "S-*TSh*: $n_{TSh}=2$" resonance is formed largely by the $1\widehat{E}^-$ *TL*-branch common with the basic "S-*TL*: $n_{TL}=1$" resonance;

– the non-basic "S-*TSh*: $n_{TSh}=6$" for $\dot{c}_{33}^D/\dot{c}_{44}^E\in\sim 3.8...5.1$ (M2<S> *PZT-35*) and "S-*TSh*: $n_{TSh}=8$" for $\dot{c}_{33}^D/\dot{c}_{44}^E\in\sim 6.9...9.0$ (M3<S> *PZT-5A*) resonances are formed by the $3\widehat{E}^-$ *TL*-branch common with the basic "S-*TL*: $n_{TL}=3$" resonance, otherwise they both are formed by the respective $m\widehat{E}^+$ *TSh*-branch, $m=6,8$;

– the basic "A-*TSh*: $n_{TSh}=3$" for $\dot{c}_{33}^D/\dot{c}_{44}^E\in\sim 2.0...4.0$ (M1<A> $PbTiO_3$) and "A-*TSh*: $n_{TSh}=5$" for $\dot{c}_{33}^D/\dot{c}_{44}^E\in\sim 5.8...11.0$ (M3<A> *PZT-5A*) resonances are formed by the $2\widehat{E}^-$ *TL*-branch common with the non-basic "A-*TL*: $n_{TL}=2$" resonance, otherwise they both are formed by the respective $m\widehat{E}^+$ *TSh*-branch, $m=3,5$.

The effect of transient conditions can be illustrated in M2<A> *PZT-35* for the *"*A-*TSh:3"* and *"*A-*TL:2"* resonances.

Due to separation of the *TL* and *TSh* modes influence on the dispersion as factors in the first-order derivative approach, as seen from Fig. 8a,b for the basic "S-*TL: 1*" resonance, there is no distortion from the *TSh*-mode in the dispersion $W=\mathrm{i}(\zeta_m^{oc})^2/(\zeta_m^{sc})^2$ characteristic, and it fully follows the elementary admittance $\widehat{\mathrm{Y}}_{\langle \mathrm{TL}\rangle}$. According to the numerical analysis conducted, the coincidence of the dispersion *W*- and admittance *V*-characteristics takes place for both amplitude (typically no more then several *dB*) and phase representation.

B4. *Exactly Coinciding Basic "S-TL: odd n" with non-Basic "S-TSh: even n", Basic "A-TSh: odd n" with non-Basic "A-TL: even n" resonances.*

B4-S. For the basic *"*S-*TL: odd* n_{TL}*"* and non-basic *"*S-*TSh: even* n_{TSh}*"* resonances with $\left|\tan \mathrm{K}_{\langle TL\rangle}\right|>>1$ and $\left|\cot \mathrm{K}_{\langle TSh\rangle}\right|>>1$ together, it follows $\mathrm{K}_{\langle TL\rangle}\simeq\pi n_{TL}/2$ for odd $n_{TL}=1,3,5...$ and $\mathrm{K}_{\langle TSh\rangle}\simeq\pi n_{TSh}/2$ for even $n_{TSh}=2,4,6...$. Such a condition is provided, for example, for practical values $\dot{c}_{33}^D/\dot{c}_{44}^E=\sim(2/1)^2$, $(\{6,8\}/3)^2$, $(\{8,10,12,14\}/5)^2$, $...=\left(\text{even}\, n_{TSh}/\text{odd}\, n_{\mathrm{TL}}\right)^2$, when an even-order "S-*TSh: n*" and an odd-order "S-*TL: n*" resonances coincide, respectively. The dispersion branches near the ξ-origin then are determined by the predominant terms with $\underset{\sim}{\Delta}_1^{sc,oc}$ coefficients in (56),(59) as follows:

$$\mathrm{i}\left(\zeta_m^{oc}\right)^2 \Big/ \left(\zeta_m^{sc}\right)^2 \Big|_{\substack{\text{S-}TL\text{: odd } n \\ \& \\ \text{S-}TSh\text{: even } n}} \cong \left(\underset{\sim}{\Delta}_1^{sc} \Big/ \underset{\sim}{\Delta}_1^{oc}\right) \cdot \widehat{\mathrm{Y}}_{\langle TL\rangle} \quad , \tag{92}$$

$$\left(\zeta_m^{sc}\right)^{-2} \Big|_{\substack{\text{S-}TL\text{: odd } n \\ \& \\ \text{S-}TSh\text{: even } n}} \cong -\underset{\sim}{\Delta}_1^{sc} \frac{\cot \mathrm{K}_{\langle TSh\rangle} \cdot \tan \mathrm{K}_{\langle TL\rangle}}{\mathrm{K}_{\langle TSh\rangle} \cdot \mathrm{K}_{\langle TL\rangle}} \cdot \left(-\mathrm{i}\, \widehat{\mathrm{Y}}_{\langle TL\rangle}\right) \quad , \tag{93}$$

$$\left(\zeta_m^{oc}\right)^{-2} \Big|_{\substack{\text{S-}TL\text{: odd } n \\ \& \\ \text{S-}TSh\text{: even } n}} \cong -\underset{\sim}{\Delta}_1^{oc} \frac{\cot \mathrm{K}_{\langle TSh\rangle} \cdot \tan \mathrm{K}_{\langle TL\rangle}}{\mathrm{K}_{\langle TSh\rangle} \cdot \mathrm{K}_{\langle TL\rangle}} \quad . \tag{94}$$

Decomposing (93),(94) on relatively small parameters of loss factors and frequency displacement (71), when a non-basic *TSh* resonance $\cot \mathrm{K}_{\langle TSh\rangle} \to \infty$ coincides with a basic *TL* antiresonance $\tan \mathrm{K}_{\langle TL\rangle} \to \infty$ with $f_0 \equiv f_{r(TSh:\, even\ n)} = f_{a(TL:\, odd\ n)}$, then

$$\zeta_m^{oc} \Big|_{\substack{\text{S-}TL\text{: odd } n \\ antires. \\ \& \\ \text{S-}TSh\text{: even } n}} \simeq \frac{\pi^2}{8\sqrt{\underset{\sim}{\Delta}_1^{oc}}} \cdot \frac{n_{TL}\, n_{TSh}}{\sqrt{Q_{33}^D\, Q_{44}^E}} \left(-\mathrm{i} + y\right) \quad , \tag{95}$$

where $y = 2Q\chi$ and Q here is the mean of Q_{33}^D and Q_{44}^E. It behaves linearly (Fig. 12a) on the relative frequency displacement $\chi = f/f_0 - 1$ (71), is pure imaginary at the *TL* antiresonance with its absolute minimum value ever possible proportional to $1/Q$. For the s.c. wave-number frequency dependence

$$\zeta_m^{sc} \Big|_{\substack{\text{S-}TL\text{: odd } n \\ antires. \\ \& \\ \text{S-}TSh\text{: even } n}} \cong -\mathrm{i} \frac{\pi^2}{8\sqrt{\underset{\sim}{\Delta}_1^{sc}}} \cdot \frac{n_{TL}\, n_{TSh}}{\sqrt{Q_{33}^D Q_{44}^E}} \sqrt{\left(1 + \mathrm{i}\, 2Q_{44}^E \chi\right) \cdot \left[1 + \mathrm{i}\, 2Q_{33}^D \left(\chi + \mathrm{k}_t^2 \frac{4}{\pi^2 n_{TL}^2}\right)\right]} \quad , \tag{96}$$

with its absolute antiresonance (*a*) and resonance (*r*) minima values corresponding to ± 1, $Q = \left\langle Q_{44}^E \middle| Q_{33}^D \right\rangle$, respectively, for $k_t^2 Q \gg 1$ (Fig. 12a)

$$min\left(\zeta_m^{sc}\right)_{\langle a|r\rangle} \Big|_{\substack{\text{S-}TL\text{: odd } n \\ antires. \\ \& \\ \text{S-}TSh\text{: even } n}} \cong (\pm 1 - \mathrm{i}) \frac{\pi}{4\sqrt{\underset{\sim}{\Delta}_1^{sc}}} \cdot \frac{n_{TSh}}{\sqrt{Q}}\, \mathrm{k}_t \quad , \tag{97}$$

which is proportional typically to $1/\sqrt{Q}$ and additionally to CEMC.

Analogously, when a non-basic *TSh* resonance $\cot \mathrm{K}_{\langle TSh\rangle} \to \infty$ coincides with a basic *TL* resonance $\left|\widehat{\mathrm{Y}}_{\langle TL\rangle}\right| \to \infty$ with $f_0 \equiv f_{r(TL:\, odd\ n)} = f_{r(TSh:\, even\ n)}$ and joint frequency displacement $\chi = f/f_0 - 1$, then

$$\zeta_m^{sc} \Big|_{\substack{\text{S-}TL\text{: odd } n \\ res. \\ \& \\ \text{S-}TSh\text{: even } n}} \simeq \frac{\pi^2}{8\sqrt{\underset{\sim}{\Delta}_1^{sc}}} \cdot \frac{n_{TL}\, n_{TSh}}{\sqrt{Q_{33}^D Q_{44}^E}} \left(-\mathrm{i} + y\right) \quad , \tag{98}$$

where $y = 2Q\chi$ and Q here is the mean of Q_{33}^D and Q_{44}^E. For the o.c. wave-number frequency dependence

$$\zeta_m^{oc} \Big|_{\substack{\text{S-}TL\text{: odd } n \\ res. \\ \& \\ \text{S-}TSh\text{: even } n}} \cong -\mathrm{i} \frac{\pi^2}{8\sqrt{\underset{\sim}{\Delta}_1^{oc}}} \cdot \frac{n_{TL} n_{TSh}}{\sqrt{Q_{44}^E Q_{33}^D}} \sqrt{\left(1 + \mathrm{i}\, 2Q_{44}^E \chi\right) \cdot \left[1 + \mathrm{i}\, 2Q_{33}^D \left(\chi - \mathrm{k}_t^2 \frac{4}{\pi^2 n_{TL}^2}\right)\right]} \quad , \tag{99}$$

with its absolute antiresonance (*a*) and resonance (*r*) minima values corresponding to ± 1, $Q = \left\langle Q_{33}^D \middle| Q_{44}^E \right\rangle$, respectively, for $k_t^2 Q \gg 1$ (Fig. 12b)

$$min\left(\zeta_m^{oc}\right)_{\langle a|r\rangle} \Big|_{\substack{\text{S-}TL\text{: odd } n \\ res. \\ \& \\ \text{S-}TSh\text{: even } n}} \cong (\pm 1 - \mathrm{i}) \frac{\pi}{4\sqrt{\underset{\sim}{\Delta}_1^{oc}}} \cdot \frac{n_{TSh}}{\sqrt{Q}}\, \mathrm{k}_t \quad . \tag{100}$$

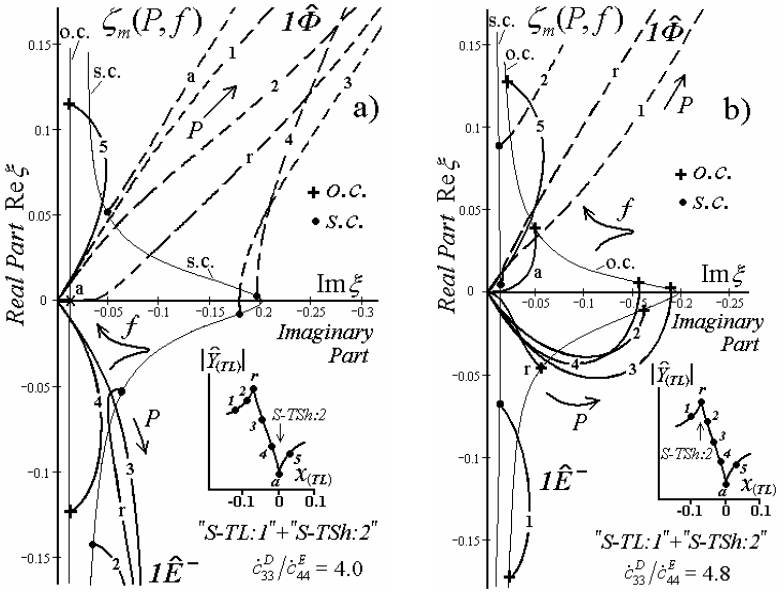

Fig. 12 a,b. *Complex dispersion characteristics* $\zeta_m(P,f)$ *(39) near the basic "*S-*TL:1" and non-basic "*S-*TSh:2" resonances with their "antiresonance" (a) and "resonance" (b) coincidence. Material constants for PZT-35 type,* $Q_{ij}^D = 200$, $\dot{c}_{44}^D \cdot 10^{-10} = 5.82\,(a), 5.03\,(b)$. *Inserted – the* $\left|\widehat{\mathrm{Y}}_{\langle TL\rangle}\right|$ *characteristic with the reference frequencies.*

For both above cases, the maximum ("peak") values of $\left|\mathrm{Im}\,\zeta_m\right|$ are respectively ($k_t^2 Q \gg 1$)

$$peak\ \ \zeta_m^{\langle sc|oc\rangle}\ \Big|_{\text{S-}TSh\text{: even } n}^{\text{S-}TL\text{: odd } n\ \text{antires.}|\,\text{res.}} \cong -\mathrm{i}\,\frac{1}{\sqrt{\underset{\sim}{\Delta}_1^{\langle sc|oc\rangle}}}\,\frac{n_{TSh}}{2n_{TL}}\,\mathrm{k}_t^2 \quad . \tag{101}$$

The exact coincidence of the "S-*TL:1*" and "S-*TSh:2*" resonances provides (98) extremely low $\sim 2/Q$ completely imaginary s.c. lateral wave-number at the thickness resonance with decay distance $x_0/2b \approx Q/4$, which in practical view can afford sufficiently widened effective radiating surface of a transducer. From the approximations (54),(55) it follows for the coupled case that the absolute minimum in (95) and (98) is near equal to the product of respective minima (77),(86) and (83),(89) for the pure basic and non-basic modes:

$$\min \zeta_m\Big|^{fully\ coupled} \simeq \min \zeta_{m1}\Big|^{pure\ basic} \cdot \min \zeta_{m2}\Big|^{pure\ non-basic} \quad . \tag{102}$$

B4-A. For the basic *"*A-*TSh: even* n_{TL}*"* and non-basic *"*A-*TL: odd* n_{TSh}*"* resonances with $\left|\tan \mathrm{K}_{\langle TSh\rangle}\right| >> 1$ and $\left|\cot \mathrm{K}_{\langle TL\rangle}\right| >> 1$ together, it follows $\mathrm{K}_{\langle TSh\rangle} \simeq \pi n_{TSh}/2$ for odd $n_{TSh} = 1,3,5...$ and $\mathrm{K}_{\langle TL\rangle} \simeq \pi n_{TL}/2$ for even $n_{TL} = 2,4,6....$ Such a condition is provided, for example, for practical values $\dot{c}_{33}^D/\dot{c}_{44}^E = (\{3,5\}/2)^2$, $(\{7,9,11\}/4)^2$, $... = \left(\mathrm{odd}\, n_{TSh}/\mathrm{even}\, n_{\mathrm{TL}}\right)^2$, when an odd-order "A-*TSh: n*" and an even-order "A-*TL: n*" resonances coincide, respectively. The dispersion branches near the ξ-origin then are determined by the predominant terms with $\underset{\sim}{\Delta}_1^{sc,oc}$ coefficients in (63),(66) as follows:

$$\mathrm{i}\left(\zeta_m^{oc}\right)^2 \Big/ \left(\zeta_m^{sc}\right)^2 \ \Big|_{\text{A-}TL\text{: even } n}^{\text{A-}TSh\text{: odd } n} \cong \left(\underset{\sim}{\Delta}_1^{sc} \Big/ \underset{\sim}{\Delta}_1^{oc}\right) \cdot \widehat{\mathrm{Y}}_{\langle TSh\rangle} \quad , \tag{103}$$

$$\left(\zeta_m^{sc}\right)^{-2} \ \Big|_{\text{A-}TL\text{: even } n}^{\text{A-}TSh\text{: odd } n} \cong -\underset{\sim}{\Delta}_1^{sc} \cdot \frac{\cot \mathrm{K}_{\langle TL\rangle} \cdot \tan \mathrm{K}_{\langle TSh\rangle}}{\mathrm{K}_{\langle TL\rangle} \cdot \mathrm{K}_{\langle TSh\rangle}} \quad , \tag{104}$$

$$\left(\zeta_m^{oc}\right)^{-2}\Big|_{\substack{\text{A-}TSh\text{: odd } n\\ \&\\ \text{A-}TL\text{: even } n}} \cong -\underline{\Delta}_1^{oc}\cdot\frac{\cot \mathrm{K}_{\langle TL\rangle}\cdot\tan \mathrm{K}_{\langle TSh\rangle}}{\mathrm{K}_{\langle TL\rangle}\cdot\mathrm{K}_{\langle TSh\rangle}}\cdot\left(-\mathrm{i}\widehat{\mathrm{Y}}_{\langle TSh\rangle}\right)^{-1} \quad . \tag{105}$$

Decomposing (104),(105) on small parameters of losses and frequency displacement (71), when a non-basic *TL* resonance $\cot \mathrm{K}_{\langle TL\rangle}\to\infty$ coincides with a basic *TSh* resonance $\tan \mathrm{K}_{\langle TSh\rangle}\to\infty$ with $f_0\equiv f_{r(TL\text{: even } n)}=$ $=f_{r(TSh\text{: odd } n)}$, then

$$\zeta_m^{sc}\Big|_{\substack{\text{A-}TSh\text{: odd } n\\ res.\\ \&\\ \text{A-}TL\text{: even } n}} \simeq \frac{\pi^2}{8\sqrt{\underline{\Delta}_1^{sc}}}\cdot\frac{n_{TL}\,n_{TSh}}{\sqrt{Q_{33}^D Q_{44}^E}}\left(-\mathrm{i}+y\right) \quad , \tag{106}$$

where $y=2Q\chi$ and Q is here the mean of Q_{33}^D and Q_{44}^E. It behaves linearly on frequency displacement $\chi=f/f_0-1$ (71), is pure imaginary at the *TSh* resonance with its minimum absolute value ever possible proportional to $1/Q$. For the o.c. wave-number frequency dependence

$$\zeta_m^{oc}\Big|_{\substack{\text{A-}TSh\text{: odd } n\\ res.\\ \&\\ \text{A-}TL\text{: even } n}} \cong -\mathrm{i}\frac{\pi^2}{8\sqrt{\underline{\Delta}_1^{oc}}}\cdot\frac{n_{TL}\,n_{TSh}}{\sqrt{Q_{33}^D Q_{44}^E}}\sqrt{\left(1+\mathrm{i}\,2Q_{33}^D\chi\right)\cdot\left[1+\mathrm{i}\,2Q_{44}^E\left(\chi-\mathrm{k}_{15}^2\frac{4}{\pi^2 n_{TSh}^2}\right)\right]} \tag{107}$$

with its absolute antiresonance (*a*) and resonance (*r*) minima values corresponding to ± 1, $Q=\left\langle Q_{44}^E\middle|Q_{33}^D\right\rangle$, respectively, for $k_{15}^2 Q\gg 1$

$$min\left(\zeta_m^{oc}\right)_{\langle a|r\rangle}\Big|_{\substack{\text{A-}TSh\text{: odd } n\\ res.\\ \&\\ \text{A-}TL\text{: even } n}} \cong \left(\pm 1-\mathrm{i}\right)\frac{\pi}{4\sqrt{\underline{\Delta}_1^{oc}}}\cdot\frac{n_{TL}}{\sqrt{Q}}\,\mathrm{k}_{15} \quad . \tag{108}$$

Analogously, when a non-basic *TL* resonance $\cot \mathrm{K}_{\langle TL\rangle}\to\infty$ coincides with a basic *TSh* antiresonance $\widehat{\mathrm{Y}}_{\langle TSh\rangle}\to 0$ with $f_0\equiv f_{r(TL\text{: even } n)}=f_{a(TSh\text{: odd } n)}$ and joint frequency displacement $\chi=f/f_0-1$, then

$$\zeta_m^{oc}\Big|_{\substack{\text{A-}TSh\text{: odd } n\\ antires.\\ \&\\ \text{A-}TL\text{: even } n}} \simeq \frac{\pi^2}{8\sqrt{\underline{\Delta}_1^{oc}}}\cdot\frac{n_{TL}\,n_{TSh}}{\sqrt{Q_{33}^D Q_{44}^E}}\left(-\mathrm{i}+y\right) , \tag{109}$$

where $y=2Q\chi$ and Q is here the mean of Q_{33}^D and Q_{44}^E. For the s.c. wave-number frequency dependence

$$\zeta_m^{sc}\Big|_{\substack{\text{A-}TSh\text{: odd } n\\ antires.\\ \&\\ \text{A-}TL\text{: even } n}} \cong -\mathrm{i}\frac{\pi^2}{8\sqrt{\underline{\Delta}_1^{sc}}}\cdot\frac{n_{TL}\,n_{TSh}}{\sqrt{Q_{33}^D Q_{44}^E}}\sqrt{\left(1+\mathrm{i}\,2Q_{33}^D\chi\right)\cdot\left[1+\mathrm{i}\,2Q_{44}^E\left(\chi+\mathrm{k}_{15}^2\frac{4}{\pi^2 n_{TSh}^2}\right)\right]} , \tag{110}$$

with its absolute antiresonance (*a*) and resonance (*r*) minima values corresponding to ± 1, $Q=\left\langle Q_{33}^D\middle|Q_{44}^E\right\rangle$, respectively, for $k_{15}^2 Q\gg 1$

$$min\left(\zeta_m^{sc}\right)_{\langle a|r\rangle}\Big|_{\substack{\text{A-}TSh\text{: odd } n\\ antires.\\ \&\\ \text{A-}TL\text{: even } n}} \cong \left(\pm 1-\mathrm{i}\right)\frac{\pi}{4\sqrt{\underline{\Delta}_1^{sc}}}\cdot\frac{n_{TL}}{\sqrt{Q}}\,\mathrm{k}_{15} \quad . \tag{111}$$

For both above cases, the maximum ("peak") values of $\left|\mathrm{Im}\,\zeta_m\right|$ are respectively ($k_{15}^2 Q\gg 1$)

$$peak\ \ \zeta_m^{\langle oc|sc\rangle}\Big|_{\substack{\text{A-}TSh\text{: odd } n\\ res.|antires.\\ \&\\ \text{A-}TL\text{: even } n}} \cong -\mathrm{i}\frac{1}{\sqrt{\underline{\Delta}_1^{\langle oc|sc\rangle}}}\cdot\frac{n_{TL}}{2n_{TSh}}\,\mathrm{k}_{15}^2 \quad . \tag{112}$$

IV. CONCLUSION

The 3-D equations of linear piezoelectricity, including electro-mechanical damping in solid and resistance in electrodes, were used to obtain solutions for lateral dispersion characteristics of descending plane harmonic waves of arbitrary direction in an infinite thickness-polarized piezoceramic plate with traction-free surfaces. The effects of cumulative energy dissipation on the wave propagation under regimes raging from the s.c. condition through the relaxation *RC*-type dispersion resonance to the o.c. condition are examined in detail for PZT piezoceramics with three characteristic values of the *TL*-mode energy-trap figure-of-merit $\dot{c}_{33}^{D}/\dot{c}_{44}^{E}$ – less, near equal, and higher 4. The symmetric and antisymmetric eigenmodes of *TL* up to 3rd harmonic and *TSh* up to 9th harmonic vibrations of odd- and even-orders were analyzed analytically and numerically.

All branches can not be pure real any longer due to dissipation and significant characteristic changes of the dispersion curves occur mostly near the cut-off frequencies inherent to non-dissipative waves. Varying the dissipation parameters of internal loss and electrode resistance, the interaction of different branches was demonstrated – deformed and inter-connected dispersion branches with singularities take place due to acoustical and electrical coupling between surrounding regions of the plate.

The electrode resistivity effect is primarily described by the relaxation time parameter τ of unit surface running electrode resistance and PR capacitance. The extracted dispersion surfaces are located between and connect the respective classical limit dispersion s.c. (ideal electrodes) and o.c. (electrodeless) branches of planar, *TSh* and *TL* modes, and "electric potential" branches. The calculated dispersion dependences on frequency and electrode resistance are found to follow the universal scaling formula similar to those for the dielectrics characterization. Represented as a Cole-Cole diagram of the complex lateral wave-number, most dispersion branches exhibit a Debye-like semicircle dependence with extremum at $\omega\tau \simeq 1$. The lowest "potential" branch, going out from the wave-number origin at a frequency out of any thickness resonances, obeys the modified Devidson-Cole dependence linear as $(1-\mathrm{i})\sqrt{\omega\tau}$ for relatively low electrode resistances, which corresponds to the laterally uncoupled elementary space-regions. For the basic *TL* resonances of any order, the dispersion branch slope near the origin follows the character of the corresponding elementary *TL*-mode admittance: with the direction $(1-\mathrm{i})$ for its capacitive character out of the resonance-antiresonance frequency interval, $(-1-\mathrm{i})$ for its inductive character inside the resonance-antiresonance interval, and $(0-\mathrm{i})$ exactly at the resonance and antiresonance frequencies.

Stated as the Theorem, the determinant ratio of the o.c. to s.c. characteristic matrices in the **S-** (**A-**) configuration in the limit of zero lateral wave-number equals the corresponding elementary normalized complex admittance of the *TL*(*TSh*)-mode. The dispersion branches of any thickness resonance tend to reach the origin with the absolute minimums inversely proportional to the quality factors and respective first-order derivatives of the characteristic equation. The developed first-derivative approach based on characteristic matrices differentiation reveals a simple presentation and explanation of the coupled *TL*-*TSh* modes

dispersion behavior near the thickness resonances, showing the close connection between the propagation and excitation problems in a homogeneous medium. Separating the *TL* and *TSh* resonance factors, it was stated based on the Theorem that the ratio of the o.c. to s.c. lateral wave-numbers squared near the basic and/or non-basic thickness resonances is largely determined by the corresponding complex elementary admittance. As a consequence, the frequencies and bandwidth of the resonance dispersion minimums coincide with those for the elementary admittance; for the basic modes, the ratio of their consecutive s.c. and o.c. minimums is determined by the ratio of the resonance and antiresonance quality factors of the elementary admittance; and for the non-basic modes, the ratio of simultaneous s.c. and o.c. dispersion minimums is determined by the corresponding effective CEMC. The exact coincidence of the basic and non-basic thickness resonances for certain $\dot{c}_{33}^{D}/\dot{c}_{44}^{E}$ ratios provides minimal resonance lateral dispersion ever possible.

Real PR electrodes are resistive – that adds extra energy losses and hence changes the wave dispersion relationships. It especially becomes significant for up-to-date thin high-frequency PRs with large major surfaces when the lateral vibration characteristics distribution is critical. The developed approach can be applied to a piezoceramic plate with polarization direction along the major surfaces (a “shear” plate), and to piezoelectrics of different symmetry.

REFERENCES

[1] D.A. Berlincourt, D.R. Curran, and H. Jaffe, *Piezoelectric and Piezomagnetic Materials and Their Function in Transducers. Physical Acoustics*, vol. 1, part A, Editor - W.P.Mason, New York: Academic Press, 1964.

[2] OCT 11 0444-87. *Piezoceramic Materials. Specifications*, Moscow: ElectronStandard, 1988.

[3] T.R. Meeker, "Thickness mode piezoelectric transducers,” *Ultrasonics*, vol. 10-1, pp. 26-36, 1972.

[4] K. Yamada and H. Shimizu, “Thickness-extensional trapped-energy mode transducers with no inharmonic spurious modes for any size of vibration area,” *Proc. IEEE Ultrasonics Symposium*, 1984, pp. 383-387.

[5] T. Yamada and N. Niizeki, “Admittance of piezoelectric plates vibrating under the perpendicular field excitation,” *Proc. IEEE*, vol. 58, no. 6, pp. 941–942, 1970.

[6] IEC Standard. *Guide to Dynamic Measurements of Piezoelectric Ceramics with High Electro-Mechanical Coupling*, Publication 483, 1976.

[7] R. Holland and E.P. EerNisse, *Design of Resonant Piezoelectric Devices*, Cambridge: MIT Press, 1968.

[8] M. Onoe, H.F. Tiersten, and A.H. Meitzler, "Shift in the location of resonant frequencies caused by large electromechanical coupling in thickness-mode resonators," *JASA*, vol. 35, no. 1, pp. 36-42, 1963.

[9] A.V. Mezheritsky, “Elastic, dielectric and piezoelectric losses in piezoceramics – how it works all together,” *IEEE Trans. Ultrason., Ferroelect., Freq. Contr*., vol. 51, no. 6, pp. 695-707, 2004.

[10] D.C. Gazis and R.D. Mindlin, “Extensional vibrations and waves in a circular disk and a semi-infinite plate,” *J. App. Mech.*, vol. 27, pp. 541-547, 1960.

[11] H.F. Tiersten, “Wave propagation in an infinite piezoelectric plate,” *J. Acoust. Soc. Amer*., vol. 35, pp. 234–239, 1963

[12] A.A. Comparini and J.J. Hannon, “Flexural, width-shear, and width-twist vibrations of thin rectangular crystal plates,” *IEEE Trans. Ultrason., Ferroelect., Freq. Contr*., vol. SU-21, no. 2, pp. 130-135, 1974.

[13] P.C.Y. Lee and N. Liu, “Plane harmonic waves in an infinite piezoelectric plate with dissipation,” *IEEE Trans. Ultrason., Ferroelect., Freq. Contr*., vol. 51, no. 12, pp. 1629-1638, 2004.

[14] I.A. Viktorov, *Rayleigh and Lamb waves - Physical Theory and Applications,* New York: Plenum, 1967.

[15] A.V. Mezheritsky, “Electrical measurements of a high-frequency, high-capacitance piezoceramic

resonator with resistive electrodes," *IEEE Trans. Ultrason., Ferroelect., Freq. Contr.*, vol. 52, no. 8, pp. 1229-1238, 2005.
[16] P. Schnabel, "Dispersion of thickness vibration of piezoceramic disk resonators," *IEEE Trans. Ultrason., Ferroelect., Freq. Contr.*, vol. SU-25, no. 1, pp. 16-24, 1978.
[17] K. Blatekjaer, K.A. Ingebrigtsen, and H. Skeie, "A method for analyzing waves in structures consisting of metal strips on dispersive media," *IEEE Trans. ED-20*, pp. 1133-1138, 1973.
[18] G.S. Kino, *Acoustic Waves: Devices, Imaging and Analog Signal Processing*. Englewood Cliffs, NJ: Prentice-Hall, 1987.
[19] V.P. Plessky, S.V. Biryukov, and J. Koskela , "Harmonic admittance and dispersion equations – the Theorem," *IEEE Trans. Ultrason., Ferroelect., Freq. Contr.*, vol. 49, no. 4, pp. 528-534, 2002.
[20] Yu.V. Gulyaev, I.E. Kuznetsova, B.D. Zaitsev, S.G. Joshi, and I.A. Borodina, "Influence of a thin layer with arbitrary conductivity on the characteristics of acoustic waves in potassium niobate," *Technical Physics Letters*, vol. 25, no. 4, pp. 302-303, 1999 (English translation of the journal, *Pis'ma v Zhurnal Tekhnicheskoi Fiziki* (Russia)).
[21] Y.-C. Lee and S.H. Kuo, "Leaky Lamb waves of a piezoelectric plate subjected to conductive fluid loading: an experimental study," *IEEE Trans. Ultrason., Ferroelect., Freq. Contr.*, vol. 53, no. 9, pp. 1617-1626, 2006.
[22] D. Damjanovic, *Hysteresis in Piezoelectric and Ferroelectric Materials. The Science of Hysteresis*, vol. 3, chapter 4, Editors - I. Mayergoyz and G. Bertotti, Amsterdam: Elsevier, 2005, pp. 337-465.
[23] I. Bunget and M. Popescu, *Physics of Solid Dielectrics*, Amsterdam: Elsevier, 1984.
[24] S. Havriliak and S. Negami, "A complex plane representation of dielectric and mechanical relaxation processes in some polymers," *Polymer*, vol. 8, no. 4, pp. 161-210, 1967.
[25] V.I. Pustovoit, "Interaction of electron flows with elastic lattice waves," *Uspekhi Fizicheskikh Nauk* (Russia), vol. 97, no. 2, pp. 257-306, 1969.
[26] R. Huang, P.C.Y. Lee, W.-S. Lin, and J.-D. Yu, "Extensional, thickness-stretch and symmetric thickness-shear vibrations of piezoceramic disks," *IEEE Trans. Ultrason., Ferroelect., Freq. Contr.*, vol. 49, no. 11, pp. 1507-1515, 2002.
[27] A.V. Mezheritsky, "Quality factor of piezoceramics," *Ferroelectrics*, vol. 266, pp. 277-304, 2002.
[28] B.R. Vasant, "Delay analysis of the distributed RC line," *Proc. 32 ACM/IEEE Conference on Automation Design*, 1995, pp. 370-375.

Appendix I : **Proof of the Theorem**

I-A. ***Proof for the*** **S-*configuration*** (basic *TL*-mode):

The determinants of the matrices $|\mathbf{MS}|$ and $|\mathbf{NS}|$ (24)-(26) with generalized elements p_{ij} are both of the same dimension and are finite at $\xi \to 0$. They can be represented with non-zero elements as

$$\left\|\mathbf{MS}_{ij}\right\|_{\xi=0} = F_0 \equiv \begin{Vmatrix} p_{11} & p_{12} & 0 \\ p_{21} & p_{22} & 0 \\ p_{31} & p_{32} & p_{33} \end{Vmatrix} = \left(p_{11}\, p_{22} - p_{12}\, p_{21}\right) p_{33} \ , \tag{I-1}$$

$$\left\|\mathbf{NS}_{ij}\right\|_{\xi=0} = U_0 \equiv \begin{Vmatrix} -p_{11} & 0 & 0 \\ p_{21} & p_{22} & 0 \\ p_{31} & p_{32} & p_{33} \end{Vmatrix} = -p_{11}\, p_{22}\, p_{33} \ , \quad i,j = 1,2,3 \ . \tag{I-2}$$

Then $$\left.\frac{\|\mathbf{MS}\|}{\|\mathbf{NS}\|}\right|_{\xi=0} = -\left(1 - \frac{p_{21}}{p_{11}} \cdot \frac{p_{12}}{p_{22}}\right) , \qquad \frac{p_{21}}{p_{11}} = \frac{e_{33}^2}{c_{33}^E \varepsilon_{33}^S} \ , \tag{I-3}$$

$$\frac{p_{12}}{p_{22}}=\frac{c_{33}^{E}\varepsilon_{33}^{S}}{e_{33}^{2}}\cdot\left(1+\frac{c_{33}^{E}}{e_{33}}\cdot\frac{\tilde{A}_{z\,(2)}}{\tilde{A}_{\varphi\,(2)}}\right)^{-1}\cdot\left.\frac{\tan(K_{(2)})}{K_{(2)}}\right|_{\xi\to 0}\quad,\qquad \left.1+\frac{c_{33}^{E}}{e_{33}}\cdot\frac{\tilde{A}_{z\,(2)}}{\tilde{A}_{\varphi\,(2)}}\right|_{\xi\to 0}=1+\frac{c_{33}^{E}\varepsilon_{33}^{S}}{e_{33}^{2}}\quad. \tag{I-4}$$

I-B. ***Proof for the*** **A-*configuration*** (basic *TSh*-mode)***:***

The determinants of the matrices $\left|\mathbf{M}\mathrm{A}\right|$ and $\left|\mathbf{N}\mathrm{A}\right|$ (24)-(26) are both of the same dimension and at $\xi\to 0$ the expressions $F(\xi)\equiv\left\|\mathbf{M}\mathrm{A}\right\|\cdot\xi$ and $U(\xi)\equiv\left(\varepsilon_{33}^{S}/\varepsilon_{11}^{S}\right)\left\|\mathbf{N}\mathrm{A}\right\|\cdot\xi^{-1}$ are finite. They can be represented with non-zero elements a_{ij} as

$$\left\|\mathbf{M}\mathrm{A}\right\|\cdot\xi=\begin{Vmatrix}\mathbf{M}\mathrm{A}_{11}\cdot\xi & \mathbf{M}\mathrm{A}_{12} & \mathbf{M}\mathrm{A}_{13}\\ \mathbf{M}\mathrm{A}_{21}\cdot\xi & \mathbf{M}\mathrm{A}_{22} & \mathbf{M}\mathrm{A}_{23}\\ \mathbf{M}\mathrm{A}_{31}\cdot\xi & \mathbf{M}\mathrm{A}_{32} & \mathbf{M}\mathrm{A}_{33}\end{Vmatrix}\quad,\qquad \left(\left\|\mathbf{M}\mathrm{A}_{ij}\right\|\cdot\xi\right)\Big|_{\xi=0}=\begin{Vmatrix}a_{11}^{sc} & a_{12} & 0\\ 0 & a_{22} & 0\\ a_{31} & a_{32} & a_{33}\end{Vmatrix}=a_{11}^{sc}\,a_{22}a_{33}\ , \tag{I-5,6}$$

$$\frac{\left\|\mathbf{N}\mathrm{A}\right\|}{\xi}=\begin{Vmatrix}\mathbf{N}\mathrm{A}_{11}\cdot\xi^{-1} & \mathbf{N}\mathrm{A}_{12} & \mathbf{N}\mathrm{A}_{13}\cdot\xi^{-2}\\ \mathbf{N}\mathrm{A}_{21}\cdot\xi^{-1} & \mathbf{N}\mathrm{A}_{22} & \mathbf{N}\mathrm{A}_{23}\cdot\xi^{-2}\\ \mathbf{N}\mathrm{A}_{31}\cdot\xi & \mathbf{N}\mathrm{A}_{32}\cdot\xi^{2} & \mathbf{N}\mathrm{A}_{33}\end{Vmatrix}\quad,\quad \left.\left(\frac{\left\|\mathbf{N}\mathrm{A}_{ij}\right\|}{\xi}\right)\right|_{\xi=0}=\begin{Vmatrix}a_{11}^{oc} & 0 & a_{13}\\ a_{21} & a_{22} & a_{23}\\ a_{31} & 0 & a_{33}\end{Vmatrix}=a_{22}\left(a_{11}^{oc}\,a_{33}-a_{13}\,a_{31}\right).$$

Then $$\left.\left(\xi^{-2}\cdot\frac{\left\|\mathbf{N}\mathrm{A}\right\|}{\left\|\mathbf{M}\mathrm{A}\right\|}\right)\right|_{\xi=0}=\frac{a_{11}^{oc}}{a_{11}^{sc}}\left(1-\frac{a_{13}}{a_{33}}\cdot\frac{a_{31}}{a_{11}^{oc}}\right)\ , \tag{I-7}$$

$$\frac{a_{31}}{a_{11}^{sc}}=-\frac{e_{33}e_{15}}{c_{44}^{E}\varepsilon_{33}^{S}}\quad,\qquad \frac{a_{11}^{oc}}{a_{11}^{sc}}=-\frac{\varepsilon_{11}^{S}}{\varepsilon_{33}^{S}}\quad,\qquad \left.\frac{a_{13}}{a_{33}}=-\frac{e_{15}}{e_{33}}\frac{\tan(K_{(3)})}{K_{(3)}}\right|_{\xi\to 0}\quad. \tag{I-8}$$

As $K_{(2)}(0)\equiv\mathrm{K}_{\langle TL\rangle}$, $K_{(3)}(0)\equiv\mathrm{K}_{\langle TSh\rangle}$ and $\mathrm{k}_{t}^{2}=e_{33}^{2}/c_{33}^{D}\varepsilon_{33}^{S}$, $\mathrm{k}_{15}^{2}=e_{15}^{2}/c_{44}^{E}\varepsilon_{11}^{S}$, *the Theorem is proven.*

Appendix II: **Proof sketch - Basics for the Statement substantiation:**

Generally the thickness $K_{(j)}$ wave-numbers (14) can be represented near the ξ^{2}-origin as

$$K_{(j)}^{2}(\xi^{2})=K_{(j)}^{2}(0)-\vartheta_{1(j)}\cdot\xi^{2}-(1/2)\,\vartheta_{2(j)}\cdot(\xi^{2})^{2}-(1/6)\,\vartheta_{3(j)}\cdot(\xi^{2})^{3}+\ldots\ , \tag{II-1}$$

where $\quad K_{(1)}^{2}(0)=0\,,\qquad K_{(2)}^{2}(0)=\omega^{2}\rho b^{2}/c_{33}^{D}\equiv\mathrm{K}_{\langle TL\rangle}^{2}\,,\qquad K_{(3)}^{2}(0)=\omega^{2}\rho b^{2}/c_{44}^{E}\equiv\mathrm{K}_{\langle TSh\rangle}^{2}\,,$ (II-2)

$\vartheta_{i(j)}=-\left\{K_{(j)}^{2}\right\}_{,\xi^{2}}^{(i)}(0)$ is the *i*-order derivative, $j=1,2,3.$ In an isotropic non-piezoelectric case with the only single dielectric permittivity, elastic and Poisson constants, the derivatives $\vartheta_{1(j)}=1$, $\vartheta_{2(j)}=0$. For the polarized isotropic piezoceramics under consideration, $\vartheta_{1(1)}=\varepsilon_{11}^{S}/\varepsilon_{33}^{S}$ and $\left|\vartheta_{1(2,3)}\right|\cong 1\pm 0.3$ depending on elastic, dielectric, and piezoelectric anisotropy, and they are independent of frequency (exact expressions):

$$\vartheta_{1(2)}=\frac{c_{44}^{E}}{c_{33}^{D}}+\frac{2e_{33}e_{15}}{\varepsilon_{33}^{S}c_{33}^{D}}-\frac{\varepsilon_{11}^{S}}{\varepsilon_{33}^{S}}\mathrm{k}_{t}^{2}+\frac{c_{44}^{E}}{c_{33}^{D}}\cdot\frac{\left[1+\dfrac{c_{13}^{E}}{c_{44}^{E}}+\dfrac{e_{33}(e_{31}+e_{15})}{\varepsilon_{33}^{S}c_{44}^{E}}\right]^{2}}{c_{33}^{D}/c_{44}^{E}-1}\ ,$$

$$\vartheta_{1(3)} = \frac{c_{11}^E}{c_{44}^E} + \frac{(e_{31}+e_{15})^2}{\varepsilon_{33}^S c_{44}^E} - \frac{\left[1+\frac{c_{13}^E}{c_{44}^E}+\frac{e_{33}(e_{31}+e_{15})}{\varepsilon_{33}^S c_{44}^E}\right]^2}{c_{33}^D/c_{44}^E - 1} \ . \qquad \text{(II-3)}$$

The second-order derivatives $\vartheta_{2(j)} \propto \Theta \cdot \left(c_{44}^E / \omega^2 \rho b^2\right)$ are inversely proportional to the frequency squared in presence of piezoelectricity (the parameter of anisotropy $\Theta = 0$ for isotropic non-piezoelectric case), and $\left|\vartheta_{2(j)}\right| \approx 1$ for the lowest fundamental thickness resonances, and is much less 1 at higher harmonics, so that

$$\vartheta_{2(1)} = 2\frac{\varepsilon_{11}^S}{\varepsilon_{33}^S}\frac{c_{44}^E}{\omega^2 \rho b^2}\left\{\frac{(e_{31}+e_{15})^2}{\varepsilon_{33}^S c_{44}^E} - \left(\mathrm{k}_{15} - \sqrt{\frac{\varepsilon_{11}^S}{\varepsilon_{33}^S}\frac{c_{33}^D}{c_{44}^E}}\cdot \mathrm{k}_t\right)^2\right\} \ . \qquad \text{(II-4)}$$

The third-order derivative $\vartheta_{3(1)} \propto \widehat{\Theta} \cdot \left[c_{44}^E c_{33}^D / (\omega^2 \rho b^2)^2\right]$.

Glossary

φ, ε_0 – electric potential and vacuum dielectric permittivity

Q_m, $Q_{ij}^{E,D}$, $Q_{r(a)}$, Q – standardized material, elastic constant's, PR resonance (antiresonance) and generalized quality factors

$c_{ij}^{E,D}\left(s_{ij}^{E,D}\right)$, $e_{ij}(h_{ij}, d_{ij})$, $\varepsilon_{ij}^{T,S}$ – complex piezomaterial constants (real ones are with an upper point)

ρ, $\nu = \varepsilon_{11}^S / \varepsilon_{33}^S$ – material density and dielectric anisotropy parameter

s^*, ε^* – effective elastic compliance and dielectric permittivity

k_t, k_{15} ($\tilde{\mathrm{k}}_{15}$), k_{31}, k_p – complex CEMC (generalized notation k with its real value k)

D, E, T, S – electric field induction and strength, mechanical stress and strain

$C_{\{33,11\}}^{T,S}$ $\left(\breve{C}_0 \equiv \breve{C}_{33}^S = \varepsilon_{33}^S / 2b\right)$ – PR capacitance (unit surface value)

$\omega = 2\pi f$, χ, $y = 2Q\chi$ – angular frequency, relative and generalized frequency displacements

f_r, f_a, n – resonance (r) and antiresonance (a) frequencies, harmonic order of the elementary admittance $\widehat{\mathrm{Y}}$

x, z ($\bar{x}$, $\bar{z}$) and u_x, u_z – space coordinates (normalized) and local respective displacements

Υ, Ψ, $2b$, $\vec{\mathrm{P}}$ – length, width and thickness of an elementary PR, and its polarization direction

$|\mathrm{B}|$ – characteristic matrix of motion and charge equations

$\left|\mathbf{\Phi}\langle \mathrm{S|A}\rangle\right|$, $\left|\mathbf{G}\langle \mathrm{S|A}\rangle\right|$ and $\left\|\mathbf{M}\langle \mathrm{S|A}\rangle\right\|$, $\left\|\mathbf{N}\langle \mathrm{S|A}\rangle\right\|$ – s.c. and o.c. characteristic matrices of boundary conditions, and corresponding determinants for **S**- and **A**- configurations, respectively

$A_{\{z,x,\varphi\}}\left(\bar{A}_{\{z,x,\varphi\}}, \tilde{A}_{\{z,x,\varphi\}}\right)$, L_j – characteristic amplitudes and weighting coefficients in eigen-mode solutions

$\mathrm{K}_{\langle TL\rangle}$, $\mathrm{K}_{\langle TSh\rangle}$ (K) – wave-number of 1-D elementary *TL* and *TSh* vibrations (generalized notation)

$\widehat{\mathrm{Y}}_{\langle TL\rangle}$, $\widehat{\mathrm{Y}}_{\langle TSh\rangle}$, $\widehat{\mathrm{Y}}$ – normalized complex admittance of the elementary (non-coupled) *TL* and *TSh* mode, and their generalized notation

K, ξ – coupled complex thickness and lateral wave-numbers

$\vartheta_{i(j)}$ – i-order derivative $\left\{-K_{(j)}^2\right\}_{,\xi^2}^{(i)}$ of the j-order wave-number, $j = 1, 2, 3$

$\zeta_m(\omega, P)$, $\zeta_m^{sc}(\omega)$, $\zeta_m^{oc}(\omega)$ – m- branch lateral complex wave-number, s.c. ($P = 0$) and o.c. ($P = \infty$) dispersion

eigen-values

$\breve{R}_{el} = 1/\sigma h_{el}$, h_{el}, σ – unit surface resistance of the electrode, its thickness and unit conductance

λ, $\vec{\mathrm{v}}$ and x_0, μ – wave-length, velocity and characteristic decay parameters

$Z(\breve{Z})$, ϕ, $R_{r(a)}(\breve{R}_{r(a)})$ – PR impedance, its phase, resonance/antiresonance resistances (unit surface values)

$|\mathrm{X}|$, $\|\mathrm{X}\|$, $\|\|\mathrm{X}\|\|$ – notations for a complex **X** matrix, its determinant and determinant's absolute value

$\mathrm{X}_{,x}$, $\mathrm{X}'_{,x}(\mathrm{X}')$, $\partial \mathrm{X}/\partial x$ – notations for a first-order x-derivative of some **X** function

$F(\xi)$, $U(\xi)$ – generalized s.c. and o.c. characteristic matrix's functions of the lateral wave-number

$\Delta_i^{sc,oc}$, $\theta_i^{sc,oc}$ – coefficients in first-order derivative representation of the characteristic matrices

p_{ij}, a_{ij} – elements of generalized F_0 and U_0 matrix's functions for **S-** and **A-**configurations

$P^2 = b^2 \omega \breve{C}_0 \breve{R}_{el} = \omega\tau$, $P_0^2 = \omega_0 \tau$, $\tau = b^2 \breve{R}_{el} \breve{C}_0$ – relaxation parameters of electrode resistivity influence

α, β – relaxation parameters of the Havriliak-Negami equation

$\mathrm{i} = \sqrt{-1}$ – imaginary unit

i, j – integer numbers (as subscripts)

S-*TL:n* , S-*TSh:n* – *n*-order basic *TL* (odd n_{TL}) and non-basic *TSh* (even n_{TSh}) resonances in **S**-configuration

A-*TSh:n* , A-*TL:n* – *n*-order basic *TSh* (odd n_{TSh}) and non-basic *TL* (even n_{TL}) resonances in **A**-configuration

κ_{TL} , κ_{TSh} – effective CEMC for "A-*TL: even n*" and "S-*TSh: even n*" resonances, respectively

$\ldots\&\ldots$, $\langle \ldots | \ldots \rangle$ – "*and*" and "*or*" signs with respective elements

Upper point denotes a real value of the complex parameter.

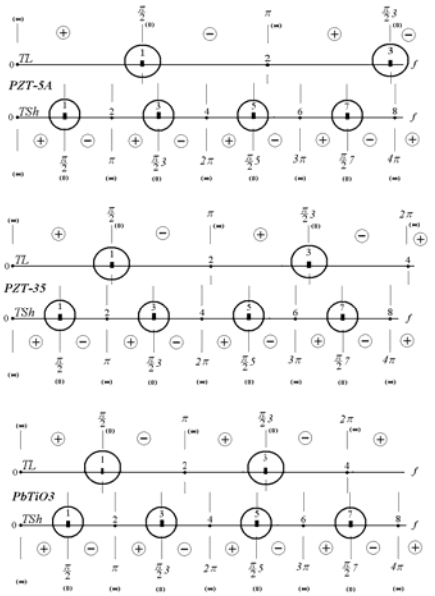

The authors A.A. Mezheritsky, A.V. Mezheritsky :
Brooklyn, NY 11218
aam80@optonline.net , mav5@optonline.net
* *M.Sc. in Computer Science (City University of New York), Ph.D. Student, IEEE Student Member (2005)*
** *Ph.D. in Physics (1985, MIPT, Moscow, Russia), IEEE Member*

Dependences of Dispersion Characteristics on Electrode Resistivity and Frequency for the Symmetric S- configuration with Basic TL-Mode.

PCM PbTiO3

$$\xi^2 \cdot \|\mathbf{MS}\| - 2iP^2 \cdot \|\mathbf{NS}\| = 0 \quad \rightarrow \quad \xi = \zeta_m(\omega, P) \quad with \quad Im\,\zeta_m < 0$$

Losses:

$\dot{c}_{nm}^D = \dot{c}_{nm}^D(1 + i/Q)$

Constants : $c_{33}^E/c_{44}^E\left(c_{33}^D/c_{44}^E\right) = 2.36\ (2.98)$

$\dot{c}_{33}^D = 16.8 \cdot 10^{10}\ N/m^2$ $\quad \dot{c}_{11}^D = 14.4 \cdot 10^{10}\ N/m^2$ $\quad \dot{c}_{44}^D = 6.1 \cdot 10^{10}\ N/m^2$

$\dot{c}_{13}^D = 2.9 \cdot 10^{10}\ N/m^2$ $\quad \dot{c}_{12}^D = 3.3 \cdot 10^{10}\ N/m^2$

$\dot{h}_{33} = 5.45 \cdot 10^9\ V/m$ $\quad \dot{h}_{31} = -0.42 \cdot 10^9\ V/m$ $\quad \dot{h}_{15} = 1.59 \cdot 10^9\ V/m$

$\dot{s}_{33}^\sigma/\varepsilon_0 = 134$ $\quad \dot{s}_{11}^\sigma/\varepsilon_0 = 212$

$k_t = 0.458$ $\quad \tilde{k}_{15} = 0.279$ $\quad k_p = 0.182$

$Q = 100$ *(solid line)* $\quad (Q_{33}^E = 79,\ Q_{44}^E = 92)$

$Q = 900$ *(dash line)* $\quad (Q_{33}^E = 711,\ Q_{44}^E = 830)$

$P^2 = b^2\omega\tilde{C}_0\tilde{R}_{el}$

Notations:

$m\hat{E}^+$ – *m-branch of the TSh-set related to* $(n = m+1)$*-order shear thickness resonance,*

$m\hat{E}^-$ – *m-branch of the TL-set related to* $(n = m)$*-order longitudinal thickness resonance,*

$m\hat{\Phi}$ – *m-branch of the "potential" set,*

$\hat{R}$ – *"planar" branch,*

with odd numbers $m = 1,3,5...$ *for S- configuration.*

Relative Frequency Displacements: $\left[\chi_{(TSh)}+1\right]\sqrt{\dot{c}_{44}^E} = \left[\chi_{(TL)}+1\right]\sqrt{\dot{c}_{33}^D}$

$$\chi_{(TSh)} = f/f_{r1(TSh)} - 1 \qquad \chi_{(TL)} = f/f_{a1(TL)} - 1$$

$$f_{r1(TSh)} = \frac{1}{2(2b)} \cdot \sqrt{\frac{\dot{c}_{44}^E}{\rho}} \qquad f_{a1(TL)} = \frac{1}{2(2b)} \cdot \sqrt{\frac{\dot{c}_{33}^D}{\rho}}$$

Frequency Scale:

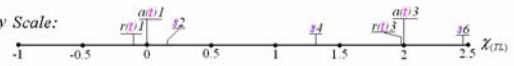

s n – n-order TSh-resonance, r(t) n – n-order TL-resonance, a(t) n – n-order TL-antiresonance

Dependences of Dispersion Characteristics on Electrode Resistivity and Frequency for the Symmetric S- configuration with Basic TL-Mode.

PCM PZT- 35

$$\xi^2 \cdot \|\mathbf{MS}\| - 2iP^2 \cdot \|\mathbf{NS}\| = 0 \quad \rightarrow \quad \xi = \zeta_m(\omega, P) \quad with \quad Im\,\zeta_m < 0$$

Losses:

$\dot{c}_{nm}^D = \dot{c}_{nm}^D(1 + i/Q)$

Constants : $\dot{c}_{33}^E/\dot{c}_{44}^E\left(\dot{c}_{33}^D/\dot{c}_{44}^E\right) = 3.49\ (4.35)$

$\dot{c}_{33}^D = 18.9 \cdot 10^{10}\ N/m^2$ $\quad \dot{c}_{11}^D = 17.2 \cdot 10^{10}\ N/m^2$ $\quad \dot{c}_{44}^D = 5.44 \cdot 10^{10}\ N/m^2$

$\dot{c}_{13}^D = 8.1 \cdot 10^{10}\ N/m^2$ $\quad \dot{c}_{12}^D = 9.0 \cdot 10^{10}\ N/m^2$

$\dot{h}_{33} = 2.8 \cdot 10^9\ V/m$ $\quad \dot{h}_{31} = -0.44 \cdot 10^9\ V/m$ $\quad \dot{h}_{15} = 1.5 \cdot 10^9\ V/m$

$\dot{s}_{33}^\sigma/\varepsilon_0 = 540$ $\quad \dot{s}_{11}^\sigma/\varepsilon_0 = 550$

$k_t = 0.445$ $\quad \tilde{k}_{15} = 0.449$ $\quad k_p = 0.408$

$Q = 100$ *(solid line)* $\quad (Q_{33}^E \approx Q_{44}^E = 80)$

$Q = 900$ *(dash line)* $\quad (Q_{33}^E \approx Q_{44}^E = 720)$

$P^2 = b^2\omega\tilde{C}_0\tilde{R}_{el}$

Notations:

$m\hat{E}^+$ – *m-branch of the TSh-set related to* $(n = m+1)$*-order shear thickness resonance,*

$m\hat{E}^-$ – *m-branch of the TL-set related to* $(n = m)$*-order longitudinal thickness resonance,*

$m\hat{\Phi}$ – *m-branch of the "potential" set,*

$\hat{R}$ – *"planar" branch,*

with odd numbers $m = 1,3,5...$ *for S- configuration.*

Relative Frequency Displacements: $\left[\chi_{(TSh)}+1\right]\sqrt{\dot{c}_{44}^E} = \left[\chi_{(TL)}+1\right]\sqrt{\dot{c}_{33}^D}$

$$\chi_{(TSh)} = f/f_{r1(TSh)} - 1 \qquad \chi_{(TL)} = f/f_{a1(TL)} - 1$$

$$f_{r1(TSh)} = \frac{1}{2(2b)} \cdot \sqrt{\frac{\dot{c}_{44}^E}{\rho}} \qquad f_{a1(TL)} = \frac{1}{2(2b)} \cdot \sqrt{\frac{\dot{c}_{33}^D}{\rho}}$$

Frequency Scale:

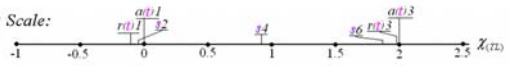

s n – n-order TSh-resonance, r(t) n – n-order TL-resonance, a(t) n – n-order TL-antiresonance

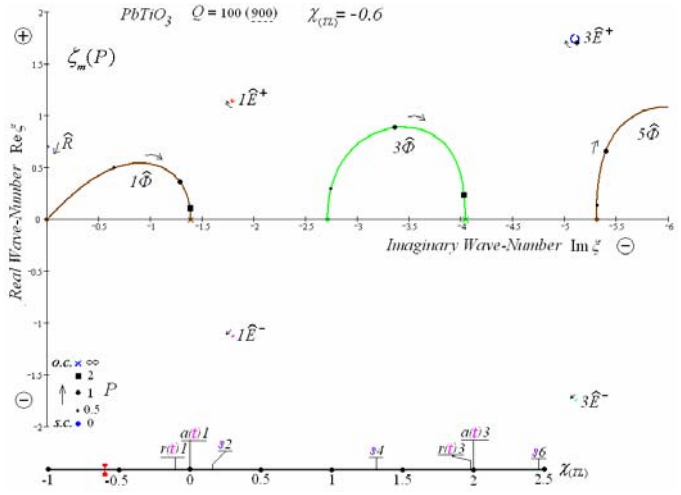

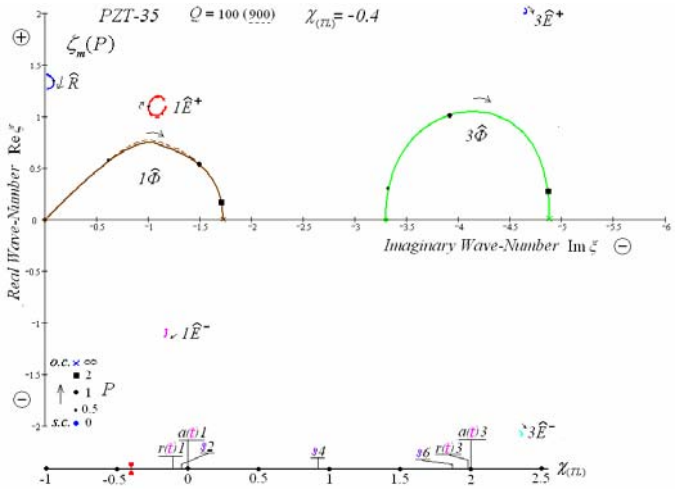

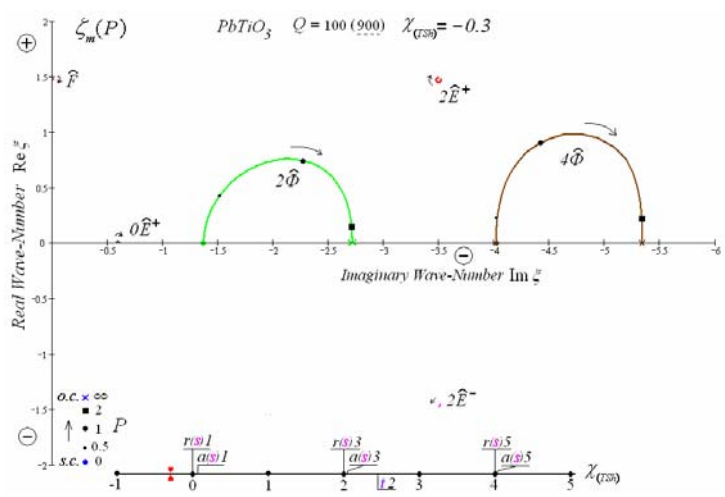

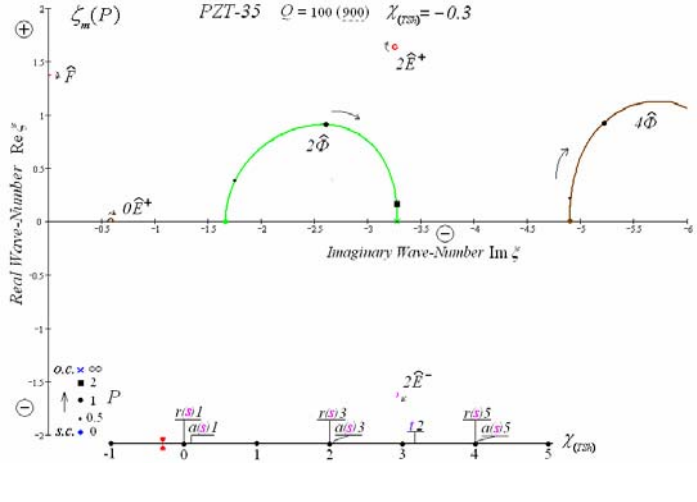

Dependences of Dispersion Characteristics on Electrode Resistivity and Frequency for the Symmetric S- configuration with Basic TL-Mode.

PCM PZT-5A

$$\xi^2 \cdot \|MS\| - 2iP^2 \cdot \|NS\| = 0 \quad \rightarrow \quad \xi = \zeta_m(\omega, P) \quad with \quad Im\,\zeta_m < 0$$

Constants : $c_{33}^E/c_{44}^E\left(c_{33}^D/c_{44}^E\right) = 5.39(7.01)$

$c_{33}^D = 14.7\cdot10^{10}\ N/m^2$ $\quad c_{11}^D = 12.6\cdot10^{10}\ N/m^2$ $\quad c_{44}^D = 3.97\cdot10^{10}\ N/m^2$

$c_{13}^D = 6.52\cdot10^{10}\ N/m^2$ $\quad c_{12}^D = 8.09\cdot10^{10}\ N/m^2$

$h_{33} = 2.15\cdot10^9\ V/m$ $\quad h_{31} = -0.73\cdot10^9\ V/m$ $\quad h_{15} = 1.52\cdot10^9\ V/m$

$\varepsilon_{33}^s/\varepsilon_0 = 830$ $\quad \varepsilon_{11}^s/\varepsilon_0 = 916$

$k_t = 0.481$ $\quad \tilde{k}_{15} = 0.687$ $\quad k_p = 0.603$

Losses:

$c_{nm}^D = \hat{c}_{nm}^D(1+i/Q)$

$Q = 100$ *(solid line)* $\quad (Q_{33}^E = 77,\ Q_{44}^E = 53)$

$Q = 900$ *(dash line)* $\quad (Q_{33}^E = 692,\ Q_{44}^E = 475)$

$P^2 = b^2\omega\tilde{C}_0\tilde{R}_{el}$

Notations:

$m\hat{E}^+$ – m-branch of the TSh-set related to (n = m+1)-order shear thickness resonance,

$m\hat{E}^-$ – m-branch of the TL-set related to (n = m)-order longitudinal thickness resonance,

$m\hat{\Phi}$ – m-branch of the "potential" set,

$\hat{R}$ – "planar" branch,

with odd numbers m = 1,3,5... for S- configuration.

Relative Frequency Displacements: $\left[\chi_{(TSh)}+1\right]\sqrt{c_{44}^E} = \left[\chi_{(TL)}+1\right]\sqrt{c_{33}^D}$

$$\chi_{(TSh)} = f/f_{r1(TSh)} - 1 \qquad \chi_{(TL)} = f/f_{a1(TL)} - 1$$

$$f_{r1(TSh)} = \frac{1}{2(2b)}\cdot\sqrt{\frac{c_{44}^E}{\rho}} \qquad f_{a1(TL)} = \frac{1}{2(2b)}\cdot\sqrt{\frac{c_{33}^D}{\rho}}$$

Frequency Scale:

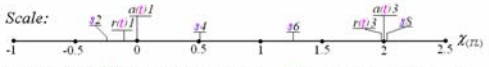

s n – n-order TSh-resonance, r(t) n – n-order TL-resonance, a(t) n – n-order TL-antiresonance

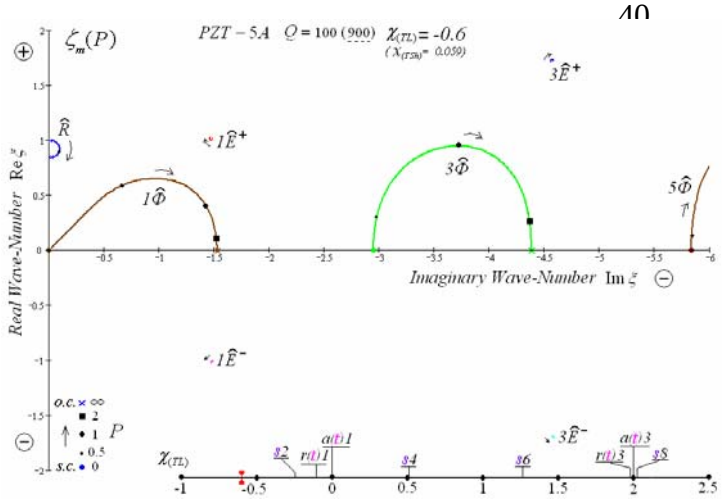

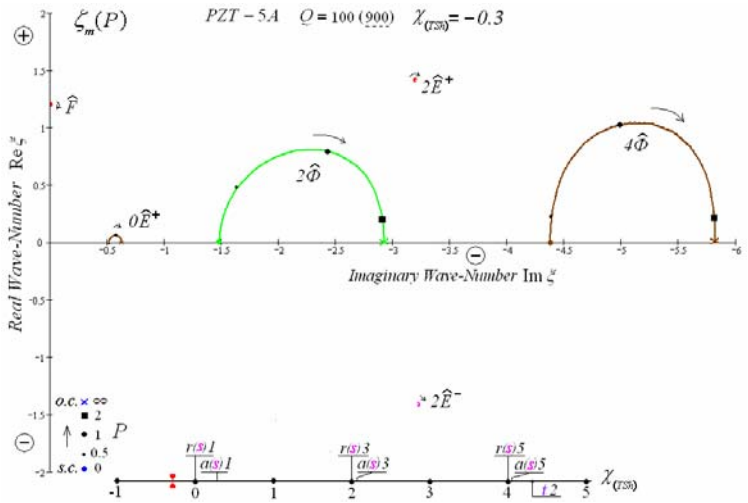

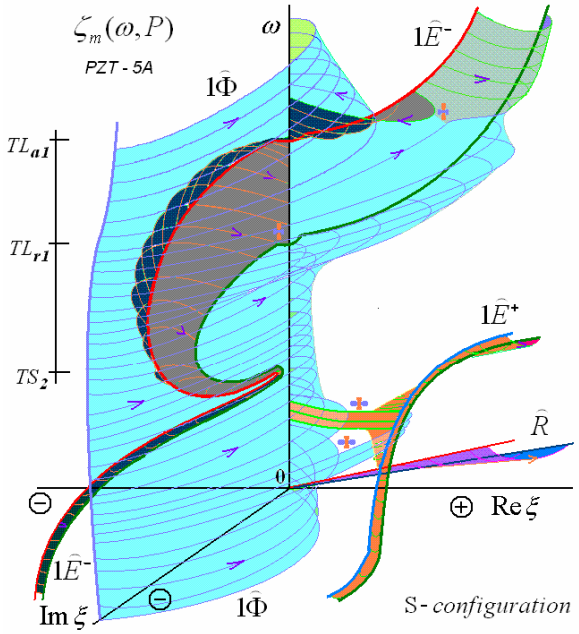

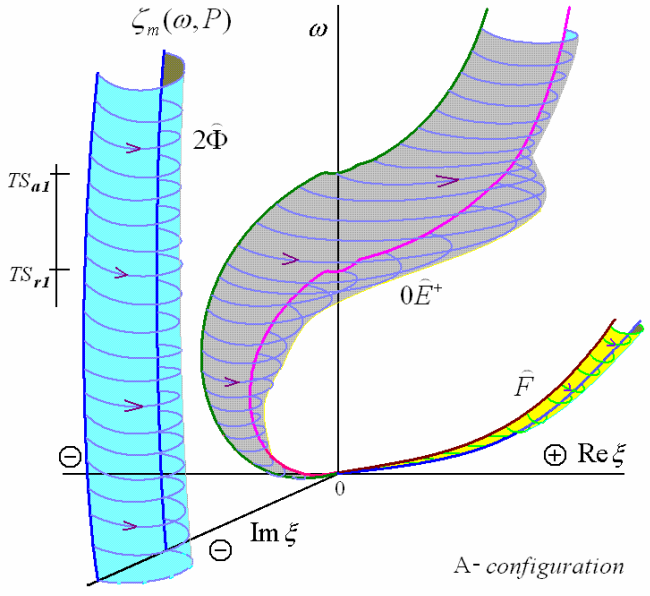

Schematic of the dispersion surfaces dependences on electrode conductivity and frequency from static up to the fundamental thickness resonance: arrows show P^{-1} changing, sings ✣ indicate the regions of dispersion singularities

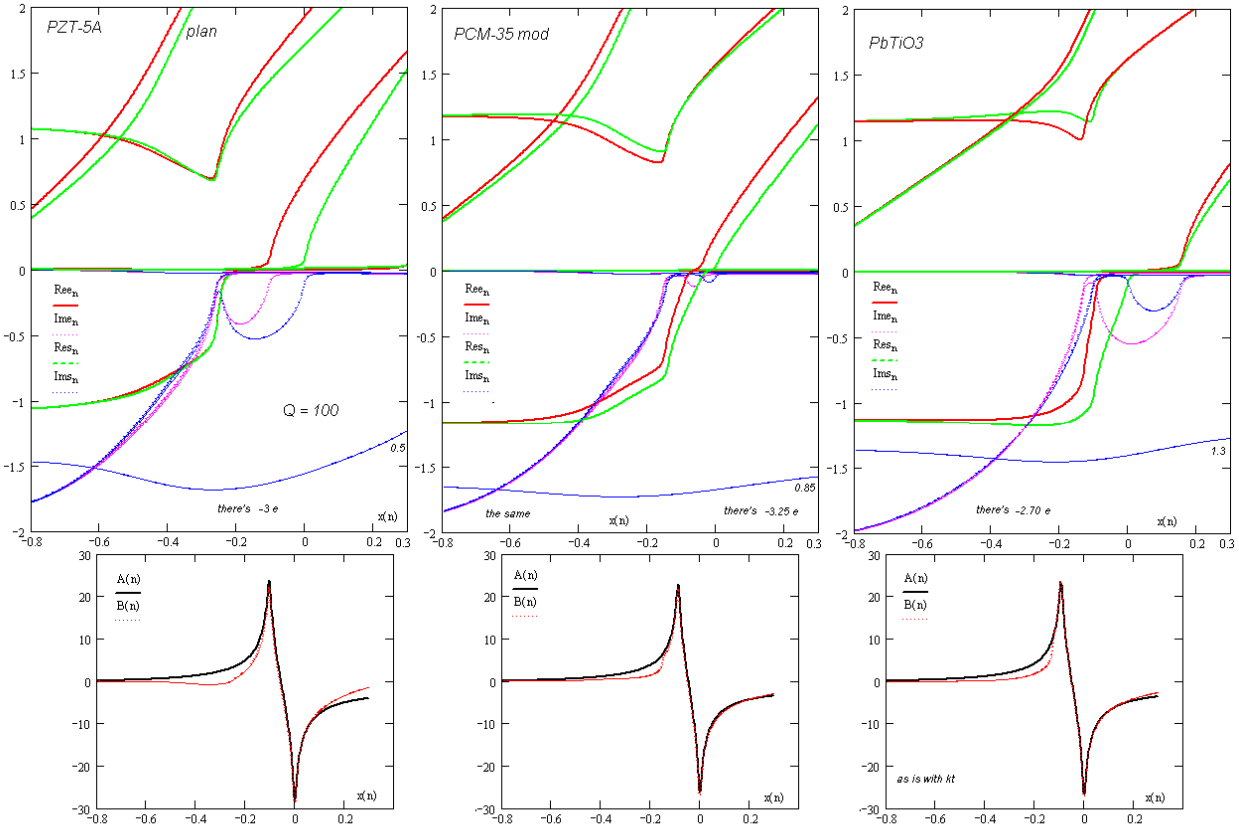

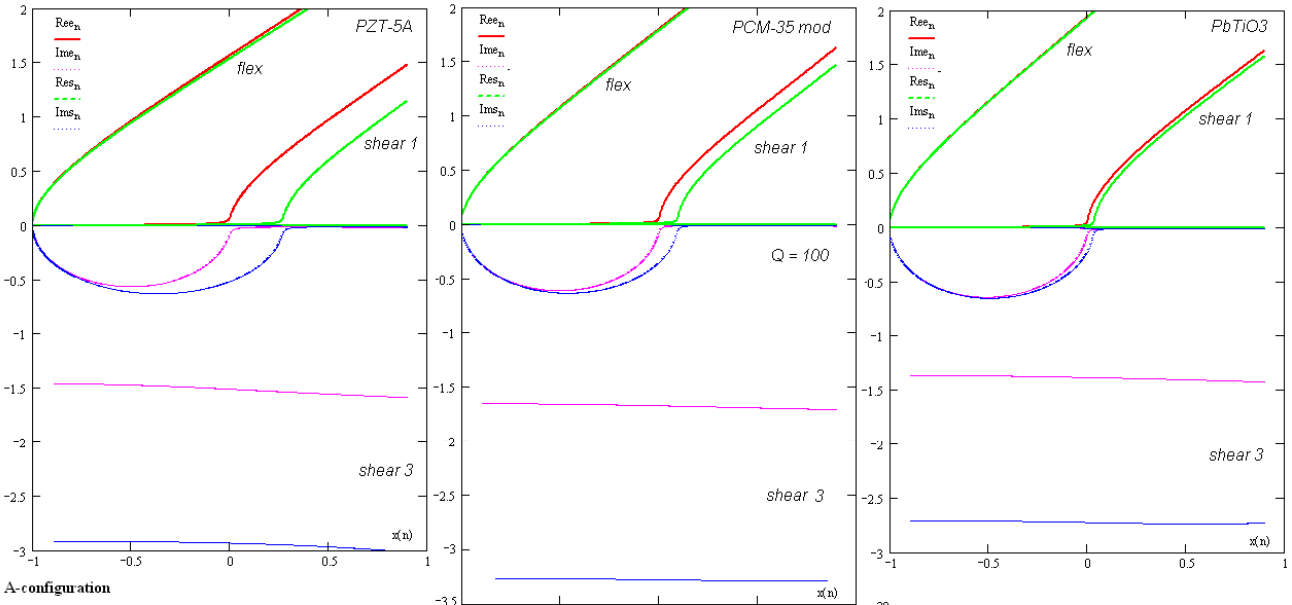

A-configuration